

Synthetic Approach towards the Formation of Cobalt Peroxynitrite Intermediate

*A dissertation submitted to the
Indian Institute of Technology Guwahati as
Partial fulfillment for the degree of
Doctor of Philosophy in Chemistry*

Submitted by

Soumen Saha

(Roll No. 126122002)

Supervisor

Prof. Biplab Mondal



Department of Chemistry

Indian Institute of Technology Guwahati

December, 2017



**Dedicated to My Family, Friends
&
Teachers**

STATEMENT

I hereby declare that this thesis entitled “**Synthetic Approach towards the Formation of Cobalt Peroxynitrite Intermediate**” is the outcome of research work carried out by me under the supervision of Prof. Biplab Mondal in the Department of Chemistry, Indian Institute of Technology Guwahati, India.

In keeping with the general practice of reporting scientific observations, due acknowledgements have been made wherever the work described is based on the findings of other investigators.

December, 2017

Soumen Saha

Indian Institute of Technology Guwahati

Acknowledgement

The success and final outcome of this thesis required a lot of guidance and assistance from many people and I am extremely privileged to have got this all along the completion of my thesis. All that I have done is only due to such supervision and assistance and I would not forget to thank them.

First and foremost I would like to thank my thesis supervisor, Prof. Biplab Mondal, who fearlessly accepted me as Ph.D student under his guidance and was the main creator of the great ideas, techniques and whole background of this thesis. We experienced together all the ups and downs of routine work, the shared happiness of success and the depression of failure. It would never have been possible for me to completion of my thesis without his incredible support and encouragement. I have been extremely lucky to have a supervisor who cared so much about my work, and who responded to my questions and queries so promptly.

Besides my advisor, I would like to thank the rest of my thesis committee member Prof. B. K. Patel, Dr. Debasis Manna and Dr. A.S. Achalkumar for their encouragement, insightful advices and valuable suggestions.

I sincerely appreciate the whole hearted cooperation and valuable help rendered by the teaching and non-teaching staff of Department of Chemistry, Indian Institute of Technology Guwahati. I am also thankful to Central Instrument facility (CIF), IITG for providing instrument facility. I wish to extend my thanks to IIT Guwahati for the financial support.

My Sincere thanks to my lab senior, Somnath Da, Hemanta Da, Vikash Da, Kanhu Da, Aswini Da, Apurba Da and Pankaj Da for their support and motivation during the initial days of my stay in the lab and immense help in my research works. My heartfelt thanks to my fellow lab mates, Kuldeep, Baishakhi, Dibyajyoti Da and Rakesh for always being there and bearing with me the good and bad times during my wonderful days of Ph.D. My special words of gratitude to Kuldeep with whom I have started my Ph.D journey and also submitting our thesis at same time. His perceptive suggestions and invaluable help were quite exciting and encouraging for me to make my career in

research. I would also like to thank all the project students with whom I had a great opportunity to work together.

I must express my gratitude to my childhood friends Sohail and Raju for their constant help and support. My appreciation and gratefulness to my school and college friends, Sugata, Maloy, Tatha, Mojo, Pintu, DK, Arka, Rudra, Tanmay, Dinesh, Hochi, Pratik, Anirban, Ayan, Pijush, Ashraf..... for their kind help and encouragement towards the success of my life.

I thank my all the PhD colleagues at IITG- Keshab, Halder, Shilaj, Kallol, Uday, Suranjan, Hiranya, Shubhadip, Arvin, Akhtar, Sayan, Manas, Rajendra, Sahnawaz, Belal, Gourab, Sabya, Subhankar, Subhra, Soumendra..... for all the fun I have shared in last five years.

I am extremely thanked to all my teachers because of their teaching at different stages of education. Without learning from them I could not able to write this thesis.

I owe my deepest gratitude towards my better half for her eternal support and understanding of my goals and aspirations. Her infallible love and support has always been my strength. Her patience and sacrifice will remain my inspiration throughout my life. It would be ungrateful on my part if I thank Juhi in these few words.

As always it is impossible to mention everybody who had an impact to this work however, there are those whose spiritual support is even more important. I feel a deep sense of gratitude for my father, mother and sister who formed part of my vision and taught me good things that really matter in life. All the support and love they have provided me over the years was the greatest gift anyone has ever given me. I am also very much grateful to all my family members for their constant inspiration and encouragement.

Finally, I would like to thank all others who are associated with my work directly or indirectly at IIT Guwahati for their help.

Soumen Saha

Indian Institute of Technology Guwahati



भारतीय प्रौद्योगिकी संस्थान गुवाहाटी
INDIAN INSTITUTE OF TECHNOLOGY GUWAHATI
North Guwahati, Assam – 781039, India

Prof. Biplab Mondal
Department of Chemistry

Phone : + 91-361-258-2317
Fax: + 91-361-258-2349
E-mail: biplab@iitg.ernet.in

Certificate

This is to certify that **Mr. Soumen Saha** has been working under my supervision since July, 2012 as a regular Ph.D. student in the Department of Chemistry, Indian Institute of Technology Guwahati. I am forwarding his thesis entitled “**Synthetic Approach towards the Formation of Cobalt Peroxynitrite Intermediate**” being submitted for the Ph.D. degree.

I certify that he has fulfilled all the requirements according to the rules of this Institute regarding the investigations embodied in his thesis and this work has not been submitted elsewhere for a degree.

December, 2017

Biplab Mondal

Contents

	Page No.
Synopsis	i
Chapter 1: Introduction	
1.1 General aspect of peroxyxynitrite	1
1.2 Formation of metal peroxyxynitrite	3
1.3 Scope of the thesis	11
1.4 References	11
Chapter 2: Nitric Oxide Reactivity of a Co(II) Complex: Reductive Nitrosylation of Co(II) followed by Release of Nitrous Oxide	
Abstract	16
2.1 Introduction	17
2.2 Results and discussion	18
2.3 Experimental section	25
2.4 Conclusion	28
2.5 References	28
Chapter 3: Reactivity of a Cobalt Nitrosyl Complex: Formation of a Cobalt Peroxyxynitrite Intermediate and Transfer of the Nitrosyl to a Cobalt Porphyrin Complex	
Abstract	33
3.1 Introduction	34
3.2 Results and discussion	35
3.3 Experimental section	41
3.4 Conclusion	46
3.5 References	46
Chapter 4: Reaction of a Nitrosyl Complex of Cobalt Porphyrin with Hydrogen Peroxide: Putative Formation of Peroxyxynitrite Intermediate	
Abstract	50
4.1 Introduction	51
4.2 Results and discussion	52
4.3 Experimental section	58

4.4 Conclusion	61
4.5 References	61

Chapter 5: Reaction of a Co(III)-Peroxo Complex and NO: Formation of a Putative Peroxynitrite Intermediate

Abstract	66
5.1 Introduction	67
5.2 Results and discussion	68
5.3 Experimental section	73
5.4 Conclusion	76
5.5 References	77
Appendix I	81
Appendix II	87
Appendix III	97
Appendix IV	104
List of publications	109

Synopsis

The thesis entitled “**Synthetic Approach towards the Formation of Cobalt Peroxynitrite Intermediate**” is divided into five chapters.

Chapter 1: Introduction

Nitric oxide (NO) is an important small molecule known as ubiquitous intercellular messenger in all vertebrates.¹⁻⁴ Only a submicromolar concentration of NO is responsible for all of its activities. It is known as a cytotoxic effector when produced in excess.⁴ Cytotoxicity of NO is due to the formation of secondary reactive nitrogen species (RNS) like peroxynitrite (ONOO⁻) or nitrogen dioxide (NO₂). The formation of these secondary RNS may result from the oxidation of NO in the presence of oxidants like superoxide radicals (O₂⁻), hydrogen peroxide (H₂O₂) and/or transition metal ions.⁵⁻⁶ Peroxynitrite can be generated by the reaction of H₂O₂ and nitrite (NO₂⁻) in the presence of the peroxidase enzymes.⁷⁻⁸ On the other hand, the oxy-heme {*i.e.* iron(III)-superoxo} species of the nitric oxide dioxygenase (NODs) react with NO to result in nitrate (NO₃⁻) ion which is biologically benign.⁹ This reaction is believed to proceed through the formation of ONOO⁻ intermediate.⁹⁻¹⁰ In literature, ONOO⁻ intermediates are exemplified to form either in the reaction of oxy-heme (formally, Fe^{III}-O₂⁻) proteins with NO or metal-nitrosyls with O₂ or O₂⁻.¹⁰⁻¹¹ Clarkson and Basolo reported the reaction of a cobalt-nitrosyl complex with O₂ to result in the formation of NO₂⁻ product through a putative ONOO⁻ intermediate.¹² Kim *et al.* reported the reaction of a non-heme dinitrosyliron with O₂ to afford NO₃⁻.¹³ In a similar reaction, [Cu(NO)] species was found to result in corresponding NO₂⁻ and O₂ *via* ONOO⁻ intermediate.¹⁴ Recently, the ONOO⁻ intermediates have been shown to form in the reaction of NO with Cr-superoxo or peroxo species. A Cr^{IV}-peroxo complex, [(12-TMC)Cr(O₂)(Cl)]⁺ {12-TMC = 1,4,8,11-tetramethyl-1,4,8,11-tetraazacyclotetradecane} is

reported to react with NO to result in a Cr(III)-nitrate complex *via* the formation of a Cr(III)-(ONOO⁻) intermediate.¹⁵ Nam *et. al.* reported the reactivity of an Fe(III)-peroxo complex, [(14-TMC)Fe(O₂)]⁺ with NO⁺ as an approach for generating the ONOO⁻ intermediate which led to the formation of an Fe(III)-nitrate complex.¹⁶

In our laboratory, we have been working on the reactivity of the metal nitrosyls with O₂⁻ anion and H₂O₂ with an aim to generate a ONOO⁻ species. For example, {CuNO}¹⁰ complex of the *bis*(2-ethyl-4-methylimidazol-5-yl)methane ligand was found to react with H₂O₂ to afford the corresponding Cu(I)-nitrite and the formation of a Cu(I)-peroxynitrite intermediate is presumed.¹⁷ The same nitrosyl complex, upon reaction with O₂⁻ anion was observed to result in Cu(II)-nitrite.¹⁸ In another example, the {CuNO}¹⁰ complex in the presence of H₂O₂ was shown to form Cu(II)-nitrite *via* a presumed ONOO⁻ intermediate.¹⁸ Recently Nam group prepared a [(12-TMC)Co(NO)]²⁺ by transferring the bound NO ligand from [(14-TMC)Co(NO)]²⁺. In addition to the NO-transfer reaction, dioxygenation of [(14-TMC)Co(NO)]²⁺ by O₂ produces [(14-TMC)Co(NO₃)]⁺ *via* the formation of a Co(II)-(ONOO⁻) intermediate.¹⁹

Metal-peroxynitrite complexes decompose readily to form either metal nitrate or metal-oxo complex and NO₂. In both cases ONOO⁻ was found to induce phenol ring nitration which may have consequences for the process of tyrosine phosphorylation. The presence of nitrated tyrosine residues has been suggested as a marker for peroxynitrite activity.²⁰⁻²¹ Karlin *et. al.* reported that NO reacts with [(thf)(F₈)Fe(O₂⁻)], followed by the addition of the tyrosine mimic 2,4-di-*tert*-butylphenol (DTBP) resulted in the formation of [(F₈)Fe(NO₃)] and effective nitration of DTBP occurs.²²

The present thesis is originated from our interest to study the formation of cobalt peroxynitrite intermediates by the reaction of a cobalt-nitrosyl with O₂⁻/ H₂O₂ or a cobalt-

peroxo complex with NO. The second chapter describes the reaction of a Co(II) complex with NO and the formation of a Co-nitrite complex *via* a thermally unstable Co-dinitrosyl complex with the release of N₂O. The third chapter discusses the reactivity of a nitrosyl complex of cobalt salen complex. The complex was found to react with KO₂ to result in the formation of a Co-nitrate complex *via* a putative Co-(ONOO⁻) intermediate. In addition, the bound NO group of the nitrosyl complex was transferred to a cobalt porphyrinate to form the corresponding nitrosyl. The fourth chapter deals with the reaction of a nitrosyl complex of cobalt porphyrinate with H₂O₂ to result in the cobalt nitrite complex through a putative formation of Co-(ONOO⁻) intermediate. The last chapter describes the formation of a Co-(ONOO⁻) intermediate in the reaction of a cobalt-peroxo complex with NO leading to the formation of a cobalt-nitrate complex.

Chapter 2: Nitric Oxide Reactivity of a Co(II) Complex: Reductive Nitrosylation of Co(II) Complex Followed by the Release of N₂O

A Co(II) complex, [(L1)₂Co]Cl₂, **2.1** was prepared by stirring a mixture of cobalt(II) chloride hexahydrate with 2 equivalents of the ligand **L1** {**L1** = *bis*(2-ethyl-4-methylimidazol-5-yl)methane} in methanol. It was characterized structurally as well as by spectral analyses. The ORTEP diagram is shown in figure S1a. The crystal structure revealed that the Co(II) center is surrounded by the four nitrogen atoms from two units of the ligand in an overall distorted tetrahedral geometry.

Gradual addition of NO gas to a dry and degassed methanol solution of **2.1** resulted in the change of color to red. The complete reaction was observed with 3 equivalents of NO. In UV-visible spectroscopic monitoring, the addition of NO resulted in the appearance of absorption bands at 516 nm ($\epsilon/M^{-1}cm^{-1}$, 300), 556 nm ($\epsilon/M^{-1}cm^{-1}$, 490), 579 nm ($\epsilon/M^{-1}cm^{-1}$, 474), 664 nm ($\epsilon/M^{-1}cm^{-1}$, 140) along with other intra-ligand transitions at lower

wavelengths (Figure S2a). This is attributed to the formation of intermediate complex **2.2**.

In absence of air and moisture, the color was found to be stable for several hours.

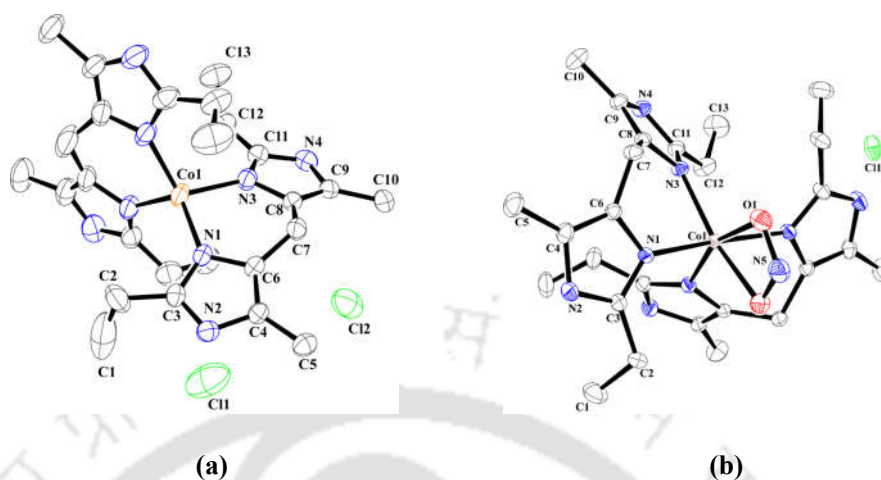


Figure S1. ORTEP diagram of complexes (a) **2.1** and (b) **2.3**. (30% thermal ellipsoid plot. H-atoms and solvent molecules are not shown for clarity).

Unfortunately we could not isolate it as solid owing to its reactive nature. However, spectroscopic characterization revealed **2.2** as a Co(I)-dinitrosyl having $\{\text{Co}(\text{NO})_2\}^{10}$ configuration.

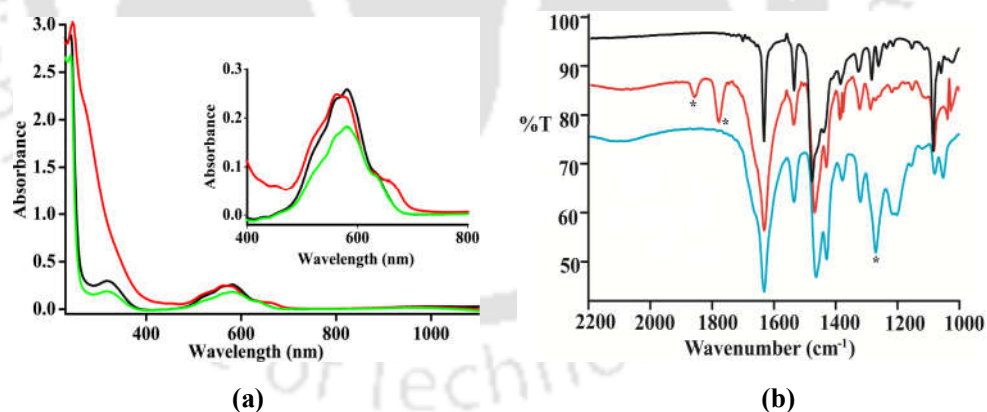


Figure S2. (a) UV-visible spectral monitoring of the reaction of complex **2.1** (black) with NO to result **2.2** (red) and **2.3** (green) in methanol. (b) Solution FT-IR spectral monitoring of the reaction of complex **2.1** (black) with NO to result **2.2** (red) and **2.3** (blue) in methanol.

The addition of successive equivalent of NO resulted in the change of color to dark brown.

In the visible region of the spectrum it shows absorption bands at 523 nm ($\epsilon/M^{-1}\text{cm}^{-1}$, 184),

558 nm ($\epsilon/M^{-1}cm^{-1}$, 312) and 579 nm ($\epsilon/M^{-1}cm^{-1}$, 360), respectively. This is attributed to the formation of complex, [(L1)₂Co(NO₂)], **2.3** (Scheme S1). In the FT-IR spectrum, **2.2** shows two new stretching frequency at 1857 and 1774 cm^{-1} , assignable to the coordinated NO stretching of {Co(NO)₂}¹⁰ moiety (Figure S2b). In the presence of further equivalent of NO, the NO stretching frequencies at 1857 and 1774 cm^{-1} disappeared with the appearance of a new one at 1261 cm^{-1} (Figure S2b). This is attributed to the coordinated NO₂⁻ stretching and this assignment is in well agreement with the formulation of **2.3**.

In the X-band EPR spectroscopy, the characteristic signals of Co(II) in tetrahedral geometry disappeared upon addition of 3 equivalents of NO (Figure S3a). However, the addition of subsequent equivalent of NO resulted in the appearance of Co(II) signals again. This suggests the formation of a diamagnetic intermediate, **2.2**, upon addition of 3 equivalent of NO to the solution of **2.1**. The intermediate resulted to a paramagnetic complex, **2.3** in presence of further equivalent of NO (Figure S3a).

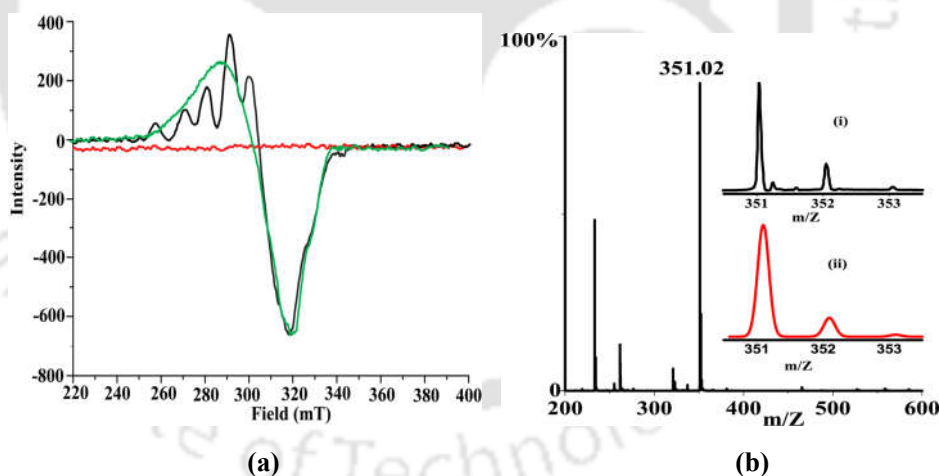


Figure S3. (a) X-band EPR spectral monitoring of the reaction of complex **2.1** (black) with NO to result, **2.2** (red) and **2.3** (green) in methanol at 77 K. (b) ESI-mass spectrum of complex **2.2** in methanol. Inset: (i) experimental and (ii) simulated isotopic distribution pattern.

¹H-NMR studies also suggested the formation of complex **2.2** via a {Co(NO)₂}¹⁰ intermediate (Figure S4). Finally, the ESI-mass spectrum also confirmed the formation of

Co(I)-dinitrosyl complex, $[(L1)Co(NO)_2] = 351.02$ (molecular ion peak)] in the reaction (Figure S3b and Scheme S1). Further, the formation of **2.3** in the reaction was confirmed by its isolation and structural characterization. The ORTEP diagram of **2.3** is shown in figure S1b.

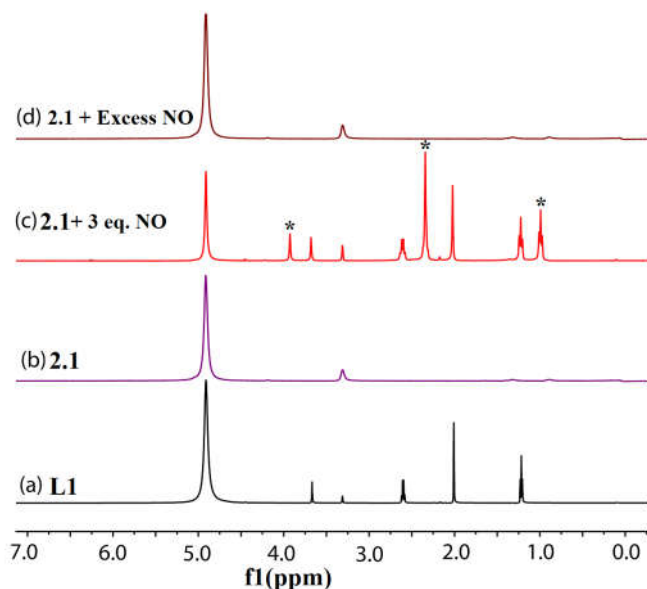
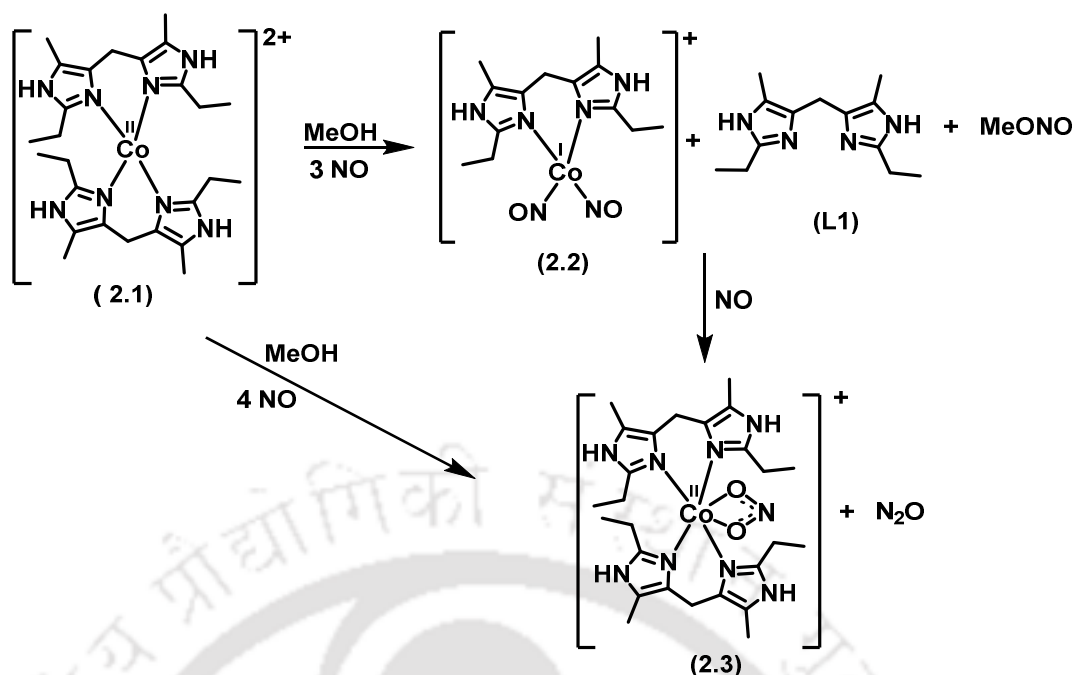


Figure S4. 1H -NMR spectrum of (a) ligand **L1** (black), (b) complex **2.1** (violet), (c) after addition of 3 equivalent of NO, **2.2+L1** and (d) after addition of excess NO, complex **2.3** in CD_3OD . The * marked signals are for complex **2.2**.

Thus, a total of 4 equivalents of NO is required to result in the formation **2.3** from **2.1** via the intermediate formation of **2.2** (Scheme S1). The reaction of **2.1** with NO can be envisaged as the reductive elimination in the first step leading to the formation of **2.2**, $[(L1)Co(NO)_2]^+$ (Scheme S1). In this case one equivalent of NO is required for the reduction of Co(II) to Co(I) and other 2 equivalents of NO form the dinitrosyl complex in subsequent step. The NO induced reduction of Co(II) was confirmed by the presence of MeONO in the reaction mixture in GC-mass analyses. In the next step, the dinitrosyl complex reacts with equivalent amount of NO to result in the nitrito complex, **2.3** (Scheme S1). It is logical to believe that the formation of NO_2^- occurs by the attack of subsequent equivalent of the NO to the $\{Co(NO)_2\}^{10}$ intermediate with concomitant release of N_2O .



Scheme S1. Reaction of complex 2.1 with NO.

Chapter 3: Reactivity of a Cobalt Nitrosyl Complex: Formation of a Peroxynitrite Intermediate and Transfer of the Nitrosyl to a Cobalt Porphyrin Complex

In this chapter the NOD reactivity of a nitrosyl of a cobalt salen complex was explored. The Co(II) complex **3.1**, [(L₂)Co] {L₂ = 6,6'-((1E,1'E)-(ethane-1,2-diyl)bis(azanylylidene))bis(methanylylidene)bis(2,4-di-*tert*-butylphenol)} have been synthesized and characterized structurally. The ORTEP diagram is shown in figure S5a. Addition of NO to the dry and degassed THF solution of the **3.1** resulted in the formation of complex **3.2**. It was isolated and characterized by spectral analyses as well as by single crystal X-ray structure determination. The ORTEP diagram is shown in figure S5b. In FT-IR spectrum complex **3.2** displayed the coordinated nitrosyl stretching frequency at 1650 cm⁻¹. Structural characterization revealed the presence of bent nitrosyl in the complex **3.2**. The reactivity of complex **3.2** towards O₂ and KO₂ has been explored. It was observed that complex **3.2** was inert towards O₂.

However, when complex **3.2** in THF solution was subjected to react with KO_2 at -40°C , it resulted in the formation of corresponding ONOO^- intermediate. Thermal instability and reactive nature precluded its isolation and spectral characterization.

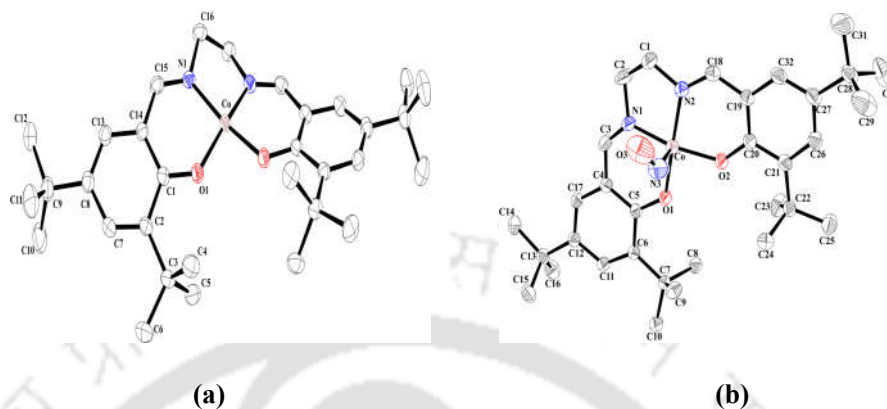
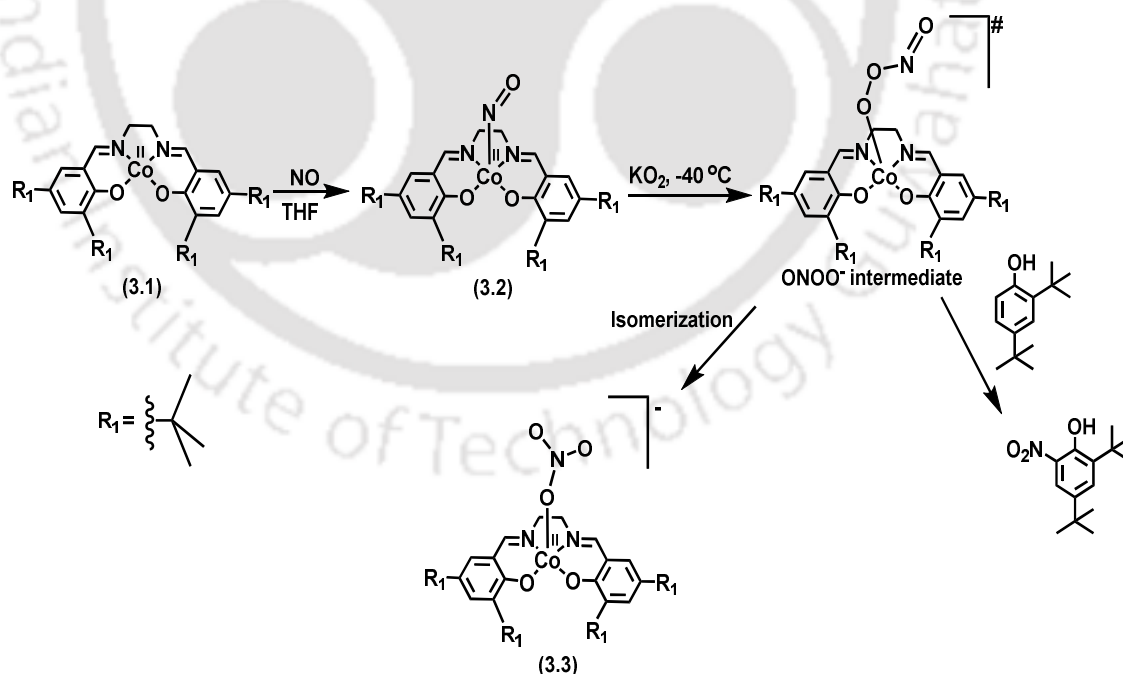


Figure S5. ORTEP diagrams of complexes (a) **3.1** and (b) **3.2**. (30% thermal ellipsoid plot. H-atoms and solvent molecules are not shown for clarity).

The formation was supported by the characteristic ring nitration reaction of 2,4-di-*tert*-butylphenol to result in 2,4-di-*tert*-butyl-6-nitrophenol (~60%) (Scheme S2).



Scheme S2. Formation of ONOO^- intermediate in THF at -40°C .

Further, isolation of corresponding NO_3^- complex, **3.3** as the isomerization product suggests the formation of the ONOO^- intermediate (Scheme S2). Complex **3.3** was characterized by elemental analyses and spectroscopic techniques. Even after several attempts, X-ray quality crystals were not obtained.

On the other hand, the NO transfer from complex **3.2** to **3.4**, $[(\text{L}3)\text{Co}] \{ \text{L}3 = 5,10,15,20\text{-tetrakis}(4'\text{-bromophenyl})\text{porphyrinate dianion} \}$ was studied (Scheme S3). When equivalent amount of **3.2** was subjected to mix with **3.4** in dry and degassed THF under Ar atmosphere, a dark red solution was formed. In UV-visible spectroscopy, the 412 nm ($\epsilon/\text{M}^{-1}\text{cm}^{-1}$, 2.01×10^5) and 527 nm ($\epsilon/\text{M}^{-1}\text{cm}^{-1}$, 2.8×10^4) bands of **3.4** were found to shift 416 nm ($\epsilon/\text{M}^{-1}\text{cm}^{-1}$, 1.85×10^5) and 540 nm ($\epsilon/\text{M}^{-1}\text{cm}^{-1}$, 2.6×10^4), respectively (Figure S6a).

In solution FT-IR spectroscopy the appearance of a new stretching at 1720 cm^{-1} suggests the formation of complex $[(\text{L}3)\text{Co}(\text{NO})]$, **3.5** (Figure S6b). It was isolated as solid and characterized *via* spectral analyses and structure determination. The ORTEP diagram is shown in figure S7b.

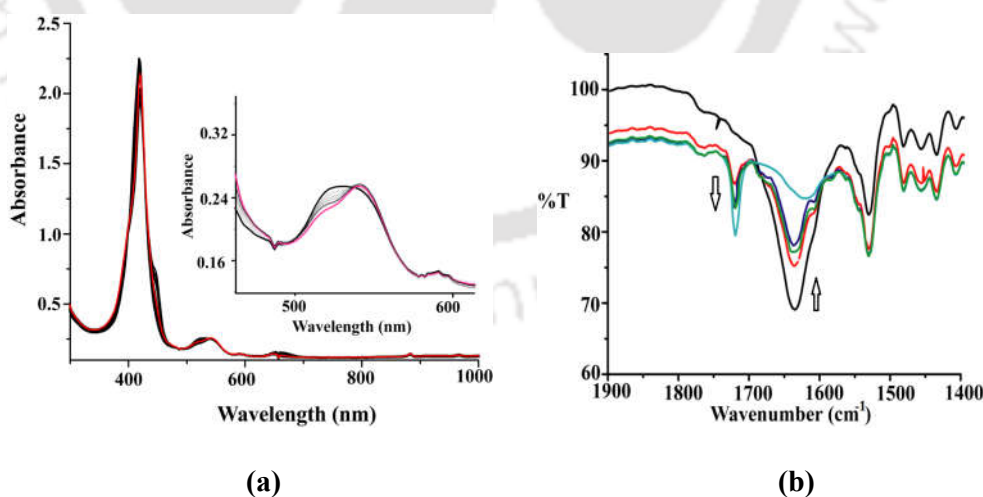


Figure S6. (a) UV-visible spectral monitoring of the reaction of complex **3.2** with **3.4** (black) to result **3.5** (red) in THF. (b) Solution FT-IR monitoring of the reaction of complex **3.2** (black) with **3.4** to result **3.5** (blue) in THF.

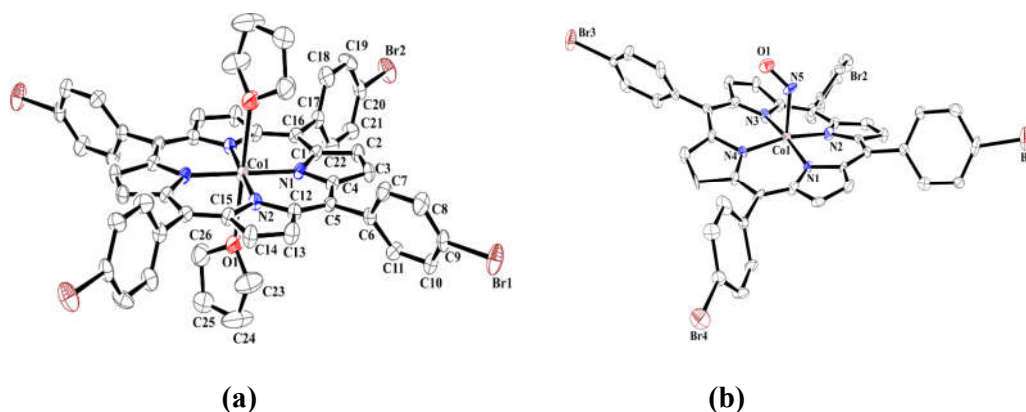
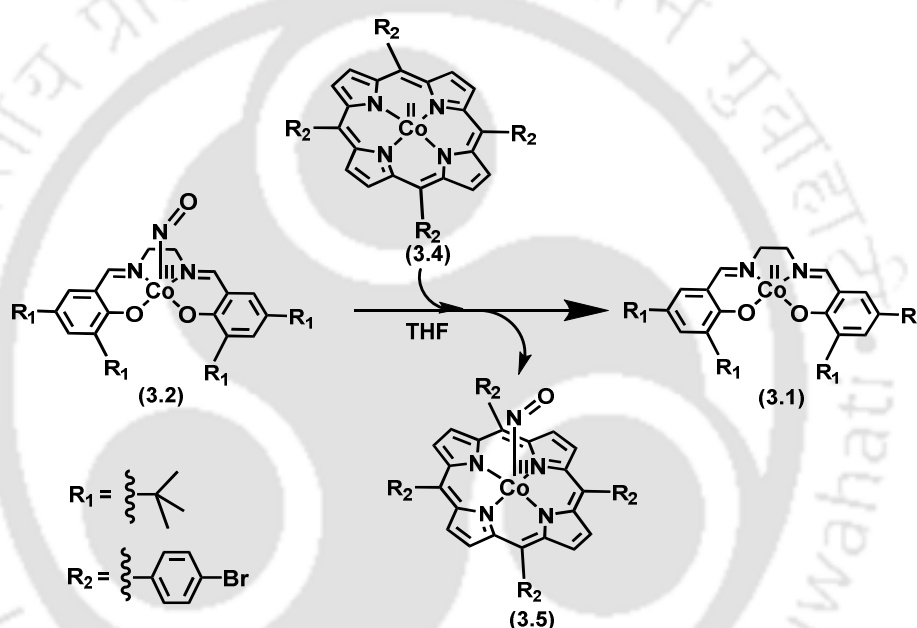


Figure S7. ORTEP diagram of complexes (a) **3.4** and (b) **3.5**. (30% thermal ellipsoid plot. H-atoms are not shown for clarity).

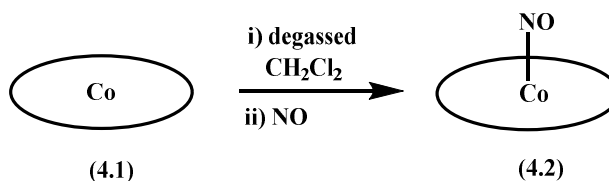


Scheme S3. NO transfer from complex **3.2** to **3.4**.

Chapter 4: Reaction of a Nitrosyl Complex of Cobalt Porphyrin with Hydrogen Peroxide: Putative Formation of Peroxynitrite Intermediate

A Co(II)-porphyrinate complex, [(L4)Co], **4.1**, {L4 = 5,10,15,20-*tetrakis*(4'-chlorophenyl) porphyrinate dianion} resulted in the corresponding nitrosyl complex, [(L4)Co(NO)], **4.2**, upon reaction with NO in dichloromethane (Scheme S4). The complex **4.2** was isolated as solid and characterized spectroscopically as well as structurally (Figure S8). In the UV-

visible spectrum, **4.2** exhibited characteristic absorption bands at 415 nm ($\epsilon/M^{-1}cm^{-1}$, 2.21×10^5) and 538 nm ($\epsilon/M^{-1}cm^{-1}$, 3.1×10^4) (Figure S9a).



Scheme S4. Synthesis of nitrosyl complex **4.2**.

Complex **4.2** was silent in the X-band EPR spectroscopy suggesting the presence of Co(III) centre having $[\text{Co}^{\text{III}}\text{-NO}]$ or $\{\text{CoNO}\}^8$ description. In the FT-IR spectrum, the NO stretching appeared at 1701 cm^{-1} (Figure S9b).

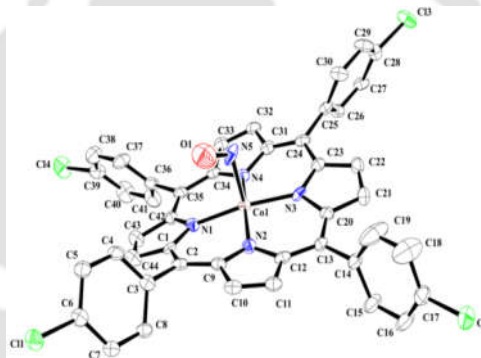


Figure S8. ORTEP diagram of complex **4.2** (30% thermal ellipsoid plot. H-atoms and solvent molecules are not shown for clarity).

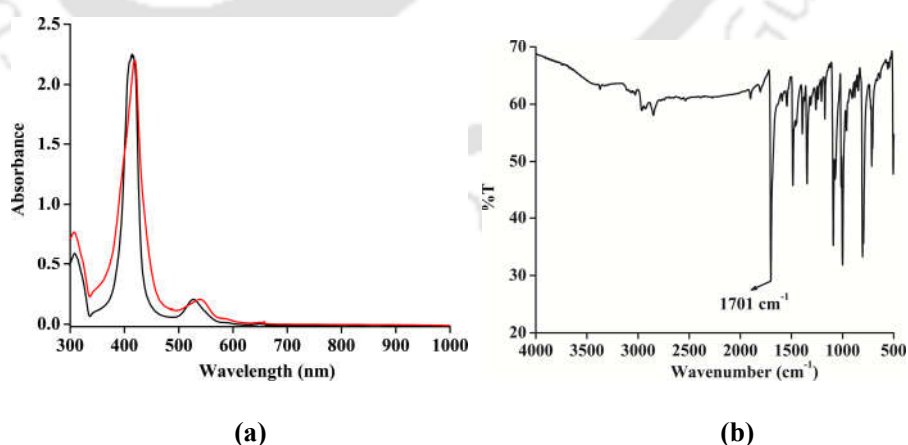
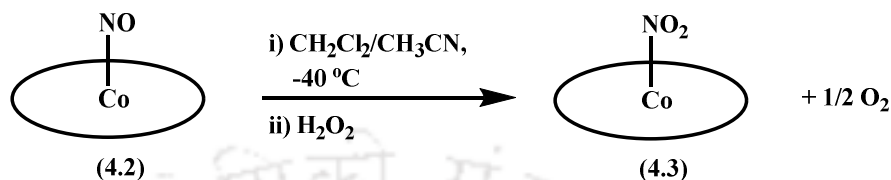


Figure S9. (a) UV-visible spectra of complexes **4.1** (black) and **4.2** (red) in dichloromethane. (b) FT-IR spectrum of complex **4.2** in KBr.

It was observed that complex **4.2** in CH_2Cl_2 solution is inert toward O_2 . However, in $\text{CH}_2\text{Cl}_2/\text{CH}_3\text{CN}$ solution it was found to react with H_2O_2 . Addition of H_2O_2 to the $\text{CH}_2\text{Cl}_2/\text{CH}_3\text{CN}$ solution of **4.2** at $-40\text{ }^\circ\text{C}$ resulted in the corresponding Co-nitrito complex, **4.3** (Scheme S5).



Scheme S5. Reaction of **4.2** with H_2O_2 in dichloromethane/acetonitrile.

In the UV-visible spectrum, the characteristic absorption bands of **4.2** at 415 and 538 nm disappeared with the formation of new ones at 430 nm ($\epsilon/\text{M}^{-1}\text{cm}^{-1}$, 2.84×10^5), 546 ($\epsilon/\text{M}^{-1}\text{cm}^{-1}$, 3.3×10^4) and 665 nm ($\epsilon/\text{M}^{-1}\text{cm}^{-1}$, 4.2×10^3), respectively (Figure S10). Spectral titration suggested that the stoichiometric ratio of complex **4.2** with H_2O_2 is 1:1. Complex **4.3** was isolated and characterized as the corresponding Co^{III} -nitrito complex.

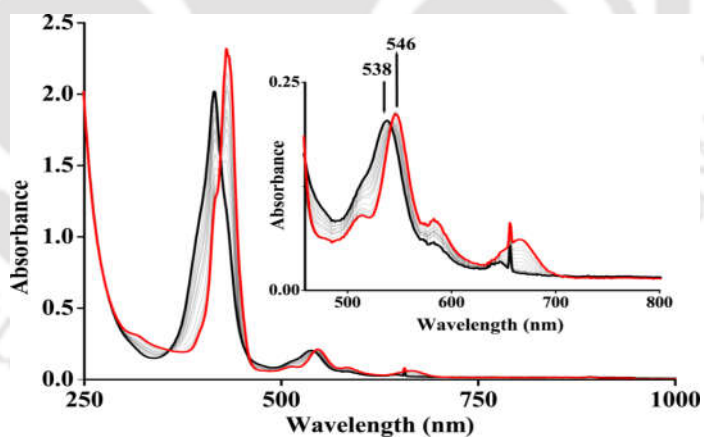
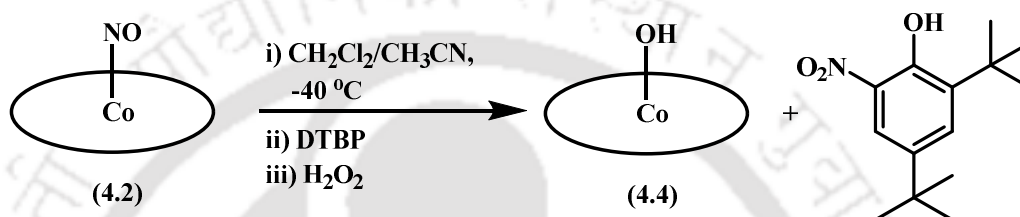


Figure S10. UV-visible spectral monitoring of the reaction of complex **4.2** (black) with H_2O_2 to result in **4.3** (red) at $-40\text{ }^\circ\text{C}$.

The ESI mass spectrum of **4.3** displayed the molecular ion peak ($\text{M}+1$) at m/z , 854.99 (calcd. 856.08). In the FT-IR spectrum, the stretching frequency at 1270 cm^{-1} is assignable

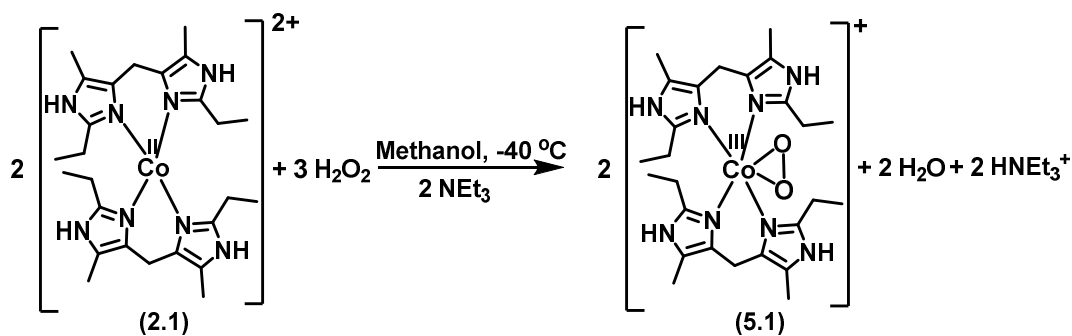
to the NO_2^- stretching. The formation of cobalt-nitrito complex is expected to be accompanied by the release of O_2 (Scheme S5). The formation of O_2 in the reaction was confirmed by its detection in the headspace gas of the reaction flask using alkaline pyrogallol test. While we do not have direct spectroscopic evidence of formation of Co-(ONOO⁻) intermediate, we sought chemical evidence for the postulated species. Effective nitration (*ca.* 50%) and corresponding Co-hydroxo product, **4.4** (*ca.* 70%) were observed when DTBP was added to complex **4.2** before the addition of H_2O_2 (Scheme S6).



Scheme S6. Phenol ring nitration by **4.2** in the presence of H_2O_2 .

Chapter 5: Reaction of a Co(III)-Peroxo Complex and NO: Formation of a Putative Peroxynitrite Intermediate

The addition of H_2O_2 in presence of NEt_3 to the methanol solution of complex **2.1** at $-40\text{ }^\circ\text{C}$ afforded Co(III)-peroxo intermediate, $[(\text{L}1)_2\text{Co}(\text{O})_2]^+$, **5.1** (Scheme S7). It displayed absorption at 452 nm ($\epsilon/\text{M}^{-1}\text{cm}^{-1}$, 890) in the UV-visible spectrum (Figure S11a). The O-O stretching for the Co(III)-peroxo intermediate appeared at 874 cm^{-1} in FT-IR spectrum (Figure S11b). As expected for a Co(III)-peroxo species, the intermediate was silent in X-band EPR study (Figure S12a). The ESI-mass spectrum of the intermediate was sensitive towards ^{18}O -labelling and found to appear at m/z 559.41 when $\text{H}_2^{18}\text{O}_2$ was used (Figure S12b). The addition of NO to the freshly generated complex **5.1** in methanol at $-40\text{ }^\circ\text{C}$ followed by warming at room temperature resulted in the formation of complex, $[(\text{L}1)_2\text{Co}(\text{NO}_3)]\text{Cl}$, **5.2**. The ORTEP diagram of **5.2** is shown in figure S13.



Scheme S7. Reaction of complex **2.1** with H_2O_2 in methanol at -40°C .

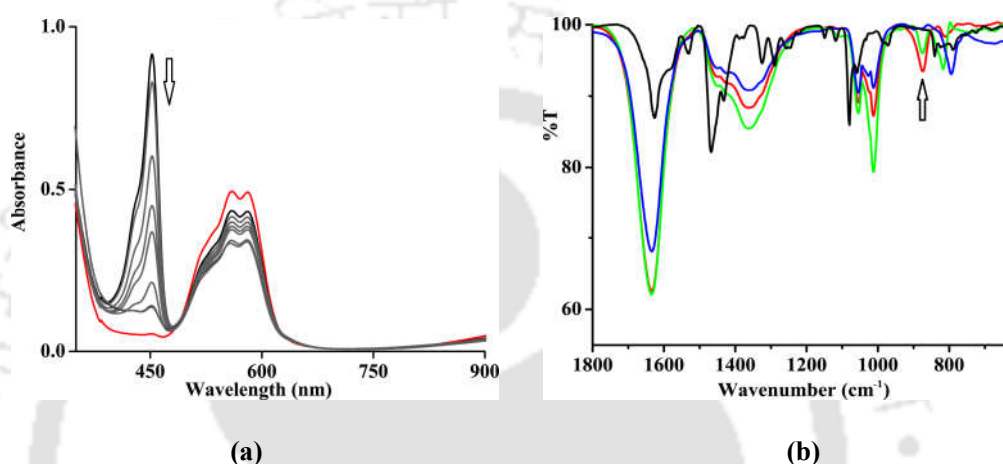


Figure S11. (a) UV-visible spectra of complex **2.1** (red), after addition of H_2O_2 {complex **5.1**} (grey), in methanol at -40°C . (b) Solution FT-IR spectra of complexes **2.1** (black), **5.1** (red) in methanol. Green and blue traces represent the gradual decomposition of **5.1** at room temperature.

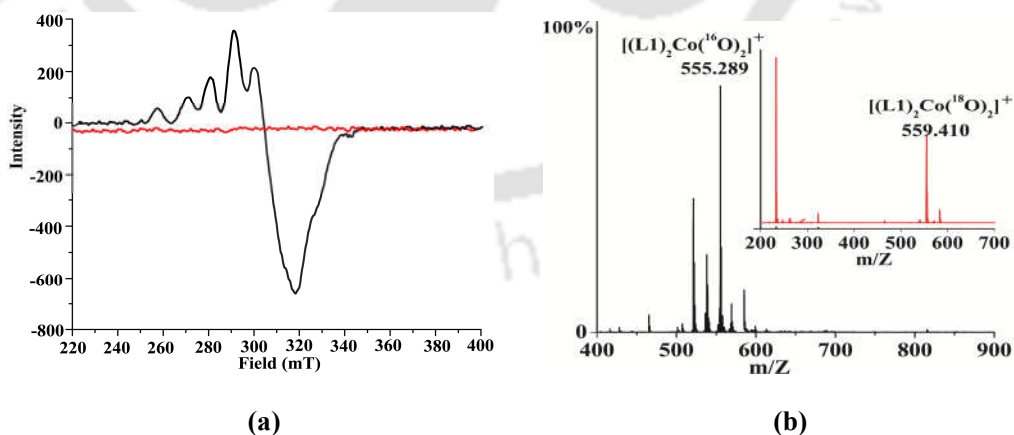


Figure S12. (a) X-band EPR spectra of complexes **2.1** (black) and **5.1** (red) in methanol at 77 K. (b) ESI-Mass spectra of complex **5.1** obtained from the reaction of **2.1** and $\text{H}_2^{16}\text{O}_2$ in methanol. Inset shows the same when the reaction was carried out with $\text{H}_2^{18}\text{O}_2$.

The crystal structure revealed that the Co(II) center is bonded with two units of the ligand and a nitrate (NO_3^-) anion in a distorted octahedral geometry (Figure S13).

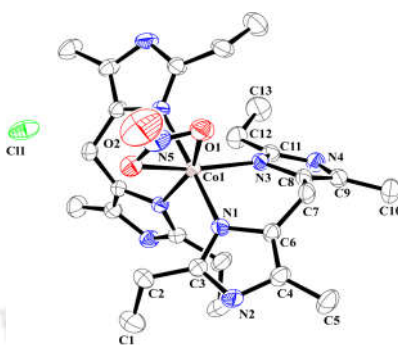
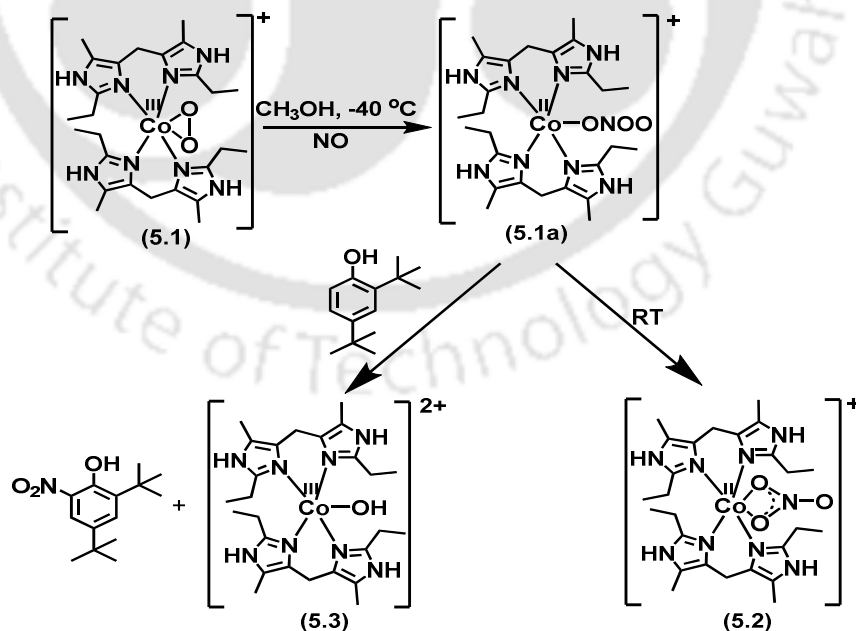


Figure S13. ORTEP diagram of complex **5.2** (30% thermal ellipsoid plot. H-atoms and solvent molecule are not shown for clarity).

The formation of **5.2** can be envisaged through the formation of a putative ONOO⁻ intermediate (**5.1a**) in the course of the reaction (Scheme S8). When DTBP was added before the addition of NO to the solution of **5.1**, an appreciable nitration (*ca.* 60%) was observed. Work-up of the reaction mixture revealed the formation of the corresponding Co-hydroxo product, **5.3** (*ca.* 70%).



Scheme S8. Formation of ONOO⁻ intermediate in methanol at $-40\text{ }^\circ\text{C}$.

References

- (1) (a) Culotta, E.; Koshland, D. E. Jr. *Science* **1992**, *258*, 1862. (b) Moncada, S.; Palmer, R. M. J.; Higgs, E. A. *Pharmacol. Rev.* **1991**, *43*, 109.
- (2) (a) Furchgott, R. F. *Angew. Chem. Int. Ed.* **1999**, *38*, 1870. (b) Ignarro, L. J.; Buga, G. M.; Wood, K. S.; Byrns, R. E.; Chaudhuri, G. *Proc. Natl. Acad. Sci. U. S. A.* **1987**, *84*, 9265. (c) Palmer, R. M. J.; Ferrige, A. G.; Moncada, S. *Nature* **1987**, *327*, 524.
- (3) (a) Ignarro, L. J. *Nitric Oxide: Biology and Pathobiology* Ed. Academic Press, San Diego, CA, **2000**. (b) Richter-Addo, G. B.; Legzdins, P. *Metal Nitrosyls* Oxford University Press, New York, **1992**. (c) Butler, A. R.; Williams, D. *Chem. Soc. Rev.* **1993**, 233. (d) Feelisch, M.; Stamler, J. S. *Methods in Nitric Oxide Research*, John Wiley and Sons, Chichester, England, **1996**. (e) Jia, L.; Bonaventura, C.; Bonaventura J.; Stamler, J. S. *Nature* **1996**, *380*, 221.
- (4) Fang, F. C. *Nitric Oxide and Infection* Ed. Kluwer Academic/ Plenum Publishers, New York, **1999**.
- (5) (a) Radi, R. *Proc. Natl. Acad. Sci. U. S. A.* **2004**, *101*, 4003. (b) Tran, N. G.; Kalyvas, H.; Skodje, K. M.; Hayashi, T.; Moënne-Loccoz, P.; Callan, P. E.; Shearer, J.; Kirschenbaum, L. J.; Kim, E. *J. Am. Chem. Soc.* **2011**, *133*, 1184.
- (6) (a) Goldstein, S.; Lind, J.; Merenyi, G. *Chem. Rev.* **2005**, *105*, 2457. (b) Blough, N. V.; Zafiriou, O. C. *Inorg. Chem.* **1985**, *24*, 3502. (c) Nauser, T.; Koppenol, W. H. *J. Phys. Chem. A* **2002**, *106*, 4084. (d) Speelman, A. L.; Lehnert, N. *Acc. Chem. Res.* **2014**, *47*, 1106. (e) Fry, N. L.; Mascharak, P. K. *Acc. Chem. Res.* **2011**, *44*, 289.
- (7) Qiao, L.; Lu, Y.; Liu, B.; Girault, H. H. *J. Am. Chem. Soc.* **2011**, *133*, 19823.

- (8) Vilet, A.; Eiserich, J. P.; Halliwell, B.; Cross, C. E. *J. Biol. Chem.* **1997**, *272*, 7617.
- (9) (a) Pfeiffer, S.; Gorren, A. C. F.; Schmidt, K.; Werner, E. R.; Hansert, B.; Bohle, D. S.; Mayer, B. *J. Biol. Chem.* **1997**, *272*, 3465. (b) Coddington, J. W.; Hurst, J. K.; Lyman, S. V. *J. Am. Chem. Soc.* **1999**, *121*, 2438. (c) Koppenol, W. H.; Bounds, P. L.; Nauser, T.; Kissner, R.; Rügger, H. *Dalton Trans.* **2012**, *41*, 13779.
- (10) (a) Schopfer, M. P.; Wang, J.; Karlin, K. D. *Inorg. Chem.* **2010**, *49*, 6267. (b) Ouellet, H.; Ouellet, Y.; Richard, C.; Labarre, M.; Wittenberg, B.; Wittenberg, J.; Guertin, M. *Proc. Natl. Acad. Sci. U. S. A.* **2002**, *99*, 5902. (c) Gardner, P. R.; Gardner, A. M.; Martin, L. A.; Salzman, A. L. *Proc. Natl. Acad. Sci. U. S. A.* **1998**, *95*, 10378. (d) Ford, P. C.; Lorkovic, I. M. *Chem. Rev.* **2002**, *102*, 993. (e) Gardner, P. R.; Gardner, A. M.; Brashear, W. T.; Suzuki, T.; Hvitved, A. N.; Setchell, K. D. R.; Olson, J. S. *J. Inorg. Biochem.* **2006**, *100*, 542.
- (11) Kurtikyan, T. S.; Ford, P. C. *Chem. Commun.* **2010**, *46*, 8570.
- (12) (a) Clarkson, S. G.; Basolo F. *J. Chem. Soc. Chem. Commun.* **1972**, *119*, 670. (b) Clarkson, S. G.; Basolo F. *Inorg. Chem.* **1973**, *12*, 1528.
- (13) Skodje, K. M.; Williard, P. G.; Kim, E. *Dalton Trans.* **2012**, *41*, 7849.
- (14) Park, G. Y.; Deepalatha, S.; Puiu, S. C.; Lee, D.-H.; Mondal, B.; Sarjeant, A. A. N.; Del Rio, D.; Pau, M. Y. M.; Solomon, E. I.; Karlin, K. D. *J. Biol. Inorg. Chem.* **2009**, *14*, 1301.
- (15) (a) Yokoyama, A.; Han, J. E.; Cho, J.; Kubo, M.; Ogura, T.; Siegler, M. A.; Karlin, K. D.; Nam, W. *J. Am. Chem. Soc.* **2012**, *134*, 15269. (b) Yokoyama, A.; Cho, K. B.; Karlin, K. D.; Nam, W. *J. Am. Chem. Soc.* **2013**, *135*, 14900.
- (16) Yokoyama, A.; Han, J. E.; Karlin, K. D.; Nam, W. *Chem. Commun.* **2014**, *50*, 1742.

- (17) Kalita, A.; Kumar, P.; Mondal, B. *Chem. Commun.* **2012**, 48, 4636.
- (18) Kalita, A.; Deka, R. C.; Mondal, B. *Inorg. Chem.* **2013**, 52, 10897.
- (19) Kumar, P.; Lee, Y.-M.; Hu, L.; Chen, J.; Park, Y. J.; Yao, J.; Chen, H.; Karlin, K. D.; Nam, W. *J. Am. Chem. Soc.* **2016**, 138, 7753.
- (20) Mondoro, T. H.; Shafer, B. C.; Vostal, J. G. *Free Radical Biol. Med.* **1997**, 22, 1055.
- (21) Kong, S. K.; Yim, M. B.; Stadtman, E. R.; Chock, P. B. *Proc. Natl. Acad. Sci. U. S. A.* **1996**, 93, 3377.
- (22) Schopfer, M. P.; Mondal, B.; Lee, D.-H.; Sarjeant, A. A. N.; Karlin, K. D. *J. Am. Chem. Soc.* **2009**, 131, 11304.

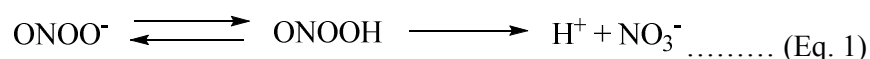


Chapter 1

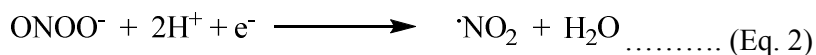
Introduction

1.1 General aspect of peroxynitrite

Nitric oxide (NO) is an important small molecule known as ubiquitous intercellular messenger in all vertebrates, modulating blood flow, thrombosis, and many more neural activities. Only a small concentration of NO is required for its function.¹⁻³ However, over production of it has a detrimental effect due to the reaction of NO with superoxide (O_2^-) to form the peroxynitrite ($ONOO^-$, PN).⁴ Under physiological conditions, the concentration of O_2^- is regulated by superoxide dismutase (SOD) enzymes and NO is present in pM to nM concentrations. Enhanced release of NO results in the reaction with O_2^- at a diffusion-limited rate to form $ONOO^-$.^{5,6} Alternatively, $ONOO^-$ can be generated by the reaction of hydrogen peroxide (H_2O_2) and nitrite (NO_2^-) in the presence of the peroxidase enzymes.^{7,8} Peroxynitrite induces oxidation and nitrosation of biomolecules. It is also known to play roles in diverse chemical modifications to lipids, proteins and nucleic acids.^{5,9,10} For example, Beckman *et al.* showed $ONOO^-$ as a far more effective means of producing hydroxyl radical than the widely accepted reaction of reduced iron with H_2O_2 (known as the Fenton reaction or the iron-catalyzed Haber-Weiss reaction).¹¹ Peroxynitrite, being a strong oxidant can react with electron-rich groups, such as sulfhydryls¹², iron-sulfur centers¹³, zinc-thiolates¹⁴ and the active site of sulfhydryl in tyrosine phosphatases.¹⁵⁻¹⁷ At near neutral pH, $ONOO^-$ rapidly decomposes ($t_{1/2} < 1s$) to peroxynitrous acid ($ONOOH$), which has pKa of 6.75 at 37 °C. It is unstable and rapidly isomerizes to nitrate (NO_3^-) (Eq. 1).¹⁸

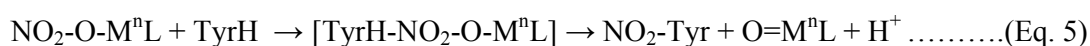
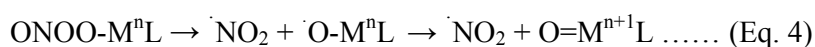


ONOOH is strong oxidant in reactions of both one and two electron mechanisms (Eq. 2 & 3). In the presence of biological targets these reactions lead to a range of oxidized products. ONOO⁻ also reacts rapidly with CO₂ to form the nitroso peroxycarbonate anion.¹⁹



The primary effect of ONOO⁻ on proteins is the nitration of the tyrosine residues.^{20,21} Nitrated tyrosine residues in peptides cannot be phosphorylated by tyrosine kinases in vitro. Thus, nitration of proteins can prevent or modulate cellular signal transduction, which requires tyrosine phosphorylation.^{22,23} The transition metal ions have been found to catalyse the reaction of ONOO⁻, in either one or two electron redox processes.²⁴ Nitric Oxide Deoxygenases enzymes (NODs) is known to control the over production of NO in vivo by converting it to the biologically benign NO₃⁻. This reaction is also believed to proceed through a ONOO⁻ intermediate.⁴

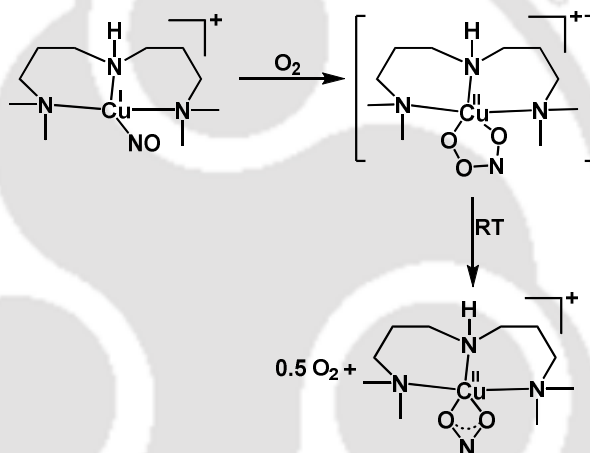
Metal-peroxynitrite complexes decompose readily to form either metal nitrate (isomerisation product) or metal-oxo complex and NO₂ (Eq. 4). In both cases ONOO⁻ appears to bring about tyrosine nitration. The presence of nitrated tyrosine residues has been suggested as a marker for ONOO⁻ activity. The formation of NO₂ has been proposed as an essential step in tyrosine nitration by ONOO⁻. The NO₂ itself could attack tyrosine as a two-electron acceptor to yield a nitroarenium ion intermediate and gives a nitration product (Eq. 5).^{25,26}



1.2 Formation of metal peroxynitrite

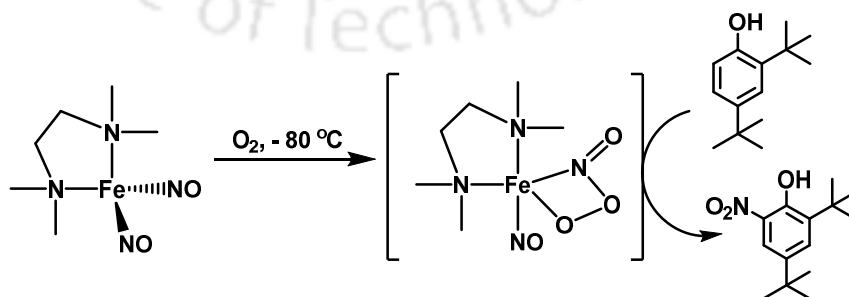
1.2.1 Reaction of metal nitrosyls with reactive oxygen species

Clarkson and Basolo reported the involvement of a few cobalt-nitrosyl complexes with O_2 in the formation of corresponding cobalt-peroxynitrite intermediate which decomposes to yield corresponding cobalt nitrite product.²⁷ Karlin group have reported that the reaction of NO with a Cu(I) complex possessing a tridentate alkylamine ligand gives a Cu(I)-(NO) adduct, which when exposed to O_2 generates a Cu(II)-(ONOO⁻) species. This undergoes thermal decomposition to produce a Cu(II)-(NO₂⁻) complex and 0.5 mol equivalent of O_2 (Scheme 1.1).²⁸



Scheme 1.1. Reaction of Cu(I)-nitrosyl complex with O_2 to form Cu(II)-(ONOO⁻) intermediate.

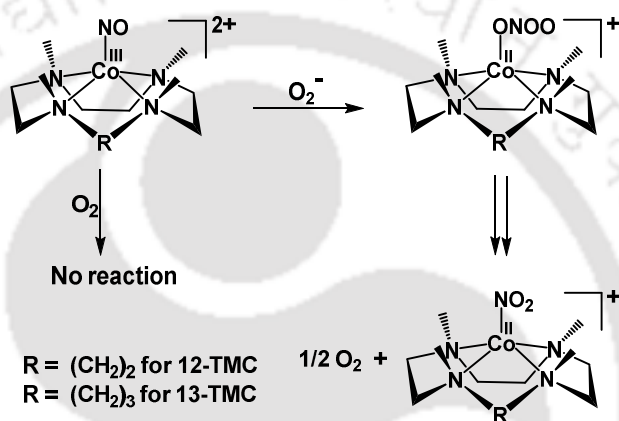
Kim *et al.* reported a N-bound $\{Fe(NO)_2\}^{10}$ DNIC complex, $[(TMEDA)Fe(NO)_2]$ {TMEDA = *N,N,N',N'*-tetramethylethylenediamine} which reacts with O_2 and acts as a



Scheme 1.2. Reaction of Fe-DNIC with O_2 to form Fe-(ONOO⁻) intermediate.

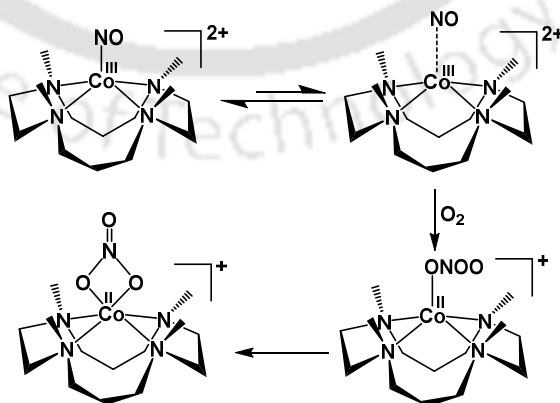
nitrating agent that converts 2,4-di-*tert*-butylphenol to 2,4-di-*tert*-butyl-6-nitrophenol via the formation of a ONOO⁻ intermediate [(TMEDA)Fe(NO)(ONOO)] which is stable at -80 °C (Scheme 1.2).²⁹

Recently Nam group have reported two Co(III)-nitrosyl complexes bearing N-tetramethylated cyclam (TMC) ligands, [(12-TMC)Co(NO)]²⁺ and [(13-TMC)Co(NO)]²⁺ which do not react with O₂; but reacts with O₂⁻ to form the corresponding Co(II)-nitrito complexes and O₂ via a presumed Co(II)-(ONOO⁻) intermediate (Scheme 1.3).³⁰



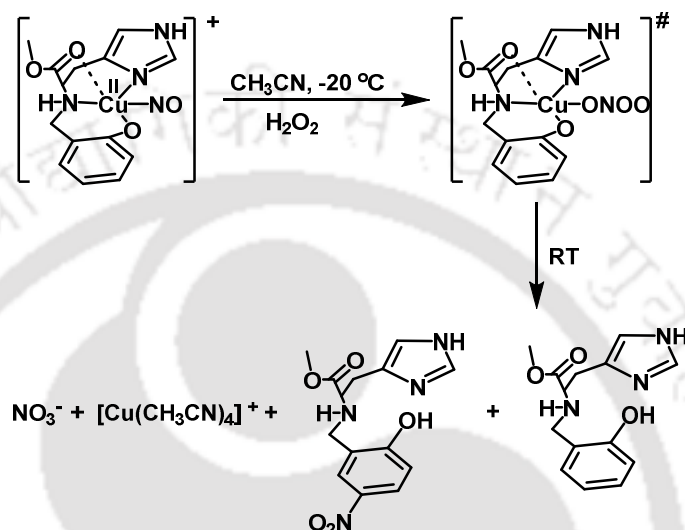
Scheme 1.3. Reaction of Co(III)-nitrosyl with O₂⁻ to form Co(II)-(ONOO⁻) intermediate.

Whereas the Co(III)-nitrosyl complex bearing 14-TMC ligand, [(14-TMC)Co(NO)]²⁺ on dioxygenation produces [(14-TMC)Co(NO₃)]⁺. The reaction is proposed to occur via the formation of a putative Co(II)-(ONOO⁻) intermediate (Scheme 1.4).³¹



Scheme 1.4. Reaction of Co(III)-nitrosyl with O₂ to form Co(II)-(ONOO⁻) intermediate.

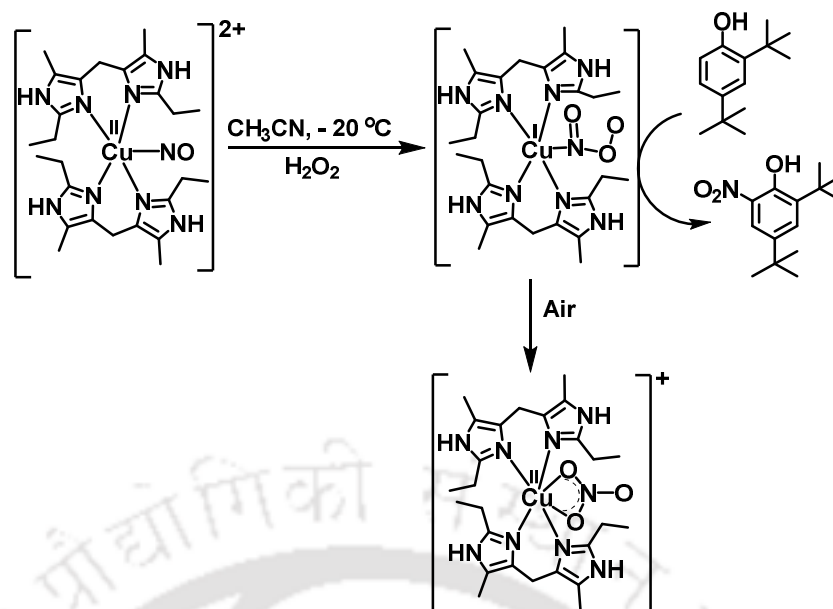
Our laboratory has been actively involved in studying the formation and decomposition pathways of metal peroxynitrite. In this regard, a Cu(II)-nitrosyl complex with histidine-derived ligand, methyl 2-(2-hydroxybenzylamino)-3-(1*H*-imidazol-5-yl)propanoate) have been reported.³² In acetonitrile medium, the presence of H₂O₂ resulted in the formation of the corresponding Cu(I)-(ONOO⁻) (Scheme 1.5).



Scheme 1.5. Reaction of Cu(II)-nitrosyl with H₂O₂ to form Cu(I)-(ONOO⁻) intermediate.

The formation of ONOO⁻ species is confirmed by characteristic phenol ring nitration reaction which resembles the tyrosine nitration in biological systems. Further, isolation of the nitrate (NO₃⁻) as the decomposition product from nitrosyl complex at room temperature also supports the involvement of ONOO⁻ (Scheme 1.5).

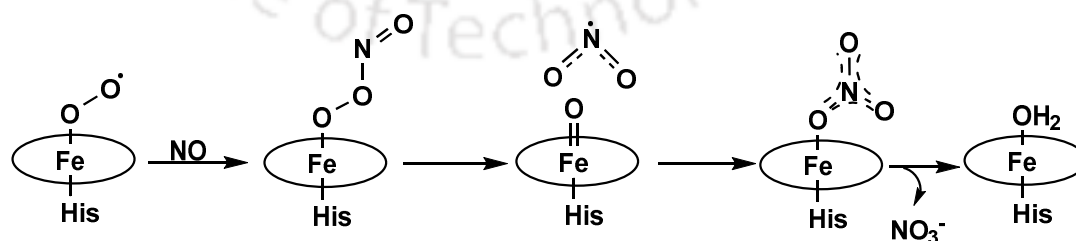
Another Cu(II)-nitrosyl complex with bis(2-ethyl-4-methyl-imidazol-5-yl)methane ligand has been found to react with H₂O₂ at -20 °C in acetonitrile to result in the formation of the Cu(I)-nitrite *via* putative formation of the corresponding Cu(I)-peroxynitrite intermediate. The formation of the ONOO⁻ intermediate also confirmed by its characteristic phenol ring nitration (Scheme 1.6).³³



Scheme 1.6. Reaction of Cu(II)-nitrosyl with H_2O_2 to form Cu(I)-(ONOO⁻).

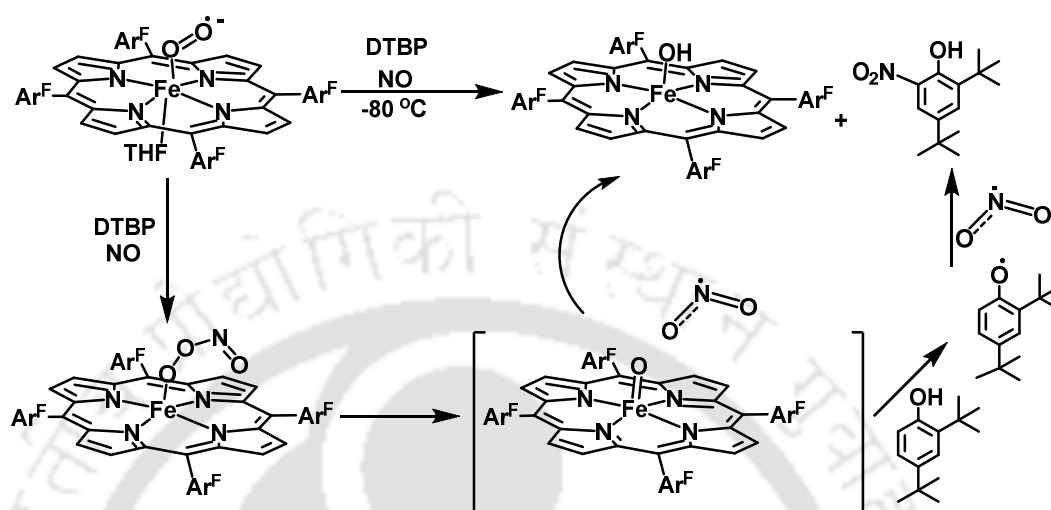
1.2.2 Reaction of metal-oxygenated species with NO

Alternatively, there are examples in literatures which demonstrate the in situ generation of ONOO⁻ in the reaction of reactive metal-dioxygen complexes with NO. Hemoglobin (Hb) and myoglobin (Mb) exhibit NODs activity.³⁴ NO reacts with oxyHb [$\text{Hb}(\text{Fe}^{\text{III}}-\text{O}_2^-)$], oxyMb [$\text{Mb}(\text{Fe}^{\text{III}}-\text{O}_2^-)$] and oxyflavo-hemoglobin [$\text{flavoHb}(\text{Fe}^{\text{III}}-\text{O}_2^-)$] and gives nitrate product.³⁵ The generally stated mechanism of NODs involves direct reaction of the Fe(III)-(O₂⁻) oxy complex with NO, giving a ONOO⁻ intermediate. Subsequent homolytic O-O bond cleavage produces an oxo-ferryl ($\text{Fe}^{\text{IV}}=\text{O}$) species and NO₂; the latter attacks the ferryl O-atom to produce a N-O bond giving nitrate (Scheme 1.7).³⁶



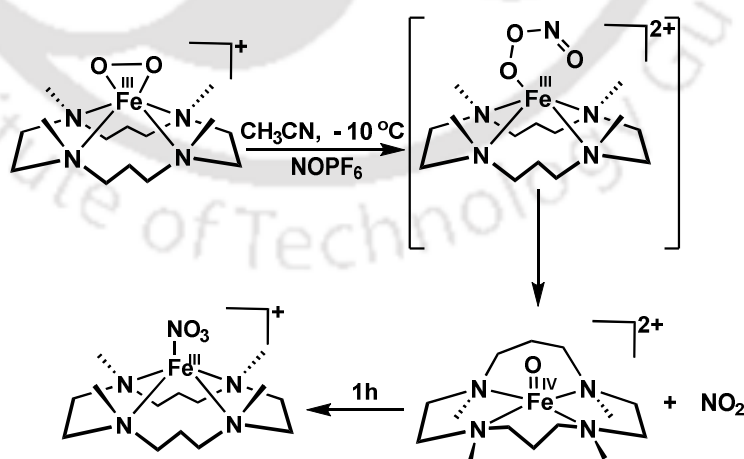
Scheme 1.7. Reaction of Fe(III)-superoxo with NO to form Fe(III)-(ONOO⁻) intermediate.

Karlin *et al.* reported that NO reacts with $[(\text{thf})(\text{F}_8)\text{Fe}^{\text{III}}-(\text{O}_2^-)]$ which can lead to the formation of $[(\text{F}_8)\text{Fe}^{\text{III}}-(\text{NO}_3^-)]$.³⁷ Effective nitration was observed when DTBP (≥ 1 equiv) was added prior to the addition of NO (Scheme 1.8).



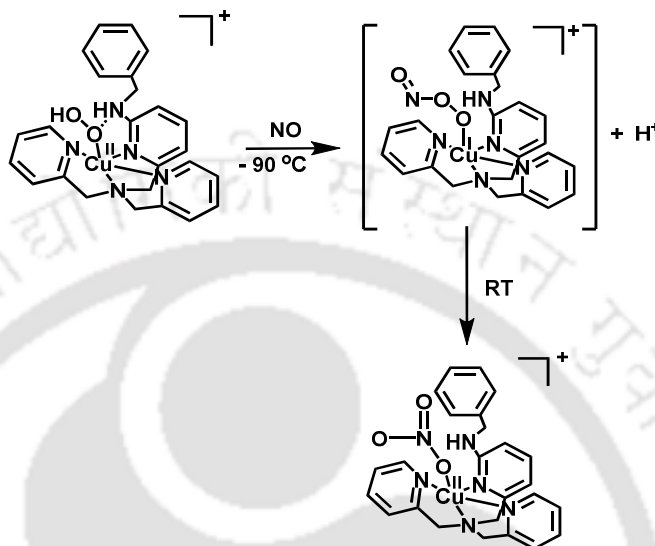
Scheme 1.8. Reaction of Fe(III)-superoxo with NO to form Fe(III)-(ONOO⁻) intermediate.

Nam group describes the reaction of a (14-TMC)Fe(III)-peroxo complex with NO⁺ to produce an (14-TMC)Fe(IV)-oxo complex and NO₂ *via* the formation of a putative Fe(III)-(ONOO⁻) species which undergoes O–O bond homolysis. Finally the reaction mixture leads to the formation of a (14-TMC)Fe(III)-nitrate complex (Scheme 1.9).³⁸



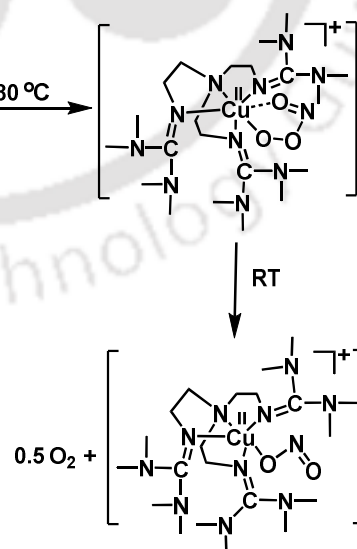
Scheme 1.9. Reaction of Fe(III)-peroxo with NO to form Fe(III)-(ONOO⁻) intermediate.

The reaction of a Cu(II)-hydroperoxo species with NO resulted in the generation of ONOO⁻. The copper-hydroperoxo complex, [(BA)Cu(OOH)]⁺ (BA, a tetradentate N₄ ligand possessing a pendant -N(H)CH₂C₆H₅ group), reacts with excess NO in acetone at -90 °C to form a Cu(II)-nitrate *via* an intermediacy of a ONOO⁻ species (Scheme 1.10).³⁹



Scheme 1.10. Reaction of Cu(II)-hydroperoxo with NO to form Cu(I)-(ONOO⁻) intermediate.

The same group reported a discrete Cu(II)-(ONOO⁻) complex, [(TMG₃tren)Cu(OONO)]⁺ (TMG₃tren = 1,1,1-tris{2-[N₂-(1,1,3,3-tetramethylguanidino)]ethyl}amine)

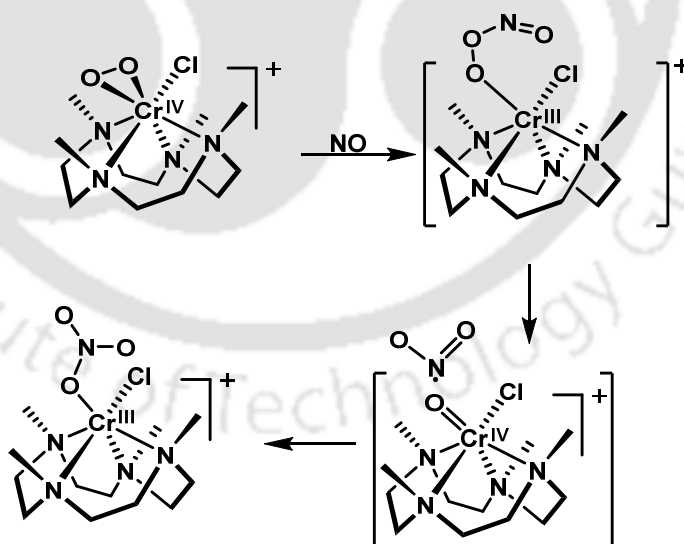


Scheme 1.11. Reaction of Cu(II)-superoxo with NO to form Cu(II)-(ONOO⁻).

from the reaction of NO with a Cu(II)-O₂ adduct, [(TMG₃tren)Cu(O₂)]⁺ which finally resulted in a nitrite complex, [(TMG₃tren)Cu(ONO)]⁺ and O₂ (Scheme 1.11).⁴⁰

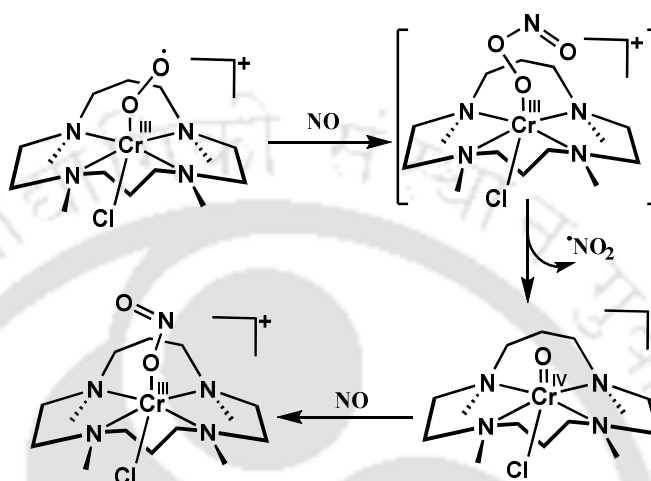
Kurtikyan group reported an oxy-coboglobin model compounds (Py)Co(Por)(O₂) [por = meso-tetraphenyl- and meso-tetra-*p*-tolylporphyrinato dianions], which react with NO at low temperature to form a six coordinated nitrato complex (Py)Co(Por)(η¹-ONO₂) *via* initial formation of a six-coordinate ONOO⁻ intermediate (Py)Co(Por)(η¹-OONO).⁴¹ The nitrato complex, (Py)Co(Por)(η¹-ONO₂), is also not thermally stable and decomposes to give NO₃⁻ and oxidized cationic complex, (Py)₂Co(Por). However, in the presence of excess NO, the nitro-pyridine complexes (Py)Co(Por)(NO₂) are predominantly formed, indicating the oxo-transfer reactivity of (Py)Co(Por)(η¹-ONO₂) with regard to NO.

A stable peroxo complex, [(12-TMC)Cr(O₂)(Cl)]⁺ was reported to react with NO to form a Cr-nitrato complex *via* the formation of a Cr(III)-(ONOO⁻) intermediate. A Cr(IV)-oxo species and NO₂ radical was formed during the decomposition of ONOO⁻ intermediate (scheme 1.12).⁴²



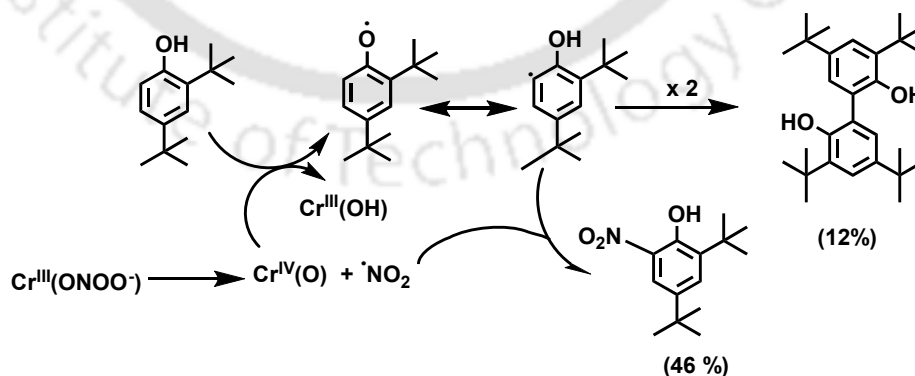
Scheme 1.12. Reaction of Cr(IV)-peroxo with NO to form Cr(III)-(ONOO⁻) intermediate.

The reaction of an end-on Cr(III)-superoxo complex bearing a 14-membered tetraazamacrocyclic TMC ligand, $[(14\text{-TMC})\text{Cr}(\text{O}_2)(\text{Cl})]^+$, with NO resulted in the generation of a stable Cr(IV)-oxo species, $[(14\text{-TMC})\text{Cr}(\text{O})(\text{Cl})]^+$, via the formation of a Cr(III)-peroxynitrite intermediate and homolytic O-O bond cleavage of the peroxynitrite ligand (Scheme 1.13).



Scheme 1.13. Reaction of Cr(III)-superoxo with NO to form Cr(III)-(ONOO⁻) intermediate.

The formation of a Cr(III)-hydroxo complex ($[(14\text{-TMC})\text{Cr}(\text{OH})(\text{Cl})]^+$) as well as 40% of nitrated DTBP (2,4-di-*tert*-butyl-6-nitrophenol, nitro-DTBP) and 12% of oxidatively dimerized DTBP (2,2'-dihydroxy-3,3',5,5'-tetra-*tert*-butylbiphenol, DTBP dimer) product was observed via radical mechanism (Scheme 1.14).^{43,44}



Scheme 1.14. Decomposition pathways of ONOO⁻ intermediate in presence of 2,4-DTBP.

1.3 Scope of the thesis

The present thesis is originated from our interest to study the formation of cobalt peroxy-nitrite intermediates by the reaction of cobalt-nitrosyls with $\text{H}_2\text{O}_2/\text{O}_2^-$ or a cobalt-peroxo complex with NO. The second chapter describes the reaction of a Co(II) complex with NO and the formation of a Co-nitrite complex *via* a thermally unstable Co-dinitrosyl intermediate. The third chapter discusses the reactivity of a nitrosyl complex of cobalt with salen ligand. The complex was found to react with KO_2 to result in the formation of a Co-nitrate complex *via* a putative Co-(ONOO⁻) intermediate. In addition, the bound NO group of the nitrosyl complex was transferred to a cobalt porphyrinate. The fourth chapter deals with the reaction of a nitrosyl complex of cobalt porphyrinate with H_2O_2 to result in the cobalt nitrite complex through a putative formation of Co-(ONOO⁻) intermediate. The last chapter describes the formation of a Co-(ONOO⁻) intermediate in the reaction of a cobalt-peroxo complex with NO leading to the formation of a cobalt-nitrate complex.

1.4 References

- (1) (a) Culotta, E.; Koshland, D. E. Jr. *Science* **1992**, 258, 1862. (b) Moncada, S.; Palmer, R. M. J.; Higgs, E. A. *Pharmacol. Rev.* **1991**, 43, 109.
- (2) (a) Furchgott, R. F. *Angew. Chem. Int. Ed.* **1999**, 38, 1870. (b) Ignarro, L. J.; Buga, G. M.; Wood, K. S.; Byrns, R. E.; Chaudhuri, G. *Proc. Natl. Acad. Sci. U. S. A.* **1987**, 84, 9265. (c) Palmer, R. M. J.; Ferrige, A. G.; Moncada, S. *Nature* **1987**, 327, 524.
- (3) (a) Ignarro, L. J. *Nitric Oxide: Biology and Pathobiology* Ed. Academic Press, San Diego, CA, **2000**. (b) Richter-Addo, G. B.; Legzdins, P. *Metal Nitrosyls* Oxford University Press, New York, **1992**. (c) Butler, A. R.; Williams, D. *Chem. Soc. Rev.* **1993**, 233. (d) Feelisch, M.; Stamler, J. S. *Methods in Nitric Oxide Research* Ed.

- John Wiley and Sons, New York **1996**. (e) Jia, L.; Bonaventura, C.; Bonaventura J.; Stamler, J. S. *Nature* **1996**, *380*, 221.
- (4) Ballard, R. A.; Truog, W. E.; Cnaan, A.; Martin, R. J.; Ballard, P. L.; Merrill, J. D.; Walsh, M. C.; Durand, D. J.; Mayock, D. E.; Eichenwald, E. C.; Null, D. R.; Hudak, M. L.; Puri, A. R.; Golombek, S. G.; Courtney, S. E.; Stewart, D. L.; Welty, S. E.; Phibbs, R. H.; Hibbs, A. M.; Luan, X.; Wadlinger, S. R.; Asselin, J. M.; Coburn, C. E. *N. Engl. J. Med.* **2006**, *355*, 343.
- (5) Pacher, P.; Beckman, J. S.; Liaudet, L. *Physiol. Rev.* **2007**, *87*, 315.
- (6) Beckman, J. S.; Koppenol, W. H. *Am. J. Physiol.* **1996**, *271*, 1424.
- (7) Qiao, L.; Lu, Y.; Liu, B.; Girault, H. H. *J. Am. Chem. Soc.* **2011**, *133*, 19823.
- (8) Vilet, A.; Eiserich, J. P.; Halliwell, B.; Cross, C. E. *J. Biol. Chem.* **1997**, *272*, 7617.
- (9) Szabó, C.; Ischiropoulos, H.; Radi, R. *Nat. Rev. Drug. Discov.* **2007**, *6*, 662.
- (10) (a) Beal, M. F. *Free Radical Biol. Med.* **2002**, *32*, 797. (b) Radi, R.; Cassina, A.; Hodara, R.; Quijano, C.; Castro, L. *Free Radical Biol. Med.* **2002**, *33*, 1451.
- (11) Beckman, J. S.; Beckman, T. W.; Chen, J.; Marshall, P. A.; Freeman, B. A. *Proc. Natl. Acad. Sci. U. S. A.* **1990**, *87*, 1620.
- (12) Radi, R.; Beckman, J. S.; Bush, K. M.; Freeman, B. A. *J. Biol. Chem.* **1991**, *266*, 4244.
- (13) Castro, L.; Rodriguez, M.; Radi, R. *J. Biol. Chem.* **1994**, *269*, 29409.
- (14) Crow, J. P.; Sampson, J. B.; Zhuang, Y.; Thompson, J. A.; Beckman, J. S. *J. Neurochem.* **1997**, *69*, 1936.
- (15) Takakura, K.; Beckman, J. S.; MacMillan-Crow, L. A.; Crow, J. P. *Arch. Biochem. Biophys.* **1999**, *369*, 197.
- (16) Marla, S. S.; Lee, J.; Groves, J. T. *Proc. Natl. Acad. Sci. U. S. A.* **1997**, *94*, 14243.

- (17) Minetti, M.; Mallozzi, C.; Stasi, A. M. M. D. *Free Radical Biol. Med.* **2002**, *33*, 744.
- (18) Koppenol, W. H.; Moreno, J. J.; Pryor, W. A.; Ischiropoulos, H.; Beckman, J. S. *Chem. Res. Toxicol.* **1992**, *5*, 842.
- (19) Denicola, A.; Freeman, B. A.; Trujillo, M.; Radi, R. *Arch. Biochem. Biophys.* **1996**, *333*, 49.
- (20) Beckman, J. S.; Ischiropoulos, H.; Zhu, L.; van der Woerd, M.; Smith, C.; Chen, J.; Harrison, J.; Martin, J. C.; Tsai, M. *Arch. Biochem. Biophys.* **1992**, *298*, 438.
- (21) Beckmann, J. S.; Ye, Y. Z.; Anderson, P. G.; Chen, J.; Accavitti, M. A.; Tarpey, M. M.; White, C. R. *J. Biol. Chem.* **1994**, *375*, 81.
- (22) Mondoro, T. H.; Shafer, B. C.; Vostal, J. G. *Free Radical Biol. Med.* **1997**, *22*, 1055.
- (23) Kong, S. K.; Yim, M. B.; Stadtman, E. R.; Chock, P. B. *Proc. Natl. Acad. Sci. U. S. A.* **1996**, *93*, 3377.
- (24) Ferrer-Sueta, G.; Quijano, C.; Alvarez, B.; Radi, R. *Methods Enzymol.* **2002**, *349*, 23.
- (25) Esteves, P. M.; De M Carneiro, J. W.; Cardoso, S. P.; Barbosa, A. G.; Laali, K. K.; Rasul, G.; Prakash, G. K.; Olah, G. A. *J. Am. Chem. Soc.* **2003**, *125*, 4836.
- (26) Denicola, A.; Souza, J. M.; Radi, R. *Proc. Natl. Acad. Sci. U. S. A.* **1998**, *95*, 3566.
- (27) (a) Clarkson, S. G.; Basolo, F. *J. Chem. Soc. Chem. Commun.* **1972**, *119*, 670. (b) Clarkson, S. G.; Basolo F. *Inorg. Chem.* **1973**, *12*, 1528.
- (28) Park, G. Y.; Deepalatha, S.; Puiu, S. C.; Lee, D.-H.; Mondal, B.; Sarjeant, A. A. N.; del Rio, D.; Pau, M. Y. M.; Solomon, E. I.; Karlin, K. D. *J. Biol. Inorg. Chem.* **2009**, *14*, 1301.

- (29) (a) Tran, N. G.; Kalyvas, H.; Skodje, K. M.; Hayashi, T.; Loccoz, P. M.; Callan, P. E.; Shearer, J.; Kirschenbaum, L. J.; Kim, E. *J. Am. Chem. Soc.* **2011**, *133*, 1184.
(b) Skodje, K. M.; Williard, P. G.; Kim, E. *Dalton Trans.* **2012**, *41*, 7849.
- (30) Kumar, P.; Lee, Y.-M.; Park, Y. J.; Siegler, M. A.; Karlin, K. D.; Nam, W. *J. Am. Chem. Soc.* **2015**, *137*, 4284
- (31) Kumar, P.; Lee, Y.-M.; Hu, L.; Chen, J.; Park, Y. J.; Yao, J.; Chen, H.; Karlin, K. D.; Nam, W. *J. Am. Chem. Soc.* **2016**, *138*, 7753.
- (32) Kalita, A.; Deka, R. C.; Mondal, B. *Inorg. Chem.* **2013**, *52*, 10897.
- (33) Kalita, A.; Kumar, P.; Mondal, B. *Chem. Commun.* **2012**, *48*, 4636.
- (34) Nam, W. *Acc. Chem. Res.* **2007**, *40*, 465.
- (35) (a) Ouellet, H.; Ouellet, Y.; Richard, C.; Labarre, M.; Wittenberg, B.; Wittenberg, J.; Guertin, M. *Proc. Natl. Acad. Sci. U. S. A.* **2002**, *99*, 5902. b) Gardner, P. R. *J. Inorg. Biochem.* **2005**, *99*, 247.
- (36) Gardner, P. R.; Gardner, A. M.; Brashear, W. T.; Suzuki, T.; Hvitved, A. N.; Setchell, K. D. R.; Olson, J. S. *J. Inorg. Biochem.* **2006**, *100*, 542.
- (37) Schopfer, M. P.; Mondal, B.; Lee, D.-H.; Sarjeant, A. A. N.; Karlin, K. D. *J. Am. Chem. Soc.* **2009**, *131*, 11304.
- (38) Yokoyama, A.; Han, J. E.; Karlin, K. D.; Nam, W. *Chem. Commun.* **2014**, *50*, 1742.
- (39) Kim, S.; Siegler, A. M.; Karlin, K. D. *Chem. Commun.* **2014**, *50*, 2844.
- (40) Maiti, D.; Lee, D.-H.; Sarjeant, A. A. N.; Pau, M. Y. M.; Solomon, E. I.; Gaoutchenova, K.; Sundermeyer, J.; Karlin, K. D. *J. Am. Chem. Soc.* **2008**, *130*, 6700.
- (41) (a) Kurtikyan, T. S.; Eksuzyan, S. R.; Hayrapetyan, V. A.; Martirosyan, G. G.; Hovhannisyan, G. S.; Goodwin, J. A. *J. Am. Chem. Soc.* **2012**, *134*, 13861.

- (b) Kurtikyan, T. S.; Eksuzyan, S. R.; Goodwin, J. A.; Hovhannisyan, G. S. *Inorg. Chem.* **2013**, *52*, 12046.
- (42) Yokoyama, A.; Han, J. E.; Cho, J.; Kubo, M.; Ogura, T.; Siegler, M. A.; Karlin, K. D.; Nam, W. *J. Am. Chem. Soc.* **2012**, *134*, 15269.
- (43) Yokoyama, A.; Cho, K.-B.; Karlin, K. D.; Nam, W. *J. Am. Chem. Soc.* **2013**, *135*, 14900.
- (44) Cho, J.; Woo, J.; Nam W. *J. Am. Chem. Soc.* **2012**, *134*, 11112.



Chapter 2

Nitric Oxide Reactivity of a Co(II) Complex: Reductive Nitrosylation of Co(II) followed by Release of Nitrous Oxide

Abstract

A cobalt complex, $[(L1)_2Co]Cl_2$, **2.1** of the ligand **L1** {**L1** = *bis*(2-ethyl-4-methylimidazol-5-yl)methane} has been synthesized and characterized structurally. Addition of 3 equivalents of NO to a dry and degassed methanol solution of **2.1**, resulted a Co-dinitrosyl complex, $[(L1)Co(NO)_2]Cl$, **2.2** via the reductive nitrosylation pathway. The addition of further equivalent of NO to the reaction mixture afforded the nitrite (NO_2^-) complex, $[(L1)_2Co(NO_2)]Cl$, **2.3** with simultaneous release of N_2O . Spectroscopic analyses and isotope labelling experiments confirm the formation of complex **2.2** as an intermediate, whereas **2.3** characterized structurally.

2.1 Introduction

Nitric oxide (NO) plays diverse roles in biological processes such as neurotransmission, immune response, regulation of blood pressure etc.¹⁻⁴ Most of these reactivity are attributed to the interaction of NO with the metallo-proteins.¹⁻⁵ The biological roles of NO inspire a wide range of studies of its coordination and interaction with transition metal centers.⁶⁻⁹ NO chemistry of cobalt has not been studied as extensively as that of iron, perhaps because of less significance of cobalt in biological systems. However, cobalt nitrosyls are interesting for its several unique reactions. For instance, cobalt dinitrosyls nitrosylate alkene double bonds to result in corresponding *bis*-nitroso compounds.¹⁰ Cobalt is also known to mediate the disproportionation of NO which is industrially important.¹⁰ Like iron nitrosyls, a variety of cobalt nitrosyls are known; however, cobalt mononitrosyls having $\{\text{CoNO}\}^7$ and $\{\text{CoNO}\}^9$ configurations are rare and only a few examples are there in literature.¹¹ On the other hand, recently Harrop *et al.* reported an example where cobalt nitrosyl complex in a pyrrole/imine ligand framework having $\{\text{CoNO}\}^8$ configuration could serve as potential HNO donor.¹² The reported $\{\text{CoNO}\}^8$ complex in the presence of stoichiometric amount of H^+ behaves as an HNO donor. In the absence of an HNO target, the $\{\text{Co}(\text{NO})_2\}^{10}$ dinitrosyl was found as the end product. Thus the NO reactivity of cobalt complexes is a field of current research.

It has been reported recently that the ligand denticity and geometry play a considerable role in controlling the reactivity of NO with transition metal complexes. For instance, Cu(II) complex of macrocyclic 5,5,7,12,12,14-hexamethyl-1,4,8,11-tetraazacyclotetradecane ligand does not react with NO in acetonitrile solution; whereas the same with analogous 5,5,7-trimethyl-[1,4]-diazepane ligand in acetonitrile solution reacts with NO to afford $\{\text{CuNO}\}^{10}$ intermediate followed by the reduction of the metal center.¹³ Recently, the Lippard's group demonstrated the influence of tetraazamacrocyclic

tropocoronand ligands on the NO reactivity of their Co(II) complexes. [Co(TC-3,3)] and [Co(TC-4,4)] and [Co(TC-5,5)] were found to result in the formation of corresponding mononitrosyl which have been isolated and structurally characterized. On the other hand, [Co(TC-6,6)] upon reaction with NO, resulted in $\{\text{Co}(\text{NO})_2\}^{10}$ species. This further decomposes to [Co(NO₂)(TC-6,6)] complex.¹⁴

The present study demonstrates the NO reactivity of a Co(II) complex, **2.1**, of bis-imidazole based ligand, **L1** {**L1** = *bis*(2-ethyl-4-methylimidazol-5-yl)methane} (Figure 2.1). The reaction resulted in the formation of Co(II)-nitrito complex, **2.3**. Details spectroscopic analyses suggest the involvement of a Co(I)-dinitrosyl complex, **2.2** having $\{\text{Co}(\text{NO})_2\}^{10}$ configuration. The formation of **2.2** is attributed to the reductive nitrosylation of **2.1**.

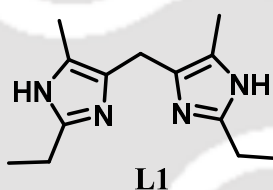


Figure 2.1. Ligand used in the present work.

2.2 Results and discussion

The ligand, **L1** {**L1** = *bis*(2-ethyl-4-methylimidazol-5-yl)methane} was synthesized by following an earlier reported procedure.¹⁵ The Co(II) complex, [(L1)₂Co]Cl₂, **2.1** was prepared by stirring a mixture of cobalt(II) chloride hexahydrate with two equivalents of the ligand in methanol (Experimental section). The complex **2.1** was characterized by spectroscopic analyses such as UV-visible, FT-IR, EPR spectroscopy and ESI-mass spectrometry (Experimental section and Appendix I). The formation of the complex was further confirmed by the single crystal X-ray structure determination. The crystallographic data and other metric parameters listed in tables A1.1, A1.2 and A1.3 (Appendix I). The

ORTEP diagram of **2.1** is shown in figure 2.2a. The crystal structure revealed that the Co(II) center is coordinated by the four nitrogen atoms from two units of the ligand in an overall distorted tetrahedral geometry. The presence of two chloride ions outside of the coordination sphere satisfied the charge of the central metal ion. The average Co-N distance (1.982 Å) was found to be within the range of analogous reported complexes.¹⁶

In methanol solution, **2.1** exhibited absorptions at 515 nm ($\epsilon/M^{-1}cm^{-1}$, 323), 559 nm ($\epsilon/M^{-1}cm^{-1}$, 494) and 581 nm ($\epsilon/M^{-1}cm^{-1}$, 490) along with the other intra-ligand transitions at lower wavelengths (Figure 2.3a). These absorption bands in the visible region of the spectrum are attributed to the ${}^4A_2 \rightarrow {}^4T_1(P)$, ${}^4A_2 \rightarrow {}^4T_1(F)$, ${}^4A_2 \rightarrow {}^4T_2$ transitions, respectively, in tetrahedral Co(II) (d^7) system.¹⁷ The crystalline **2.1** was dissolved in methanol and electron paramagnetic resonance (EPR) was recorded at 77 K (Figure 2.4a and Appendix I). The observed g_{av} was 2.29 as expected for a Co(II) ion in tetrahedral field. The observed magnetic moment was found to be 4.32 BM, which is comparable with the other reported Co(II) tetrahedral complexes.¹⁸

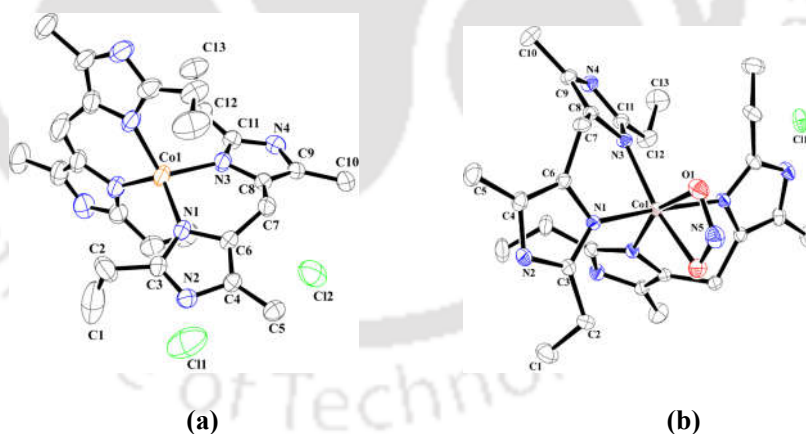


Figure 2.2. ORTEP diagram of complexes (a) **2.1** and (b) **2.3**. (30% thermal ellipsoid plot. H-atoms and solvent molecules are not shown for clarity).

NO reactivity of complex **2.1**

Gradual addition of NO gas to a dry and degassed methanol solution of **2.1** resulted in the

change of color from violet to red. The complete reaction was observed with 3 equivalents of NO. In UV-visible spectroscopic monitoring, the addition of NO resulted in the appearance of absorption bands at 516 nm ($\epsilon/M^{-1}cm^{-1}$, 300), 556 nm ($\epsilon/M^{-1}cm^{-1}$, 490), 579 nm ($\epsilon/M^{-1}cm^{-1}$, 474), 664 nm ($\epsilon/M^{-1}cm^{-1}$, 140) along with other intra-ligand transitions at lower wavelengths (Figure 2.3a). This is attributed to the formation of intermediate complex **2.2**. In absence of air and moisture, the color was found to be stable for several hours. Unfortunately we could not isolate it as solid owing to its reactive nature. However, spectroscopic characterization revealed **2.2** as a Co(I)-dinitrosyl having $\{Co(NO)_2\}^{10}$ configuration (see later). It is to be noted that in CH_2Cl_2 solution $[(TMEDA)Co(NO)_2](BPh_4)$ (TMEDA = *N,N,N',N'*-tetramethylethylenediamine) absorbs at 640 nm.¹⁹ Another $\{Co(NO)_2\}^{10}$ of mesityl derivative of ethylenediamine ligand framework exhibits *d-d* transition at 600 nm.²⁰

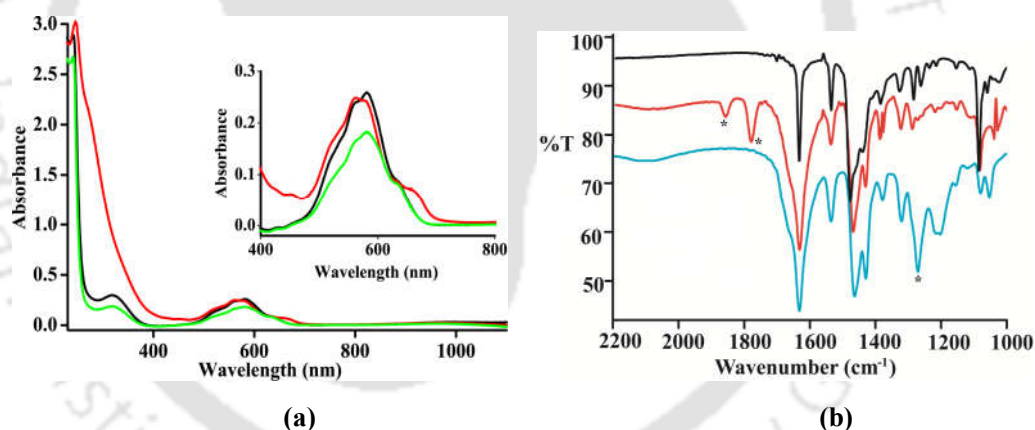


Figure 2.3. (a) UV-visible spectral monitoring of the reaction of complex **2.1** (black) with NO to result **2.2** (red) and **2.3** (green) in methanol. (b) Solution FT-IR spectral monitoring of the reaction of complex **2.1** (black) with NO to result **2.2** (red) and **2.3** (blue) in methanol.

The addition of successive equivalent of NO resulted in the change of color to dark brown. In the visible region of the spectrum it shows absorption bands at 523 nm ($\epsilon/M^{-1}cm^{-1}$, 184), 558 nm ($\epsilon/M^{-1}cm^{-1}$, 312) and 579 nm ($\epsilon/M^{-1}cm^{-1}$, 360) nm, respectively. This is attributed to the formation of complex, **2.3** (Scheme 2.1). In the FT-IR spectrum, **2.2** shows two new

stretching frequency at 1857 and 1774 cm^{-1} assignable to the coordinated NO stretching of $\{\text{Co}(\text{NO})_2\}^{10}$ moiety (Figure 2.3b). These are found to be isotope sensitive and shifted to 1825 and 1749 cm^{-1} , respectively, with ^{15}NO . In general, the $\{\text{Co}(\text{NO})_2\}^{10}$ complexes show symmetric and asymmetric NO stretching frequencies between 1820-1876 cm^{-1} and 1750-1798 cm^{-1} , respectively.²¹ The Lippard's group have reported a number of examples of Co-dinitrosyl having $\{\text{Co}(\text{NO})_2\}^{10}$ configuration where the stretching frequencies appear in the range of 1700-1900 cm^{-1} .^{14a,b} For example, in $[(\text{TC-6,6})\text{Co}(\text{NO})_2]$, NO stretching frequency appears at 1807 and 1730 cm^{-1} , whereas in case of $[(\text{TC-6,6})\text{Co}_2(\text{NO})_4]$ it was observed at 1799 and 1720 cm^{-1} .^{14a,b} It has been reported earlier that the addition of NO to a CH_2Cl_2 solution of a Co(II) complex with tmeda ligand, resulted in the formation of corresponding cobalt-dinitrosyl complex which shows NO stretching at 1866 and 1789 cm^{-1} , respectively.¹⁹

The reactions of $[\text{Co}(\text{}^i\text{PrDATI})_2]$, $[\text{Co}(\text{}^t\text{BuDATI})_2]$ and $[\text{Co}(\text{}^{\text{Bz}}\text{DATI})_2]$ (DATI = dansyl aminotroponimines) in CH_2Cl_2 solution with NO were also known to form the corresponding dinitrosyl complexes with NO stretching at 1838, 1760; 1833, 1760 and 1833, 1755 cm^{-1} , respectively.²²

In the presence of further equivalent of NO, the NO stretching frequencies at 1857 and 1774 cm^{-1} disappeared with the appearance of a new one at 1261 cm^{-1} (Figure 2.3b). This is attributed to the coordinated NO_2^- stretching and this assignment is in well agreement with the formulation of **2.3**. In case of other reported examples, the metal coordinated NO_2^- stretching appears at in the range of 1260-1485 cm^{-1} .²³

In the X-band EPR spectroscopy, the characteristic signals of Co(II) in tetrahedral geometry disappeared upon addition of 3 equivalents of NO (Figure 2.4a). However, the addition of subsequent equivalent of NO resulted in the appearance of Co(II) signals again.

The observed g_{av} is consistent with the reported examples of Co(II) in distorted octahedral geometry.²⁴ This suggests the formation of a diamagnetic intermediate, **2.2**, upon addition of 3 equivalents of NO to the solution of **2.1**. The intermediate resulted to a paramagnetic complex, **2.3** in presence of further equivalent of NO (Figure 2.4a).

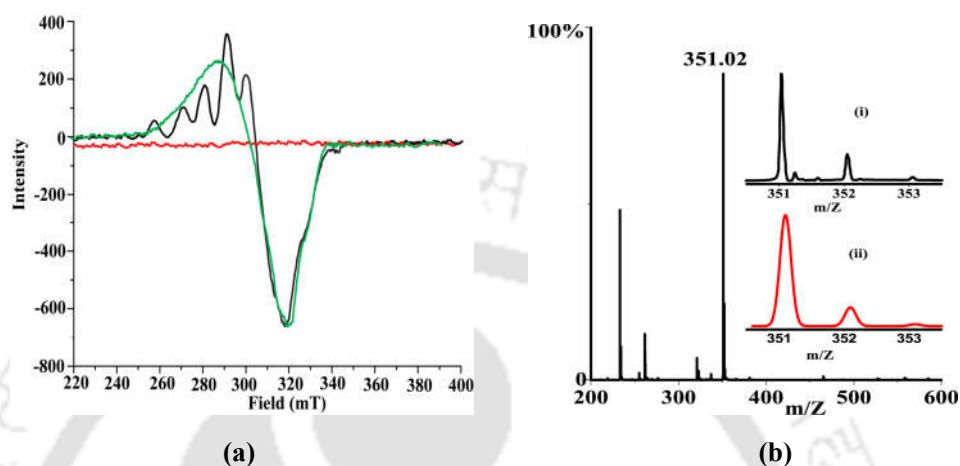


Figure 2.4. (a) X-band EPR spectral monitoring of the reaction of complex **2.1** (black) with NO to result, **2.2** (red) and **2.3** (green) in methanol at 77 K. (b) ESI-mass spectrum of complex **2.2** in methanol. Inset: (i) experimental and (ii) simulated isotopic distribution pattern.

In $^1\text{H-NMR}$ spectrum, the broad peaks of paramagnetic **2.1** in CD_3OD became well resolved in the presence of 3 equivalents of NO (Figure 2.5). The spectrum was populated with two sets of signals having same number of protons. By comparing with the spectrum of **L1** in same solvent, it has been observed that the peaks at 1.20-1.23 (t, 6H), 2.00 (s, 6H), 2.58-2.62 (q, 4H) and 3.66 (s, 2H) ppm corresponds to **L1**. The other set {0.99 (t, 6H), 2.34 (s, 10H) and 3.92 (s, 2H) ppm} shows a slight shift of the peak positions which is consistent with the metal bound ligand in Co(I)-dinitrosyl complex, **2.2**. Thus, **2.2** was formulated as $[(\text{L1})\text{Co}(\text{NO})_2]^+$. The addition of one more equivalent of NO again resulted in one set of peaks with paramagnetic broadening (Figure 2.5). This spectrum matches well with the spectrum of isolated **2.3** (Appendix I).

The formulation of **2.2** was further supported by ESI-mass spectrometric analyses. The addition of 3 equivalents of NO to the solution of **2.1** resulted in a spectrum populated by a peak at m/z 351.02 (Figure 2.4b). This is assignable to the $[(L1)Co(NO)_2]^+$ unit. The peak was found to be isotope sensitive and shifted to m/z , 353.34 upon labelling with ^{15}NO which is again consistent with the mass of $[(L1)Co(NO)_2]^+$ moiety. The simulated isotopic distribution pattern was found to be in good agreement with the observed one (Figure 2.4b). In the presence of further equivalent of NO, the peak at m/z , 351.02 disappeared and a new peak at m/z , 523.23 corresponding to $[(L1)_2Co]^+$ was observed (Appendix I).

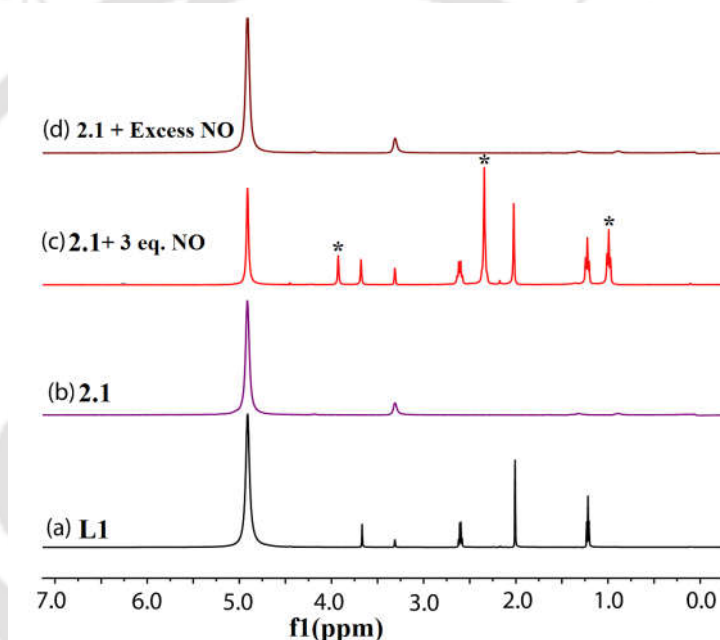
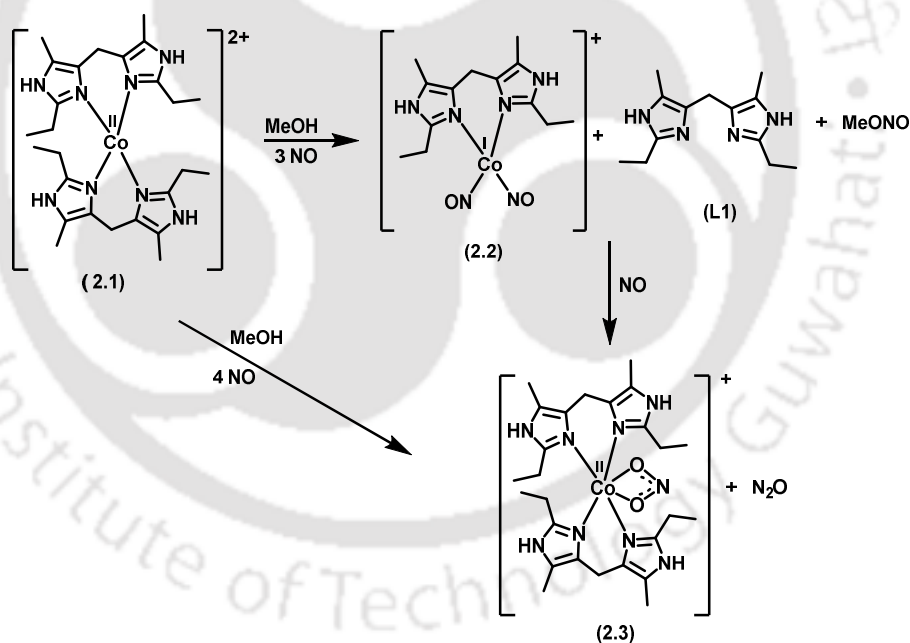


Figure 2.5. 1H -NMR spectra of (a) ligand **L1** (black), (b) complex **2.1** (violet), (c) after addition of 3 equivalents of NO, **2.2+L1** and (d) after addition of excess NO, complex **2.3** in CD_3OD . The * marked signals are for complex **2.2**.

Further, the formation of **2.3** in the reaction was confirmed by its isolation and structural characterization (Experimental section). The ORTEP diagram of **2.3** is shown in figure 2.1b. The crystal structure revealed that $Co(II)$ is co-ordinated with four N-atom from two units of ligand and two O-atoms from a nitrite anion (NO_2^-) in an distorted octahedral

geometry. The Co-O_{nitrito} bond distance is 2.23 (3) Å, and Co-O-N bond angle is 98.0 (3)° which is consistent with the previously reported Co^{II}-nitrito complexes.

Thus, a total of 4 equivalents of NO is required to result in the formation **2.3** from **2.1** via the intermediate formation of **2.2** (Scheme 2.1). The reaction of **2.1** with NO can be envisaged as the reductive elimination in the first step leading to the formation of **2.2**, [(L1)Co(NO)₂]⁺ (Scheme 2.1). In this case one equivalent of NO is required for the reduction of Co(II) to Co(I) and other 2 equivalents of NO form the dinitrosyl complex in subsequent step. The NO induced reduction of Co(II) was confirmed by the presence of MeONO in the reaction mixture in GC-mass analyses (Appendix I). In the next step, the dinitrosyl complex reacts with equivalent amount of NO to result in the nitrito complex, **2.3** (Scheme 2.1).



Scheme 2.1. Reaction of complex **2.1** with NO.

The reaction of free NO with the metal nitrosyls was reported previously. In this context, the Tolman's group observed that a Cu(I) complex of pyrazolyl borate derivative ligand, reacts with NO to form a Cu-dinitrosyl (or Cu-hyponitrite) complex and a subsequent

equivalent of NO resulted in the corresponding Cu(II)-nitrite.²⁵ A simultaneous release of N₂O was observed in this reaction. In addition, Fe(TC-5,5) and Mn(TC-5,5) were reported to react with stoichiometric 4 equivalents of NO leading to the formation of corresponding O-bound metal nitrite and N₂O.²⁶ Thus, in the present case, the release of N₂O is expected and its presence was confirmed by the head space gas analysis using GC-mass spectrometry (Appendix I).

2.3 Experimental section

2.3.1 Materials and methods

All reagents and solvents were purchased from commercial sources and were of reagent grade. HPLC grade methanol was used and dried by heating with iodine-activated magnesium with magnesium loading of *ca.* 5 g/L. The dried methanol was stored over 20% (m/v) molecular sieves (3 Å) for 3 days before use. Deoxygenation of the solvent and solutions were effected by repeated vacuum/purge cycles or bubbling with nitrogen or argon for 30 minutes. NO gas was purified by passing through KOH and P₂O₅ column. The dilution of NO was effected with argon gas using Environics Series 4040 computerized gas dilution system. UV-visible spectra were recorded on an Agilent HP 8454 spectrophotometer. FT-IR spectra were taken on a Perkin-Elmer spectrophotometer with either sample prepared as KBr pellets or in solution in a KBr cell. ¹H-NMR spectra were obtained with a 400 MHz Varian FT spectrometer. Chemical shifts (ppm) were referenced either with an internal standard (Me₄Si) for organic compounds or to the residual solvent peaks. The X-band Electron Paramagnetic Resonance (EPR) spectra were recorded on a JES-FA200 ESR spectrometer, at room temperature or at 77 K. Spectra were recorded with all the samples prepared in methanol solution at 77 K. The experimental conditions [Frequency, 9.136 GHz; Power, 0.995 mW; Field center, 336.00 mT, Width, ± 250.00 mT;

Sweep time, 30.0 s; Modulation frequency, 100.00 kHz, Width, 1.000 mT; Amplitude, 1.0 and Time constant, 0.03 s] kept same for all the samples. Mass spectra of the compounds were recorded in a Waters Q-ToF Premier and Aquity instrument. Solution electrical conductivity was checked using a Systronic 305 conductivity bridge. The magnetic moment of complexes were measured on a Cambridge Magnetic Balance. Elemental analyses were obtained from a Perkin Elmer Series II Analyzer.

Single crystals were grown by slow evaporation technique. The intensity data were collected using a Bruker SMART APEX-II CCD diffractometer, equipped with a fine focus 1.75 kW sealed tube Mo K α radiation ($\lambda = 0.71073 \text{ \AA}$) at 273(3) K, with increasing ω (width of 0.3° per frame) at a scan speed of 3 s/frame. The SMART software was used for data acquisition.²⁷ Data integration and reduction was undertaken with SAINT and XPREP software. Structures were solved by direct methods using SHELXS-97 and refined with full-matrix least squares on F^2 using SHELXL-97.²⁸ Structural illustrations have been drawn with ORTEP-3 for Windows.²⁹

2.3.2 Syntheses

2.3.2.1 Synthesis of ligand L1, [bis(2-ethyl-4-methylimidazol-5-yl)methane]

2-ethyl-4-methyl imidazole (2.2 g, 20 mmol) was taken in a round bottom flask with 50 mL of methanol; to this 0.45 g (15 mmol) of formaldehyde and aqueous solution of 5.1 g (91 mmol) potassium hydroxide was added drop wise. The reaction mixture was stirred for 24 h at room temperature. A white solid was obtained. It was filtered off and washed with water. After washing the solid was dried in air and then kept in desiccator for overnight. Yield: 1.97 g (85%). Elemental analyses for C₁₃H₂₀N₄, Calcd(%): C, 67.21; H, 8.68; N, 24.12. Found (%): C, 67.19; H, 8.68; N, 24.02. FT-IR (in KBr): 2964, 2842, 1614, 1529, 1455, 1071 cm⁻¹. ¹H-NMR (400 MHz, CDCl₃): δ_{ppm} , 1.20-1.23 (t, 6H), 2.00 (s, 6H), 2.58-

2.62 (q, 4H) and 3.66 (s, 2H). $^{13}\text{C-NMR}$ (100 MHz, CDCl_3): δ_{ppm} , 149.2, 129.1, 127.2, 23.3, 22.6, 13.7, 10.6.

2.3.2.2 Syntheses of complexes

(a) 2.1, $[(\text{L1})_2\text{Co}]^{2+}$

A solution of $\text{CoCl}_2 \cdot 6\text{H}_2\text{O}$ (1.19 g, 5 mmol) in methanol (20 mL) was added to a solution of the ligand (2.32 g, 10 mmol) in methanol (15 mL) over a period of 10 min. The resulting violet solution was stirred for 3 h and then kept at room temperature for slow evaporation. After a few days, violet color crystals of **2.1** were obtained. Yield: 2.43 g (82%). Elemental analyses for $\text{C}_{26}\text{H}_{40}\text{Cl}_2\text{CoN}_8$, Calcd. (%): C, 52.53; H, 6.78; N, 18.85, found (%): C, 52.47; H, 6.80; N, 18.93. UV-visible (MeOH): 319 nm ($\epsilon/\text{M}^{-1}\text{cm}^{-1}$, 772), 515 nm ($\epsilon/\text{M}^{-1}\text{cm}^{-1}$, 323), 559 nm ($\epsilon/\text{M}^{-1}\text{cm}^{-1}$, 494), and 581 nm ($\epsilon/\text{M}^{-1}\text{cm}^{-1}$, 490). FT-IR (in KBr): 2975, 1603, 1465, 1295, 1079, 825, 674 cm^{-1} . X-band EPR: g_{av} 2.29. Molar conductance (MeOH): 185 $\text{Scm}^2\text{mol}^{-1}$. Observed Magnetic moment: 4.32 μ_{B} . ESI-Mass (m/z): Calcd: 261.63, found: 261.60 (M/2).

(b) 2.3, $[(\text{L1})_2\text{Co}(\text{NO}_2)]^+$

Complex **2.1** was dissolved in 30 mL of dry and degassed methanol in a 50 mL schlenk flask fitted with a rubber septum connected to the schlenk line. The solution was degassed by argon gas through vacuum purge continuously for 10 min. 4 equivalents of NO was added to the solution and stirred at room temperature for 1h, after a few days a brown colour crystals of **2.3** were obtained. Elemental analyses for $\text{C}_{26}\text{H}_{40}\text{ClCoN}_9\text{O}_2$, Calcd (%): C, 51.61; H, 6.66; N, 20.84, found (%): C, 51.57; H, 6.71; N, 20.87. UV-visible (MeOH): 523 nm ($\epsilon/\text{M}^{-1}\text{cm}^{-1}$, 184), 558 nm ($\epsilon/\text{M}^{-1}\text{cm}^{-1}$, 312), 579 nm ($\epsilon/\text{M}^{-1}\text{cm}^{-1}$, 360). FT-IR (in

KBr): 1634, 1535, 1452, 1428, 1323, 1261, 1208, 1073, 1050 cm^{-1} . X-band EPR: g_{av} 1.89. Molar Conductance: $135 \text{ Scm}^2\text{mol}^{-1}$. Observed magnetic moment: $1.78 \mu_B$.

2.4 Conclusion

In conclusion, the present study demonstrates an example of the reaction of a Co(II) complex, **2.1** with 3 equivalents of NO to result in a Co-dinitrosyl complex, **2.2** via the reductive nitrosylation pathway. The addition of further equivalent of NO to the reaction mixture afforded the nitrito complex, **2.3** simultaneous release of N_2O . Spectroscopic analyses and isotope labelling experiments revealed the formulation of **2.2** as $[(L1)\text{Co}(\text{NO})_2]^+$, whereas structural characterization confirmed the formation of **2.3**.

2.5 References

- (1) (a) Ignarro, L. J. *Nitric Oxide: Biology and Pathobiology* Ed. Academic Press; San Diego, CA **2000**. (b) Richter-Addo, G. B.; Legzdins, P. *Metal Nitrosyls* Oxford University Press, New York **1992**. (c) Moncada, S.; Palmer, R. M. J.; Higgs, E. A. *Pharmacol. Rev.* **1991**, *43*, 109. (d) Bredt, D. S.; Snyder, S. H. *Annu. Rev. Biochem.* **1994**, *63*, 175. (e) Butler, A. R.; Williams, D. L. *Chem. Soc. Rev.* **1993**, 233. (f) Hunt, A. P.; Lehnert, N. *Acc. Chem. Res.* **2015**, *48*, 2117.
- (2) (a) Feelisch, M.; Stamler, J. S. *Methods in Nitric Oxide Research* Ed. John Wiley and Sons, New York **1996**. (b) Jia, L.; Bonaventura, C.; Bonaventura, J.; Stamler, J. S. *Nature* **1996**, *380*, 221. (c) Galdwin, M. T.; Lancaster Jr., J. R.; Freeman, B. A.; Schechter, A. N. *Nat. Med.* **2003**, *9*, 496.
- (3) (a) Ye, R. W.; Toro-Suarez, I.; Tiedje, J. M.; Averill, B. A. *J. Biol. Chem.* **1991**, *266*, 12848. (b) Hulse, C. L.; Averill, B. A.; Tiedje, J. M. *J. Am. Chem. Soc.* **1989**, *111*, 232. (c) Jackson, M. A.; Tiedje, J. M.; Averill, B. A. *FEBS Lett.* **1991**, *291*, 41.

- (4) (a) Godden, J. W.; Turley, S.; Teller, D. C.; Adman, E. T.; Liu, M. Y.; Payne, W. J.; LeGall, J. *Science* **1991**, *153*, 438. (b) Adman, E. T.; Turley, S.; Karlin, K. D.; Tyeklir, Z. *Bioinorganic Chemistry of Copper* Ed. Chapman & Hall, Inc.: New York **1993**, 397. (c) Ferguson, S. J. *Curr. Opin. Chem. Biol.* **1998**, *2*, 182.
- (5) (a) Richardson, D. J.; Watmough, N. J. *Curr. Opin. Chem. Biol.* **1999**, *3*, 207. (b) Moura, I.; Moura, J. J. G. *Curr. Opin. Chem. Biol.* **2001**, *5*, 168. (c) Tocheva, E. I.; Rosell, F. I.; Mauk, A. G.; Murphy, M. E. P. *Biochem.* **2007**, *46*, 12366. (d) Zhou, X.; Espey, M. G.; Chen, J. X.; Hofseth, L. J.; Miranda, K. M.; Hussain, S. P.; Winks, D. A.; Harris, C. C. *J. Biol. Chem.* **2000**, *275*, 21241.
- (6) (a) Tonzetich, Z. J.; McQuade, L. E.; Lippard, S. J. *Inorg. Chem.* **2010**, *49*, 6338. (b) McCleverty, J. A. *Chem. Rev.* **2004**, *104*, 403. (c) Tennyson, A. G.; Lippard, S. J. *J. Chem Biol.* **2011**, *18*, 1211. (d) Rose, M. J.; Butterley, N. M.; Mascharak, P. K. *J. Am. Chem. Soc.* **2009**, *131*, 8340. (e) Sun, N.; Liu, L. V.; Dey, A.; Villar-Acevedo, A. G.; Kovacs, J. A.; Darensbourg, M. Y.; Hodgson, K. O.; Hedman, B.; Solomon, E. I. *Inorg. Chem.* **2010**, *50*, 427.
- (7) (a) Lu, T.-T.; Lai, S.-H.; Li, Y.-W.; Hsu, I.-J.; Jang, L.-Y.; Lee, J.-F.; Chen, I.-C.; Liaw, W.-F. *Inorg. Chem.* **2011**, *50*, 5396. (b) Pellegrino, J.; Bari, S. E.; Bikiel, D. E.; Doctorovich, F. *J. Am. Chem. Soc.* **2009**, *132*, 989. (c) Berto, T. C.; Praneeth, V. K. K.; Goodrich, L. E.; Lehnert, N. *J. Am. Chem. Soc.* **2009**, *131*, 17116. (d) Goodrich, L. E.; Paulat, F.; Praneeth, V. K. K.; Lehnert, N. *Inorg. Chem.* **2010**, *49*, 6293. (e) Dudle, B.; Rajesh, K.; Blacque, O.; Berke, H. *Organometallics* **2011**, *30*, 2986.
- (8) (a) Hess, J. L.; Hsieh, C.-H.; Reibenspies, J. H.; Darensbourg, M. Y. *Inorg. Chem.* **2011**, *50*, 8541. (b) Hsieh, C.-H.; Darensbourg, M. Y. *J. Am. Chem. Soc.* **2010**, *132*,

14118. (c) Tsai, F.-T.; Chen, P.-L.; Liaw, W.-F. *J. Am. Chem. Soc.* **2010**, *132*, 5290. (d) Fry, N. L.; Mascharak, P. K. *Acc. Chem. Res.* **2011**, *44*, 289.
- (9) Hess, J. L.; Hsieh, C.-H.; Brothers, S. M.; Hall, M. B.; Darensbourg, M. Y. *J. Am. Chem. Soc.* **2011**, *133*, 20426. (b) Lehnert, N.; Scheidt, W. R.; Wolf, M. W. *Struct. Bond.* **2014**, *154*, 155. (c) Mariela, F. R.; Slep, V. L. D.; Olabe, J. A. *Coord. Chem. Rev.* **2007**, *251*, 1903. (d) Wright, A. M.; Hayton, T. W. *Comments Inorg. Chem.* **2012**, *33*, 207. (e) Wasser, I. M.; De Vries, S.; Loccoz, P. M.; Schroeder, I.; Karlin, K. D. *Chem. Rev.* **2002**, *102*, 1201.
- (10) (a) Brunner, H. *J. Organomet. Chem.* **1968**, *12*, 517. (b) Brunner, H.; Loskot, S. *Angew. Chem. Int. Ed.* **1971**, *10*, 515. (c) Weiner, W. P.; White, M. A.; Bergman, R. G. *J. Am. Chem. Soc.* **1981**, *103*, 3612. (d) Becker, P. N.; Bergman, R. G. *J. Am. Chem. Soc.* **1983**, *105*, 2985. (e) Becker, P. N.; Bergman, R. G. *Organometallics* **1983**, *2*, 787. (f) Weiner, W. P.; Hollander, F. J.; Bergman, R. G. *J. Am. Chem. Soc.* **1984**, *106*, 7462.
- (11) (a) Richter-Addo, G. B.; Hodge, S. J.; Yi, G.-B.; Khan, M. A.; Ma, T.; Van Caemelbecke, E.; Guo, N.; Kadish, K. M. *Inorg. Chem.* **1996**, *35*, 6530. (b) Di Vaira, M.; Ghilardi, C. A.; Sacconi, L. *Inorg. Chem.* **1976**, *15*, 1555. (c) Thyagarajan, S.; Incarvito, C. D.; Rheingold, A. L.; Theopold, K. H. *Inorg. Chim. Acta* **2003**, *345*, 333.
- (12) Rhine, M. A.; Rodrigues, A. V.; Urbauer, R. L. B.; Urbauer, J. L.; Stemmler, T. L.; Harrop, T. C. *J. Am. Chem. Soc.* **2014**, *136*, 12560.
- (13) Kalita, A.; Kumar, P.; Deka, R. C.; Mondal, B. *Inorg. Chem.* **2011**, *50*, 11868.
- (14) (a) Kozhukh, J.; Lippard, S. J. *J. Am. Chem. Soc.* **2012**, *134*, 11120. (b) Franz, K. J.; Doerrer, L. H.; Springler, B.; Lippard, S. J. *Inorg. Chem.* **2001**, *40*, 3774. (c) Scott, M. J.; Lippard, S. J. *J. Am. Chem. Soc.* **1997**, *119*, 341. (d) Villacorta, G. M.;

- Lippard, S. J. *Pure Appl. Chem.* **1986**, *58*, 1474. (e) Zask, A.; Gonnella, N.; Nakanishi, K.; Turner, C. J.; Imajo, S.; Nozoe, T. *Inorg. Chem.* **1986**, *25*, 3400. (f) Jaynes, B. S.; Doerrer, L. H.; Liu, S.; Lippard, S. J. *Inorg. Chem.* **1995**, *34*, 5735.
- (15) (a) Kalita, A.; Kumar, P.; Deka, R. C.; Mondal, B. *Chem. Commun.* **2012**, *48*, 1251. (b) Ghosh, S.; Deka, H.; Dangat, Y. B.; Saha, S.; Gogoi, K.; Vanka, K.; Mondal, B. *Dalton Trans.* **2016**, *45*, 10200.
- (16) Song, Y. S.; Kofod, P.; Madsen, A. S.; Larsen, E. *Inorg. Chem.* **2009**, *48*, 7159.
- (17) (a) Jesson, J. P. *J. Chem. Phys.* **1968**, *48*, 161. (b) Drake, A. F.; Hirst, S. J.; Kuroda, R.; Mason, S. F. *Inorg. Chem.* **1982**, *21*, 533. (c) Dzwigaj, S.; Che, M. *J. Phys. Chem. B* **2006**, *110*, 12490.
- (18) Romerosa, A.; Bello, C. S.; Ruiz, M. S.; Caneschi, A.; McKee, V.; Peruzzini, M.; Sorace, L.; Zanobini, F. *Dalton Trans.* **2003**, 3233.
- (19) Fujisawa, K.; Soma, Shoko.; Kurihara, H.; Dong, H. T.; Bilodeaub, M.; Lehnert, N. *Dalton Trans.* **2017**, *46*, 13273.
- (20) Deka, H.; Ghosh, S.; Saha, S.; Gogoi, K.; Mondal, B. *Dalton Trans.* **2016**, *45*, 10979.
- (21) (a) Sarma, M.; Kalita, A.; Kumar, P.; Singh, A.; Mondal, B. *J. Am. Chem. Soc.* **2010**, *132*, 7846. (b) Sarma, M.; Mondal, B. *Inorg. Chem.* **2011**, *50*, 3206. (c) Sarma, M.; Mondal, B. *Dalton Trans.* **2012**, *41*, 2927. (d) Haymore, B. L.; Huffman, J. C.; Butler, N. E. *Inorg. Chem.* **1983**, *22*, 168.
- (22) (a) Franz, K. J.; Singh, N.; Spingler, B.; Lippard, S. J. *Inorg. Chem.* **2000**, *39*, 4081. (b) Tomson, N. C.; Crimmin, M. R.; Petrenko, T.; Rosebrugh, L. E.; Sproules, S.; Boyd, W. C.; Bergman, R. G.; DeBeer, S.; Toste, F. D.; Wieghardt, K. *J. Am. Chem. Soc.* **2011**, *133*, 18785. (c) Hilderbrand, S. A.; Lippard, S. J. *Inorg. Chem.* **2004**, *43*, 5294. (d) Lim, M. H.; Lippard, S. J. *Acc. Chem. Res.* **2007**, *40*, 41.

- (23) (a) Goodwin, J.; Kurtikyan, T.; Standard, J.; Walsh, R.; Zheng, B.; Parmley, D.; Howard, J.; Green, S.; Marduykov, A.; Przybyla, D. E. *Inorg. Chem.* **2005**, *44*, 2215. (b) Gogoi, K.; Deka, H.; Kumar, V.; Mondal, B. *Inorg. Chem.* **2015**, *54*, 4799. (c) Lehnert, N.; Cornelissen; Neese, F.; Ono, T.; Noguchi, Y.; Okamoto, K.-I.; Fujisawa, K. *Inorg. Chem.* **2007**, *46*, 3916.
- (24) Sengupta, A.; Rajput, A.; Barman, S. K.; Mukherjee, R. *Dalton Trans.* **2017**, *46*, 11291.
- (25) Schneider, J. L.; Carrier, S. M.; Ruggiero, C. E.; Young, J. V. E.; Tolman, W. B. *J. Am. Chem. Soc.* **1998**, *120*, 11408.
- (26) (a) Franz, K. J.; Lippard, S. J. *J. Am. Chem. Soc.* **1999**, *121*, 10504. (b) Franz, K. J.; Lippard, S. J. *J. Am. Chem. Soc.* **1998**, *120*, 9034.
- (27) SMART, SAINT and XPREP, Siemens Analytical X-ray Instruments Inc., Madison, Wisconsin, U. S. A. **1995**.
- (28) (a) Sheldrick, G. M.; SADABS: software for Empirical Absorption Correction, University of Gottingen, Institute for Anorganische Chemie der Universität, Tammanstrasse 4, D-3400 Gottingen, Germany **1999**. (b) Sheldrick, G. M. SHELXS-97, University of Gottingen, Germany **1997**.
- (29) Farrugia, L. J. ORTEP-3 for windows-a version of ORTEP-III with a graphical user interface (GUI). *J. Appl. Crystallogr.* **1997**, *30*, 565.

Chapter 3

Reactivity of a Cobalt Nitrosyl Complex: Formation of a Cobalt Peroxynitrite Intermediate and Transfer of the Nitrosyl to a Cobalt Porphyrin Complex

Abstract

A cobalt salen complex, $[(L2)Co]$, **3.1** $\{L2H_2 = 6,6'-((1E,1'E)-(ethane-1,2-diyl)bis(azanylylidene))bis(methanylylidene))bis(2,4-di-tert-butylphenol)\}$ in THF solution was subjected to react with nitric oxide (NO) gas and resulted in the formation of the corresponding nitrosyl complex, $[(L2)Co(NO)]$, **3.2** having $\{CoNO\}^8$ description. It was characterized by spectroscopic studies and single crystal X-ray structure determination. It did not react with dioxygen. However, in THF solution, it reacted with KO_2 to result in the Co-nitrate complex, $[(L2)Co(NO_3)]$, **3.3**. It induced ring nitration to the externally added phenol in an appreciable yield. The reaction presumably proceeds through the formation of corresponding Co-peroxynitrite intermediate. In addition, complex **3.2** in THF solution, was found to transfer the NO group to a cobalt porphyrin complex, $[(L3)Co]$, **3.4** $\{L3 = 5,10,15,20-tetrakis(4'-bromophenyl)porphyrinate\}$ dianion to result in the corresponding nitrosyl complex, $[(L3)Co(NO)]$, **3.5**.

3.1 Introduction

Nitric oxide (NO) is an important small molecule that is involved in various physiological process; e.g. neurotransmission, vasodilation, immune response etc.¹⁻⁴ Under normal conditions, NO is produced by nitric oxide synthase (NOS) at low concentration. However, excess production of NO can have detrimental effects *via* the formation of secondary reactive nitrogen species (RNS) such as nitrogen dioxide (NO₂) and peroxynitrite (ONOO⁻).⁵ Both of these RNS are known to play important roles in bio-molecule oxidation leading to the oxidative and nitrosative stress.⁶ The formation of these secondary intermediates from NO requires the presence of oxidants like hydrogen peroxide (H₂O₂), superoxide (O₂⁻) radicals and transition metal centers.^{7,8} Peroxynitrite is believed to form *in vivo* in the diffusion controlled reaction of NO and superoxide anion (O₂⁻) or hydrogen peroxide (H₂O₂) and nitrite (NO₂⁻) in presence of peroxidase enzymes.⁹ NO₂ forms either from the homolytic O-O cleavage of ONOO⁻ or by the reaction of NO with O₂. Aqueous ONOO⁻ isomerizes to nitrate (NO₃⁻) very easily. Peroxynitrite is reported to form in the reaction of oxy-heme (Fe^{III}-O₂⁻) proteins with NO and superoxo-iron or -cobalt porphyrinates with NO. Recently ONOO⁻ intermediates are shown to form in the reaction of NO with Cr-superoxo or peroxo species; a Cr(IV)-peroxo complex, [(12-TMC)Cr(O₂)(Cl)]⁺ reacted with NO to form a Cr(III)-nitrate complex, [(12-TMC)Cr(NO₃)(Cl)]⁺, whereas a Cr(III)-superoxo complex, [(14-TMC)Cr(O₂)(Cl)]⁺ and NO gave a Cr(IV)-oxo complex, [(14-TMC)Cr(O)(Cl)]⁺ and NO₂ presumably *via* the formation of a Cr(III)-peroxynitrite intermediate, [(14-TMC)Cr(OONO)(Cl)]⁺.¹⁰⁻¹² Recently Nam and his co worker has reported two mononuclear Co(III)-nitrosyl complexes, [(12-TMC)Co(NO)]²⁺ and [(13-TMC)Co(NO)]²⁺, and examined their reactions with O₂⁻ to give high yields of Co^{II}-nitrito complexes with the release of O₂ *via* the formation of presumed Co(II)-(ONOO⁻) intermediates.¹³

On the other hand, another important aspect of metal-nitrosyl is the transfer of NO centre from one metal to another. This depends on the NO-to-metal binding constant, ligand geometry, and metal oxidation state. Caulton and co-workers have reported nitrosyl transfer from $[(\text{DMGH})_2\text{Co}(\text{NO})]$ (DMGH = monoanion of dimethylglyoxime) to the various metal complexes of Fe, Co, Ni, and Ru.¹⁴ Lippard and co-workers also suggested a dissociative pathway of NO-transfer from manganese to iron bearing a tropocoronand ligand framework.¹⁵ Very recently Nam group have reported the NO-transfer from $[(14\text{-TMC})\text{Co}(\text{NO})]^{2+}$ to $[(12\text{-TMC})\text{Co}]^{2+}$.¹⁶

The present work describes the reactivity of a Co-nitrosyl complex of salen type ligand with i) superoxide ion to form Co-nitrate complex *via* a putative peroxyxynitrite intermediate and ii) NO transfer to a Co-porphyrin complex.

3.2 Results and discussion

The ligand L2H_2 $\{\text{L2H}_2 = 6,6'-((1\text{E},1'\text{E})\text{-}(\text{ethane-1,2-diyl})\text{bis}(\text{azanylylidene}))\text{-bis}(\text{methanylylidene})\text{bis}(2,4\text{-di-}t\text{ert-butylphenol})\}$ was prepared by following an earlier reported procedure of salen ligand preparation. The Co(II) complex, **3.1** was prepared by stirring a mixture of cobalt(II) acetate tetrahydrate with one equivalent of L2H_2 in methanol and diethyl ether mixture. Isolated complex **3.1** was characterized by various spectroscopic analyses as well as the single crystal X-ray structure determination. The crystallographic data and other metric parameters listed in appendix II. The perspective ORTEP view of the **3.1** is shown in figure 3.1. Structural characterization revealed that Co(II) ion is coordinated by two N_{imine} and two O_{phenol} atoms from the ligand in an overall distorted square planar geometry. The average $\text{Co-N}_{\text{imine}}$ and $\text{Co-O}_{\text{phenolato}}$ distances are 1.848 and 1.845 Å, respectively, in **3.1**. These are within the range found in earlier

reported examples.¹⁷ The phenol moieties of the ligands are coordinated to the metal ion as phenolate and thereby neutralizing the overall charge of the metal ions.

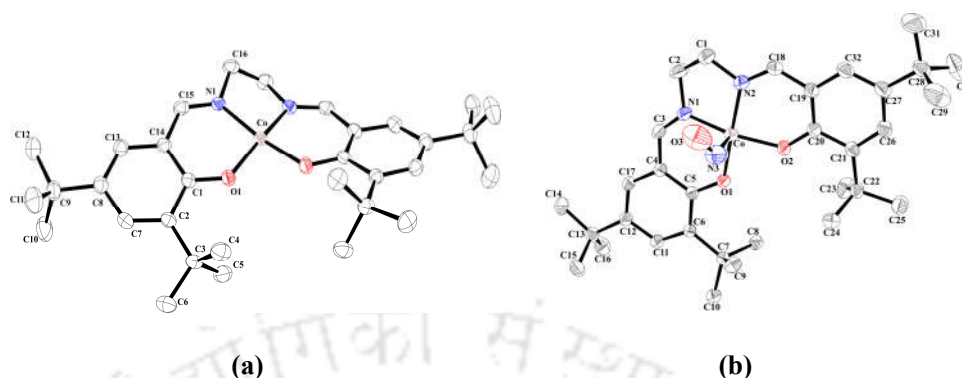


Figure 3.1. ORTEP diagram of complexes (a) **3.1** and (b) **3.2** (30% thermal ellipsoid plot. H-atoms are not shown for clarity).

NO reactivity of complex **3.1**

In dry and degassed THF solution of **3.1**, NO gas was purged for ~5 min and the red color of the solution became dark brown which corresponds to complex **3.2**. It was isolated by precipitation and characterized *via* various spectroscopic analyses as **3.2**. In UV-visible spectroscopy, the absorption bands at 406 nm ($\epsilon/M^{-1}cm^{-1}$, 1640) and 711 nm ($\epsilon/M^{-1}cm^{-1}$, 45) of **3.1** were diminished upon addition of NO (Figure 3.2a).

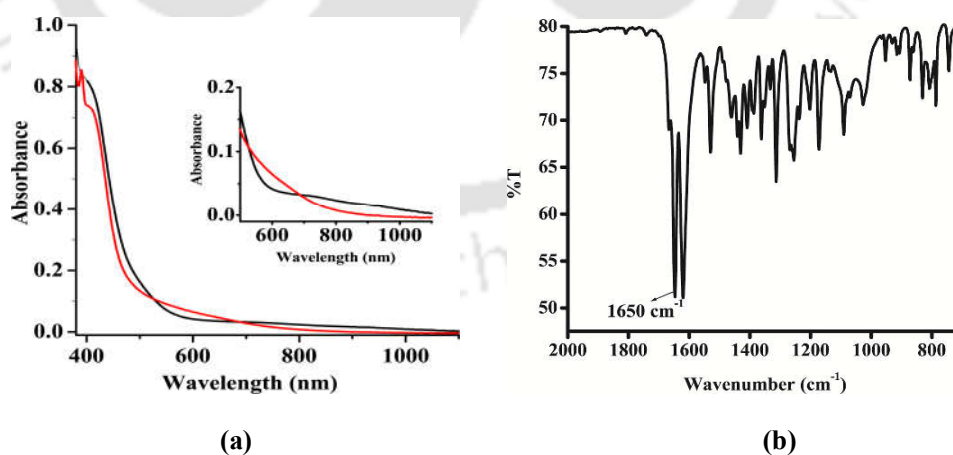


Figure 3.2. (a) UV-visible spectra of complex **3.1** (black) and after addition of NO, **3.2** (red). (b) FT-IR spectrum of complex **3.2** in KBr.

In FT-IR spectroscopy, complex **3.2** shows a strong stretching frequency at 1650 cm^{-1} which is attributed to the N-O stretching frequency of a coordinated nitrosyl group (Figure 3.2b). In case of $[(12\text{-TMC})\text{Co}(\text{NO})]^{2+}$ and $[(13\text{-TMC})\text{Co}(\text{NO})]^{2+}$, these nitrosyl stretching frequencies appeared at 1712 and 1716 cm^{-1} in solution FT-IR spectroscopy.¹³ In X-band EPR spectroscopy, **3.2** was found to be silent in THF solution at room temperature as well as at 77 K (Appendix II). ESI mass spectrum of **3.2** displayed peaks assignable to the $[(\text{L}2)\text{Co}]^+$ fragments (Appendix II). This is attributed to the facile loss of the NO group as axial ligand under reaction condition. This was observed earlier with cobalt nitrosyls of porphyrin ligands.¹⁸ Further, **3.2** was characterized by single crystal X-ray structure determination (Figure 3.1b). The crystal structure reveals that Co(II) centre is coordinated by two nitrogen atoms and two phenolato oxygen atoms of the ligand and one N-atom from nitrosyl in an overall square pyramidal geometry. The NO ligand is axially coordinated to the cobalt center in a bent fashion. The crystallographic data and other metric parameters listed in Appendix II. The N-O bond length is 1.155 \AA and the large bending of the metal-nitrosyl moiety with Co-N-O bond angle is 126.47° is also consistent with coordinated $\{\text{CoNO}\}$.^{8,19}

Reactivity of complex **3.2** with potassium superoxide (KO_2)

It was reported earlier that cobalt-nitrosyls react with molecular O_2 leading to formation of corresponding nitrite complexes.²⁰ However, **3.2** did not react with O_2 . Similar observation was reported with Co(III)-nitrosyls, $[(12\text{-TMC})\text{Co}(\text{NO})]^{2+}$ and $[(13\text{-TMC})\text{Co}(\text{NO})]^{2+}$.¹³ In those cases it was speculated that NO did not undergo dissociation in the complexes which is required for the O_2 reactivity.¹³ However, addition of KO_2 in presence of 18-crown-6 in dry THF solution **3.2** afforded a change in color. In the UV-visible spectroscopy, a new absorption band at 665 nm ($\epsilon/M^{-1}\text{cm}^{-1}$, 95) was observed, this is attributed to the formation of corresponding Co(III)-nitrate complex, **3.3** (Figure 3.3a). In FT-IR the 1650 cm^{-1}

nitrosyl stretching frequency disappeared and a new stretching frequency at 1385 cm^{-1} appeared which is assignable to the NO_3^- stretching frequency (Figure 3.3b). Even after several attempts we could not get any X-ray quality crystal of **3.3**. Other spectral and elemental analyses confirm the formation of **3.3** unambiguously. However, the formation of **3.3** suggests the formation of a putative ONOO^- intermediate in the course of the reaction (Scheme 3.1) as NO_3^- is the common isomerisation product of ONOO^- .

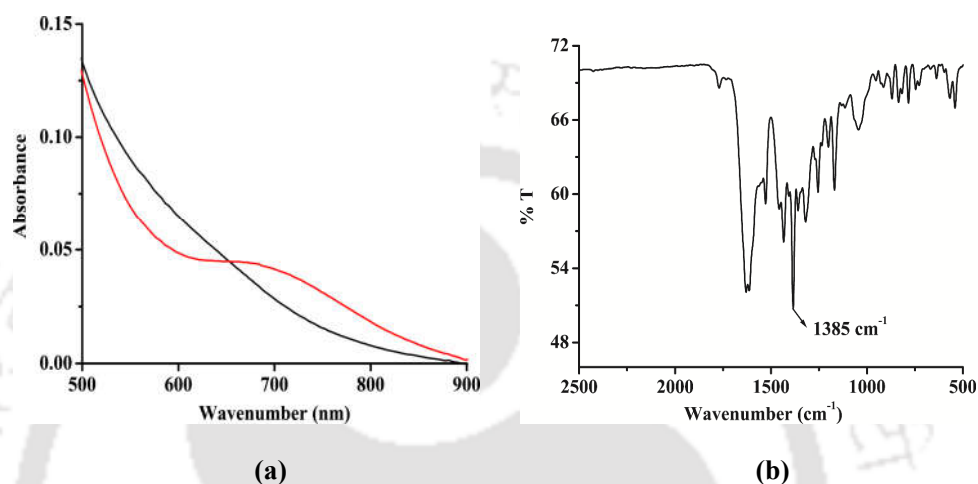
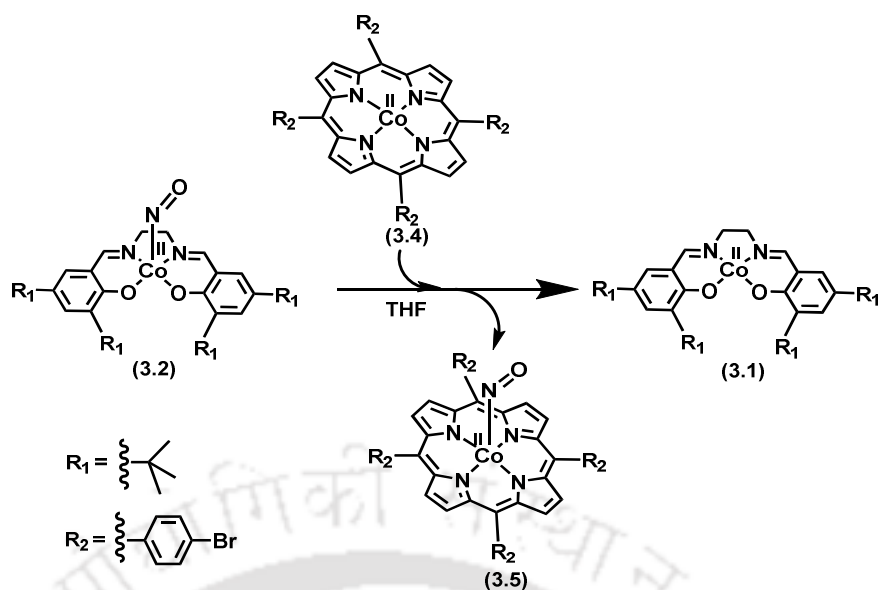


Figure 3.3. (a) UV-visible spectra of complex **3.2** (black) and after addition of KO_2 , **3.3** (red) in THF. (b) FT-IR spectrum of complex **3.3** in KBr.

Since direct spectroscopic evidence of the ONOO^- intermediate could not be obtained owing to its unstable nature, the reported methods for identification of ONOO^- have been followed.^{12b} When the reaction of **3.2** with KO_2 is carried out at $-40\text{ }^\circ\text{C}$ followed by the addition of 2,4-di-*tert*-butylphenol (DTBP), complex **3.3** is formed and unreacted DTBP is recovered. However, effective nitration (*ca.* 50%) is observed when DTBP is added before the addition of KO_2 (Scheme 3.1 and Experimental section). In this connection, nitrosyls of copper(II) complexes with methyl 2-(2-hydroxybenzylamino)-3-(1H-imidazol-5-yl)propanoate²¹ and *bis*(2-ethyl-4-methyl-imidazol-5-yl)methane²² ligands were reported to react with H_2O_2 to result in the corresponding nitrate products. They were also found to



Scheme 3.2. Transfer of nitrosyl group from complex **3.2** to **3.4**.

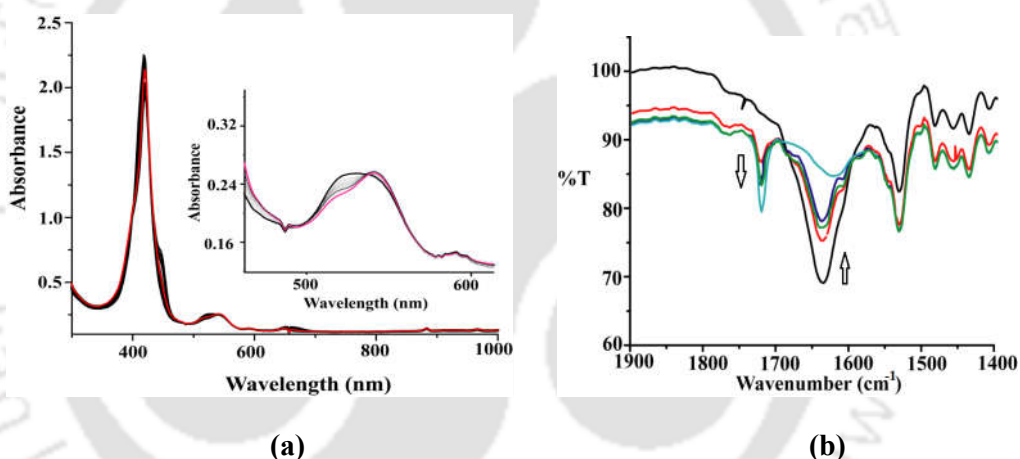


Figure 3.4. (a) UV-visible spectral monitoring of the reaction of complex **3.2** with **3.4** (black) to result **3.5** (red) in THF. (b) Solution FT-IR monitoring of the reaction of complex **3.2** (black) with **3.4** to result **3.5** (blue) in THF.

The single crystal X-ray structure of **3.5** reveals that the NO ligand is axially coordinated to the cobalt center in a bent fashion in an overall distorted square pyramidal geometry (Figure 3.5b). The crystallographic data and other metric parameters listed in appendix II. The N-O bond length is 1.195 Å and Co-N-O bond angle is 119.42° which is consistent

with coordinated $\{\text{CoNO}\}^8$.¹⁹ In a similar manner the NO transfer was reported from $[(14\text{-TMC})\text{Co}(\text{NO})]^{2+}$ to $[(12\text{-TMC})\text{Co}]^{2+}$.¹⁶

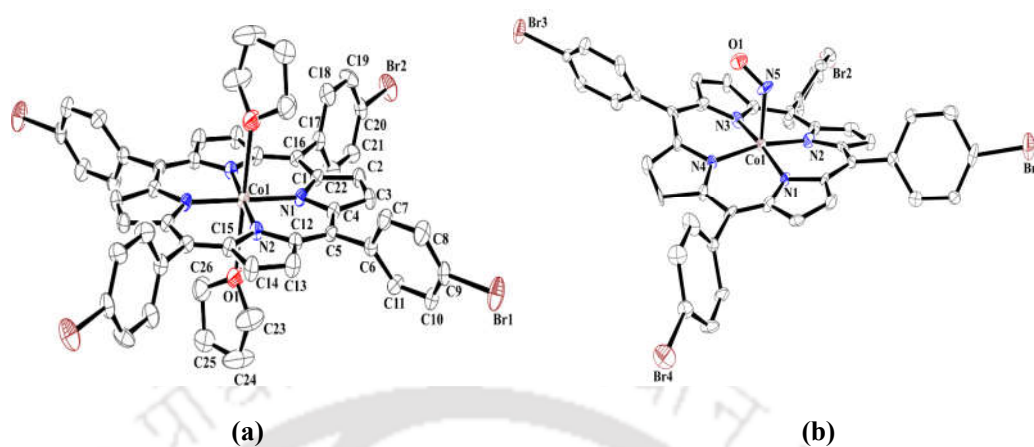


Figure 3.5. ORTEP diagram of complexes (a) **3.4** and (b) **3.5**. (30% thermal ellipsoid plot. H-atoms are not shown for clarity).

3.3 Experimental section

3.3.1 Materials and methods

All reagents and solvents of reagent grade were purchased from commercial sources and used as received except specified. Deoxygenation of the solvent and solutions was effected by repeated vacuum/purge cycles or bubbling with nitrogen or argon for 30 min. NO gas was used from a cylinder after purification using standard procedure. The dilution of NO was effected with argon gas using Environics Series 4040 computerized gas dilution system. UV-visible spectra were recorded on Agilent HP 8454 diode array UV-visible spectrophotometer. FT-IR spectra of the solid samples were taken on a Perkin Elmer spectrophotometer with samples prepared as KBr pellets. Solution electrical conductivity was measured using a Systronic 305 conductivity bridge. $^1\text{H-NMR}$ and $^{13}\text{C-NMR}$ spectra were recorded respectively in 400 MHz or 600 MHz and 100 MHz Varian FT spectrometer. Chemical shifts (ppm) were referenced either with an internal standard (Me_4Si) or to the residual solvent peaks. The X-band Electron Paramagnetic Resonance

(EPR) spectra were recorded on a JES-FA200 ESR spectrometer, at room temperature or at 77 K with microwave power, 0.998 mW; microwave frequency, 9.14 GHz and modulation amplitude, 2. Elemental analyses were obtained from a Perkin Elmer Series II Analyzer. The magnetic moment of complexes was measured on a Cambridge Magnetic Balance. Single crystals were grown by slow diffusion followed by slow evaporation technique. The intensity data were collected using a Bruker SMART APEX-II CCD diffractometer, equipped with a fine focus 1.75 kW sealed tube MoK α radiation ($\lambda = 0.71073 \text{ \AA}$) at 273(3) K, with increasing ω (width of 0.3° per frame) at a scan speed of 3 s/frame. The SMART software was used for data acquisition.²³ Data integration and reduction were undertaken with SAINT and XPREP software.²⁴ Structures were solved by direct methods using SHELXS-97 and refined with full-matrix least squares on F^2 using SHELXL-97.²⁵ Structural illustrations have been drawn with ORTEP-3 for Windows.²⁶

3.3.2 Syntheses

3.3.2.1 Syntheses of ligands

(a) L2H₂, [6,6'-((1E,1'E)-(ethane-1,2-diyl)*bis*(azanylylidene))*bis* (methanylylidene))*bis*-(2,4-di-*tert*-butylphenol)]

To the solution of ethylenediamine (0.6 g, 10 mmol) in 10 mL ethanol, 20 mL ethanol solution of 3,5-di-*tert*-butylsalicylaldehyde (4.68 g, 20 mmol) was added drop wise at room temperature. The reaction mixture was allowed to stir for 4 h till yellow colored precipitate formed. It was filtered off and washed with cold ethanol. After washing the solid was dried in air and kept in desiccator for overnight. Yield: 4.1g (83%). Elemental analyses for C₃₂H₄₈N₂O₂, Calcd. (%): C, 78.00; H, 9.82; N, 5.69. Found (%): C, 77.95; H, 9.79; N, 5.78. FT-IR (in KBr): 2961, 2869, 1629, 1481, 1466, 1439, 1361, 1270, 1253, 1041, 879, 839, 830, 773, 729, 710, 645 cm⁻¹. ¹H-NMR (400 MHz, CDCl₃): δ_{ppm} , 1.23 (s,

9H), 1.41 (s, 9H), 3.92 (s, 1H), 7.06 (s, 1H), 7.36 (s, 1H), 8.38 (s, 1H), 13.62 (s, 1H). ^{13}C -NMR (100 MHz, CDCl_3): δ_{ppm} , 29.6, 31.7, 34.3, 59.8, 118.0, 126.3, 127.2, 136.8, 140.3, 158.2, 167.8.

(b) **L3H₂, [5,10,15,20-tetrakis(4'-bromophenyl)porphyrin]**

The ligand **L3H₂** was prepared by following earlier reported general procedure of porphyrin synthesis with slight modification.²⁸ *p*-Bromobenzaldehyde (3.70 g, 20 mmol) and freshly distilled pyrrole (1.34 g, 20 mmol) were added to 37 mL of propionic acid. After refluxing for 2 h the solution was cooled to room temperature. It was then neutralized by aqueous Na_2CO_3 . A precipitate appeared and was filtered off. The crude mass was subjected to purification using column chromatography using CH_2Cl_2 and hexane as solvent to afford the desired ligand as purple solid. Yield: 0.697 g (20%). Elemental analyses for $\text{C}_{44}\text{H}_{26}\text{N}_4\text{Br}_4$. Calcd. (%): C, 56.81; H, 2.82; N, 6.02, found (%): C, 56.65; H, 2.88; N, 6.07. FT-IR (in KBr): 3439, 2922, 1473, 1394, 1071, 1010, 962, 803, 730 cm^{-1} . ^1H -NMR (600 MHz, CDCl_3): δ_{ppm} , 7.90-7.91 (d, 8H), 8.06-8.07 (d, 8H), 8.84 (s, 8H). Mass (m/z): Calcd: 929.885, found: 930.867 (M+1).

3.3.2.2 Syntheses of complexes

(a) **3.1, [(L2)Co]**

Complex **3.1** was prepared by following the reported procedure with some modifications.²⁷ Cobalt(II) acetate tetrahydrate (1.25 g, 5 mmol) was taken in a 50 mL round bottom flask, dissolved in 10 mL of MeOH. To this, a solution of ligand **L2H₂** (2.46 g, 5 mmol) in hot methanol (25 mL) was added and stirred for 3 h. A red color precipitate was formed, it was filtered off and washed several time by cold methanol. After washing the solid was dried in air and then kept in desiccator for overnight. Finally it was recrystallized from THF solution to obtain red crystals. Yield: 1.77 g (72%). Elemental

analyses for $C_{32}H_{46}N_2O_2Co$, Calcd (%): C, 69.92; H, 8.44; N, 5.10. Found (%): C, 69.80; H, 8.41; N, 5.16. FT-IR (in KBr): 3433, 2952, 1598, 1528, 1462, 1439, 1254, 1175, 872, 786 cm^{-1} . UV-visible (THF): 406 nm ($\epsilon/M^{-1}cm^{-1}$, 1640) and 711 nm ($\epsilon/M^{-1}cm^{-1}$, 45). Molar conductance (THF): 38 Scm^2mol^{-1} observed magnetic moment: 1.55 μ_B .

(b) 3.2, [(L2)Co(NO)]

In 20 mL of dry and degassed THF solution of **3.1** (275 mg, 0.5 mmol), freshly purified NO was bubbled till greenish brown color was appeared. The reaction mixture was kept at room temperature for crystallization. Yield: 0.250 g (88%). Elemental analyses for $C_{32}H_{46}N_3O_3Co$, Calcd (%): C, 66.31; H, 8.00; N, 7.25. Found (%): C, 66.24; H, 8.02; N, 7.34. FT-IR (in KBr): 2955, 1649, 1620, 1529, 1430, 1313, 1172, 1090, 744, 530 cm^{-1} .

(c) 3.3, [(L2)Co(NO₃)]⁻

Complex **3.3** was prepared from freshly prepared complex **3.2**, (290 mg, 0.5 mmol) and 2 equivalent of KO_2 in presence of 18-crown-6 (5 equivalent) in dry THF at $-80^\circ C$. The volume of the reaction mixture was reduced to 5 mL using vacuum and layered with hexane. The reaction mixture was kept in freezer for 24 h. The dark brown precipitate was filtered off and washed with hexane for several times. The solid mass was kept at desiccator for overnight. Yield: 0.195 g (64%). Elemental analyses for $C_{32}H_{46}N_3O_5Co$, Calcd (%): C, 62.84; H, 7.58; N, 6.87. Found (%): C, 62.77; H, 7.69; N, 6.88. FT-IR (in KBr): 1630, 1613, 1434, 1385, 1359, 1321, 1255, 1170, 1046, 834, 784, 540 cm^{-1} . UV-visible (THF): 665 nm ($\epsilon/M^{-1}cm^{-1}$, 95). Molar conductance (THF): 35 Scm^2mol^{-1} .

(d) 3.4, [(L3)Co]

To a mixture of ligand, **L3H₂** (0.232 g, 0.25 mmol) in $CHCl_3$ (12 mL) and AcOH (12 mL), $Co(OAc)_2 \cdot 4H_2O$ (0.622 g, 2.50 mmol) was added. After refluxing at $120^\circ C$ for 2 h, the

precipitate was filtered and washed with MeOH (15 mL \times 4). The crude mass was subjected to column chromatography to result in complex **3.4** as violet solid. Yield: 0.160 g (65%). Elemental analyses for $C_{44}H_{24}N_4Br_4Co$, Calcd. (%): C, 53.53; H, 2.45; N, 5.68, found (%): C, 53.48; H, 2.49; N, 5.71. UV-visible (THF): 412 nm ($\epsilon/M^{-1}cm^{-1}$, 2.01×10^5), 527 nm ($\epsilon/M^{-1}cm^{-1}$, 2.8×10^4). FT-IR (in KBr): 1541, 1483, 1347, 1071, 1001, 800, 719, 486 cm^{-1} . Mass (m/z): Calcd. 986.80, found: 986.50 (molecular ion peak).

(e) **3.5**, [(L3)Co(NO)]

In 20 mL of dry and degassed THF solution of **3.2** (0.290 g, 0.5 mmol), a solution of **3.4** (490 mg, 0.5 mmol) in 50 mL of dry THF was added. After stirring at room temperature for 2 h the mixture was dried under reduced pressure. The crude mass was subjected to column chromatography using $CHCl_3$ and hexane as eluent to result in complex **3.5**. Elemental analyses for $C_{44}H_{24}N_5OBr_4Co$, Calcd. (%): C, 51.95; H, 2.38; N, 6.88, found (%): C, 51.78; H, 2.47; N, 6.76. UV-visible (THF): 416 nm ($\epsilon/M^{-1}cm^{-1}$, 1.85×10^5), 540 nm ($\epsilon/M^{-1}cm^{-1}$, 2.6×10^4). FT-IR (in KBr): 1720, 1480, 1348, 1345, 1070, 1008, 805, 762, 713, 480 cm^{-1} . 1H -NMR (600 MHz, $CDCl_3$): δ_{ppm} , 7.92-7.89 (d, 8H), 8.05-8.02 (d, 8H), 8.90 (s, 4H), 9.02 (s, 4H).

3.3.2.3 Reaction of complex 3.2 with KO_2 in presence of 2,4-di-*tert*-butylphenol

In 20 mL THF solution of freshly prepared complex **3.2** (0.290 g, 0.5 mmol), a solution of 2,4-di-*tert*-butyl phenol (DTBP) (0.620 g, 3 mmol in 5 mL dry THF), was added and the mixture was cooled to -40 $^{\circ}C$. To that $KO_2/18$ -crown-6 (~ 1 equivalent) was added, and the mixture was stirred for 20 min. After that, it was warmed to room temperature and dried under reduce pressure. The solid mass was then subjected to column chromatography using silica gel column and hexane as solvent to obtain 2, 4-di-*tert*-butyl-6-nitrophenol. Yield: 0.063 g (50%). Elemental analyses for $C_{14}H_{21}NO_3$, Calcd. (%): C, 30.40; H, 4.01; N, 7.60,

found (%): C, 30.35; H, 4.03; N, 7.75. $^1\text{H-NMR}$ (600 MHz, CDCl_3): δ_{ppm} , 1.32 (s, 9H), 1.44 (s, 9H), 5.22 (s, 1H), 7.11 (s, 1H), 7.40 (s, 1H). $^{13}\text{C-NMR}$ (150 MHz, CDCl_3): δ_{ppm} , 29.6, 31.6, 34.4, 35.2, 122.3, 124.8, 125.2, 136.1, 142.9, 149.7. Mass (m/z): Calcd: 251.15, found: 250.53 (M-1).

3.4 Conclusion

In conclusion, the present work demonstrates an example of a Co(II)-salen complex, **3.1**, which reacts with NO in THF to form a stable Co(II)-nitrosyl complex, **3.2**. This nitrosyl complex reacts with KO_2 to result in corresponding nitrato complex, **3.3**. The reaction is believed to proceed *via* formation of unstable peroxyxynitrite intermediate. The nitrosyl ligand of the Co(II)-nitrosyl complex is found to be transferable. Nitrosyl transfer reaction of this nitrosyl complex was performed with a modified tetraphenylporphyrinato Co(II) complex, **3.4** which results in the formation of corresponding cobalt-porphyrinate nitrosyl complex, **3.5**.

3.5 References

- (1) (a) Culotta, E.; Koshland, D. E. Jr. *Science* **1992**, 258, 1862. (b) Moncada, S.; Palmer, R. M. J.; Higgs, E. A. *Pharmacol. Rev.* **1991**, 43, 109.
- (2) (a) Furchgott, R. F. *Angew. Chem. Int. Ed.* **1999**, 38, 1870. (b) Ignarro, L. J.; Buga, G. M.; Wood, K. S.; Byrns, R. E.; Chaudhuri, G. *Proc. Natl. Acad. Sci. U. S. A.* **1987**, 84, 9265. (c) Palmer, R. M. J.; Ferrige, A. G.; Moncada, S. *Nature* **1987**, 327, 524.
- (3) (a) Ignarro, L. J. *Nitric Oxide: Biology and Pathobiology* Ed. Academic Press, San Diego, CA, **2000**. (b) Richter-Addo, G. B.; Legzdins, P. *Metal Nitrosyls* Oxford University Press, New York **1992**. (c) Butler, A. R.; Williams, D. *Chem. Soc. Rev.* **1993**, 233. (d) Feelisch, M.; Stamler, J. S. *Methods in Nitric Oxide Research* Ed.

- John Wiley and Sons, New York **1996**. (e) Jia, L.; Bonaventura, C.; Bonaventura J.; Stamler, J. S. *Nature* **1996**, *380*, 221.
- (4) Fang, F. C. *Nitric Oxide and Infection* Ed. Kluwer Academic/Plenum Publishers, New York **1999**.
- (5) (a) Ford, P. C.; Wink, D. A.; Stanbury, D. M. *FEBS Lett.* **1993**, *326*, 1. (b) Tran, N. G.; Kalyvas, H.; Skodje, K. M.; Hayashi, T.; Moënné-Loccoz, P.; Callan, P. E.; Shearer, J.; Kirschenbaum, L. J.; Kim, E. *J. Am. Chem. Soc.* **2011**, *133*, 1184. (c) Goldstein, S.; Lind, J.; Merenyi, G. *Chem. Rev.* **2005**, *105*, 2457. (d) Speelman, A. L.; Lehnert, N. *Acc. Chem. Res.* **2014**, *47*, 1106.
- (6) (a) Pacher, P.; Beckman, J. S.; Liaudet, L. *Physiol. Rev.* **2007**, *87*, 315. (b) Beckman, J. S.; Koppenol, W. H. *Am. J. Physiol.* **1996**, *271*, 1424.
- (7) Radi, R. *Proc. Natl. Acad. Sci. U.S.A.* **2004**, *101*, 4003.
- (8) Qiao, L.; Lu, Y.; Liu, B.; Girault, H. H. *J. Am. Chem. Soc.* **2011**, *133*, 19823.
- (9) Vilet, A.; Eiserich, J. P.; Halliwell, B.; Cross, C. E. *J. Biol. Chem.* **1997**, *272*, 7617.
- (10) (a) Hughes, M. N.; Nicklin, H. G.; Sackrle, W. A. C. *J. Chem. Soc.* **1971**, 3722. (b) Babich, O. A.; Gould, E. S. *Res. Chem. Intermed.* **2002**, *28*, 575. (c) Ford, P. C.; Lorkovic, I. M. *Chem. Rev.* **2002**, *102*, 993.
- (11) (a) Herold, S.; Koppenol, W. H. *Coord. Chem. Rev.* **2005**, *249*, 499. (b) Roncaroli, F.; Videla, M.; Slep L. D.; Olabe, J. A. *Coord. Chem. Rev.* **2007**, *251*, 1903.
- (12) (a) Maiti, D.; Lee, D.-H.; Sarjeant, A. A. N.; Pau, M. Y. M.; Solomon, E. I.; Gaoutchenova, K.; Sundermeyer, J.; Karlin, K. D. *J. Am. Chem. Soc.* **2008**, *130*, 6700. (b) Yokoyama, A.; Cho, K. B.; Karlin, K. D.; Nam, W. *J. Am. Chem. Soc.* **2013**, *135*, 14900.
- (13) Kumar, P.; Lee, Y.-M.; Park, Y. J.; Siegler, M. A.; Karlin, K. D.; Nam, W. *J. Am. Chem. Soc.* **2015**, *137*, 4284.

- (14) Ungermann, C. B.; Caulton, K. G. *J. Am. Chem. Soc.* **1976**, *98*, 3862.
- (15) Franz, K. J.; Lippard, S. J. *Inorg. Chem.* **2000**, *39*, 3722.
- (16) Kumar, P.; Lee, Y.-M.; Hu, L.; Chen, J.; Park, Y. J.; Yao, J.; Chen, H.; Karlin, K. D.; Nam, W. *J. Am. Chem. Soc.* **2016**, *138*, 7753.
- (17) (a) Clarke, R. M.; Hazin, K.; Thompson, J. R.; Savard, D.; Prosser, K. E.; Storr, T. *Inorg. Chem.* **2016**, *55*, 762. (b) Deiasi, R.; Holt, S. L.; Post, A. *Inorg. Chem.* **1971**, *10*, 1498.
- (18) Richter-Addo, G. B.; Hodge, S. J.; Yi, G.-B.; Khan, M. A.; Ma, T.; Caemelbeck, E. V.; Huo, N.; Kadish, K. M. *Inorg. Chem.* **1996**, *35*, 6530.
- (19) (a) Enemark, J. H.; Feltham, R. D. *Coord. Chem. Rev.* **1974**, *5*, 686. (b) Richter-Addo, G. B.; Legzdins, P. *Metal Nitrosyls*, Oxford University Press: New York, **1992**. (c) McCleverty, J. A. *Chem. Rev.* **2004**, *104*, 403. (d) Berto, T. C.; Speelman, A. L.; Zheng, S.; Lehnert, N. *Coord. Chem. Rev.* **2013**, *257*, 244.
- (20) (a) Clarkson, S. G.; Basolo, F. *J. Chem. Soc. Chem. Commun.* **1972**, *119*, 670. (b) Clarkson, S. G.; Basolo, F. *Inorg. Chem.* **1973**, *12*, 1528. (c) Subedi, H.; Brasch, N. E. *Inorg. Chem.* **2013**, *52*, 11608. (d) Frech, C. M.; Blacque, O.; Schmalte, H. W.; Berke, H. *Dalton Trans.* **2006**, 4590.
- (21) Kalita, A.; Deka, R. C.; Mondal, B. *Inorg. Chem.* **2013**, *52*, 10897.
- (22) Kalita, A.; Kumar, P.; Mondal, B. *Chem. Commun.* **2012**, *48*, 4636.
- (23) SMART, SAINT and XPREP, Siemens Analytical X-ray Instruments Inc., Madison, Wisconsin, USA **1995**.
- (24) Sheldrick, G. M.; SADABS: University of Gottingen, Germany **1999**.
- (25) Sheldrick, G. M. SHELXS-97, University of Gottingen, Germany **1997**.
- (26) Farrugia, L. J. ORTEP-3 for Windows - a Version of ORTEP-III with a Graphical User Interface (GUI). *J. Appl. Crystallogr.* **1997**, *30*, 565.

- (27) Kochem, A.; Kanso, H.; Baptiste, B.; Arora, H.; Philouze, C.; Jarjays, O.; Vezin, H.; Luneau, D.; Orio, M.; Thomas, F. *Inorg. Chem.* **2012**, *51*, 10557.
- (28) (a) Adler, A. D.; Longo, F. R.; Finarelli.; Goldmacher, J.; Assour, J.; Korsakoff, L. *J. Org. Chem.* **1967**, *32*, 476. (b) Kadish, K. M.; Smith, K. M.; Guillard, R. *The Porphyrin Handbook* Ed. Elsevier **1999**.



Chapter 4

Reaction of a Nitrosyl Complex of Cobalt Porphyrin with Hydrogen Peroxide: Putative Formation of Peroxynitrite Intermediate

Abstract

A cobalt porphyrin complex, [(L4)Co], **4.1** {L4 = 5,10,15,20-*tetrakis*(4'-chlorophenyl)porphyrinate dianion} in dichloromethane solution was subjected to react with nitric oxide (NO) gas and resulted in the formation of the corresponding nitrosyl complex, [(L4)Co(NO)], **4.2** having {CoNO}⁸ description. It was characterized by spectroscopic studies and single crystal X-ray structure determination. It did not react with dioxygen. However, in CH₂Cl₂/CH₃CN solution, it reacted with H₂O₂ to result in the Co-nitrito complex, [(L4)Co(NO₂)], **4.3** with the simultaneous release of O₂. It induced ring nitration to the added phenol in an appreciable yield. The reaction presumably proceeds through the formation of corresponding Co-peroxynitrite intermediate.

4.1 Introduction

Nitric oxide (NO) is known to play the key roles in many physiological processes like neurotransmission, vasodilation, immune cytotoxicity, etc.^{1,2} It can also behave as a cytotoxic effector and /or pathogenic mediator when produced at high concentrations.³ It is believed that the cytotoxicity of NO is due to the formation of secondary reactive nitrogen species (RNS) like peroxynitrite (ONOO⁻) or nitrogen dioxide (NO₂).^{3,4} The formation of these secondary RNS may result from the oxidation of NO in the presence of oxidants like superoxide radicals (O₂⁻), hydrogen peroxide (H₂O₂) and/or transition metal ions.³ However, nitric oxide deoxygenases (NODs) are known to maintain the *in vivo* level of NO.^{5,6} It is known that the oxy-heme (*i.e.* iron(III)-superoxo) species of the NODs react with NO to result in nitrate (NO₃⁻) ion which is biologically benign. This reaction is believed to proceed through the formation of ONOO⁻ intermediates. The examples of discrete metal-peroxynitrite complexes are rare; only a cobalt-peroxynitrite complex is known to be discretely characterized.⁷ However, there are number of examples where metal-peroxynitrites are proposed to form as transient intermediate in the reaction of metal-oxygen species with NO. In those cases, metal-superoxo complexes of heme and non-heme iron, cobalt and copper were reported to react with NO to result in metal-peroxynitrite intermediates.^{8,9} Apart from those, recently the reaction of a non-heme Cr(IV)-peroxo complex with NO was reported to give Cr(III)-nitrate; whereas Cr(III)-superoxo has been shown to result in corresponding Cr(IV)-oxo and NO₂ through the formation of a presumed Cr(III)-peroxynitrite intermediate.¹⁰

On the other hand, a few instances involving the reaction of metal-nitrosyl and O₂ to form transient metal-peroxynitrite have been exemplified. For instance, Clarkson and Basolo reported the reaction of cobalt-nitrosyl complex with O₂ which resulted in the formation of corresponding nitrite product.¹¹ Kim *et. al* reported the reaction of a non-heme

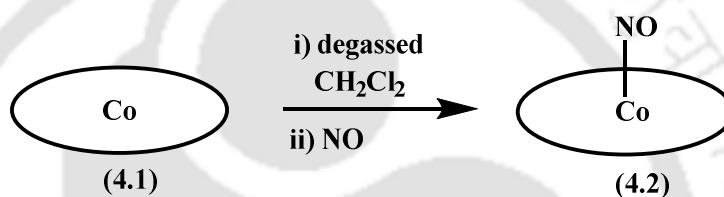
dinitrosyliron with O₂ to afford nitrate.¹² In a similar reaction {CuNO}¹⁰ species was found to result in corresponding nitrite and O₂.¹³ We reported the reaction of {CuNO}¹⁰ complex with H₂O₂ to give copper-nitrato complex *via* thermal decomposition of a presumed Cu^I-peroxynitrite intermediate.¹⁴ Thus, the metal complex mediated reaction of NO with various reduced O₂ species is of immense importance for the understanding of NO reactivity in biological systems. In addition, peroxynitrite mediated nitration of added phenols resembles the biologically well-known tyrosine nitration.

Herein we describe the synthesis, structural characterization of a nitrosyl complex of cobalt porphyrin, [(L4)Co(NO)]. In the presence of hydrogen peroxide (H₂O₂) the cobalt-nitrosyl complex exhibits NOD reactivity where the intermediate formation of peroxynitrite is implicated.

4.2 Results and discussion

The cobalt porphyrin complex, [(L4)Co], **4.1** [L4 = (5,10,15,20-tetrakis(4'-chlorophenyl)porphyrinate dianion)] was prepared following an earlier reported procedure.¹⁵ Elemental and spectral analyses confirmed the formation of the complex (Experimental section and Appendix III). Bubbling of an excess of NO gas to the degassed dichloromethane solution of **4.1** resulted in the formation of corresponding Co-nitrosyl complex [(L4)Co(NO)], **4.2** (Experimental section and Scheme 4.1). It was isolated as solid and characterized spectroscopically as well as by single crystal X-ray structure determination. The ORTEP diagram of **4.1** is shown in figure 4.1a. The crystallographic data and metric parameters are listed in the appendix III. The crystal structure revealed that the cobalt center is six coordinated with a distorted octahedral geometry. The four N-atoms from the porphyrinate dianion bind the metal ion to form a square plane and two THF units are bonded to the metal centre from the axial position. The average Co-Np bond distance

was 1.989(2) Å which is within the range observed for hexa-coordinated Co(II)-porphyrinates.^{16a} Co-O_{THF} distances were found to be 2.404 (3) Å. The average Co-O_{THF} distance of 2.204 (2) Å was reported in case of [(F₂₈TPP)Co(THF)₂].^{16b} In case of five coordinated Co(II)-porphyrinate with THF as an axial ligand, this distance was reported to be 2.206 (2) Å.^{16a} It is to be noted that for six-coordinated Co(III)-porphyrinates, the average Co-N_p distance lies in the range of 1.950 Å.^{16d} In ¹H-NMR spectrum, complex **4.1** in CDCl₃ displayed peak broadening expected for low spin cobalt(II) porphyrinates (Appendix III). In the UV-visible spectrum, **4.2** exhibited characteristic absorption bands at 415 nm ($\epsilon/M^{-1}cm^{-1}$, 2.21×10^5) and 538 nm ($\epsilon/M^{-1}cm^{-1}$, 3.1×10^4) (Figure 4.2a).



Scheme 4.1. Synthesis of nitrosyl complex **4.2**.

Complex **4.2** was silent in the X-band EPR spectroscopy suggesting the presence of Co(III) centre having [Co^{III}-NO⁻] or {CoNO}⁸ description according to the Enemark-Feltham notation.¹⁷ In ¹H-NMR spectrum, the pyrrole protons appeared as singlet at 8.94 and 8.82 ppm and the protons from the phenyl group appeared as doublet at 8.05 and 7.64 ppm (Appendix III). In the FT-IR spectrum, the NO stretching band appeared at 1701 cm⁻¹ (Figure 4.2b) which is consistent with the {CoNO}⁸ description. This frequency is slightly higher than those reported earlier for [(TPP)Co(NO)] (1689 cm⁻¹, in KBr) and [(OEP)Co(NO)] (1675 cm⁻¹, in CH₂Cl₂).¹⁸ In case of cobalt porphyrin nitrosyls of the form [{T(*p/m*-X)PP}Co(NO)] [*p/m*-X = *p*-OCH₃, *p*-CH₃, *m*-CH₃, *p*-H, *m*-OCH₃, *p*-OCF₃, *p*-CF₃, *p*-CN etc.], the $\bar{\nu}_{NO}$ band in CH₂Cl₂ was reported previously to appear in the range of 1681-1695 cm⁻¹.²²

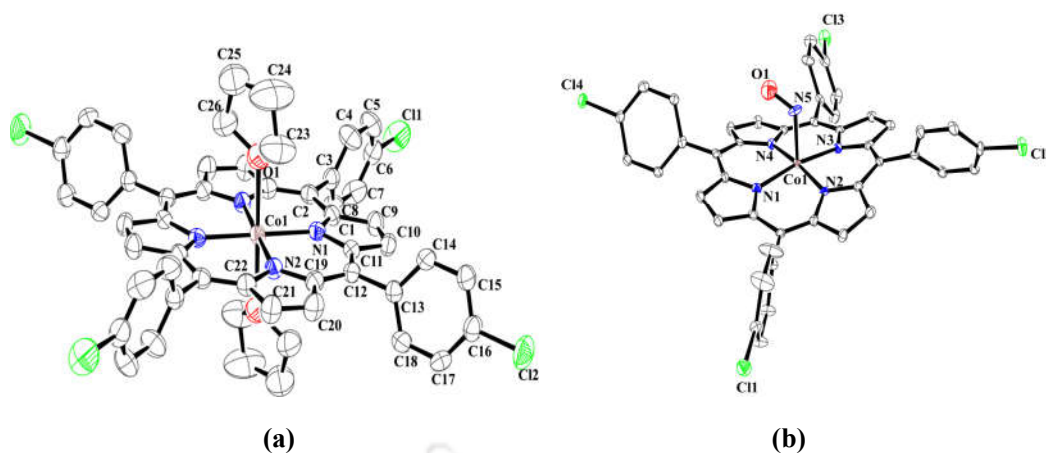


Figure 4.1. ORTEP diagram of complexes (a) **4.1** (b) **4.2**. (30% thermal ellipsoid plot. H-atoms and solvent molecules are not shown for clarity).

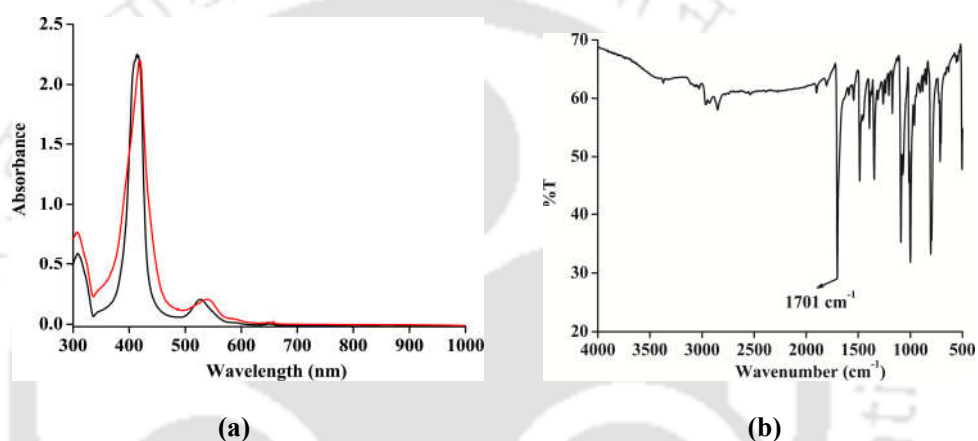


Figure 4.2. (a) UV-visible spectra of complexes **4.1** (black) and **4.2** (red) in dichloromethane. (b) FT-IR spectrum of complex **4.2** in KBr.

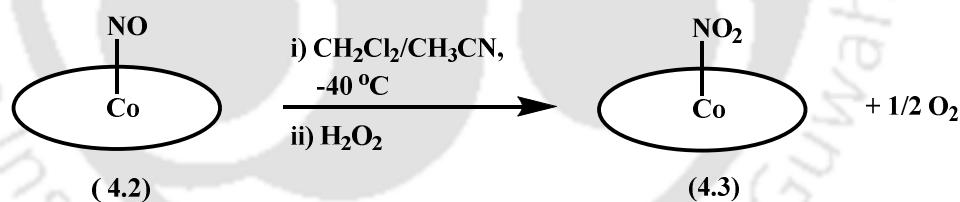
The ESI mass spectrum of **4.2** was dominated by the peak at m/z , 809.05 assignable to $[(L4)Co]^+$ [calcd. m/z , 809.00]. This is attributed to the facile loss of axial NO ligand under experimental condition.¹⁹

Furthermore, complex **4.2** was characterized by a single crystal X-ray structure determination. The ORTEP diagram is shown in figure 4.1b. The crystallographic data and other metric parameters are listed in the appendix III. The structure revealed that the NO is coordinated axially to the cobalt centre in an end-on fashion resulting in a distorted square-pyramidal geometry around the cobalt centre. Notably, the Co-N_p distances in **4.2** are in

the range of 1.974 (6) Å to 1.990 (6) Å with an average of 1.981 (6) Å. This distance is bit larger than that reported for Co(III)-porphyrinates; but in the range of Co(II)-porphyrinates.¹⁶ The Co-NO moiety is bent with a bond angle of 118.4°. The Co-N_{NO} bond distance is 1.846 (7) Å. The N-O distance was found to be 1.230 (1) Å. These are well within the range of those reported previously.¹⁹ The observation of bent NO is consistent with {CoNO}⁸ description.

Reactivity of complex **4.2** with O₂ and H₂O₂

The reactivity of **4.2** with oxidants like O₂ and H₂O₂ have been explored. It was observed that **4.2** in CH₂Cl₂ solution is inert toward O₂. This is indeed in accord with the earlier reported observations that five coordinated square pyramidal cobalt(II) nitrosyls do not react with O₂.²⁰ Similar observation was reported with Co(III)-nitrosyls of 12 and 13-membered N-tetramethylated cyclam ligands as well.²⁰ However, in CH₂Cl₂/CH₃CN solution **4.2** was found to react with H₂O₂. Addition of H₂O₂ to the CH₂Cl₂/CH₃CN solution of **4.2** at -40 °C gave corresponding Co-nitrito complex, **4.3** (Scheme 4.2).



Scheme 4.2. Reaction of complex **4.2** with H₂O₂.

In the UV-visible spectrum, the characteristic absorption bands of **4.2** at 415 nm and 538 nm disappeared with the formation of new ones at 430 nm ($\epsilon/M^{-1}\text{cm}^{-1}$, 2.84×10^5), 546 ($\epsilon/M^{-1}\text{cm}^{-1}$, 3.3×10^4) and 665 nm ($\epsilon/M^{-1}\text{cm}^{-1}$, 4.2×10^3), respectively (Figure 4.3a). Spectral titration suggested that the stoichiometric ratio of **4.2** with H₂O₂ is 1:1. Complex **4.3** was isolated and characterized as the corresponding Co(III)-nitrito complex,

[(L4)Co(NO₂)] on the basis of microanalysis and spectroscopic analyses (Experimental section and Appendix III).

The appearance of the signals in the diamagnetic range in ¹H-NMR spectrum of **4.3** in CDCl₃ is in agreement with the existence of low spin cobalt(III) centre in the complex. The pyrrole protons appeared together at 8.90 ppm; whereas the phenyl protons appeared as two doublets at 8.09 and 7.73 ppm, respectively. The ESI mass spectrum of **4.3** displayed the molecular ion peak (M+1) at m/z, 856.08 (calcd. 854.99) (Figure 4.3b). The observed isotopic distribution pattern is also in good agreement with the simulated one.

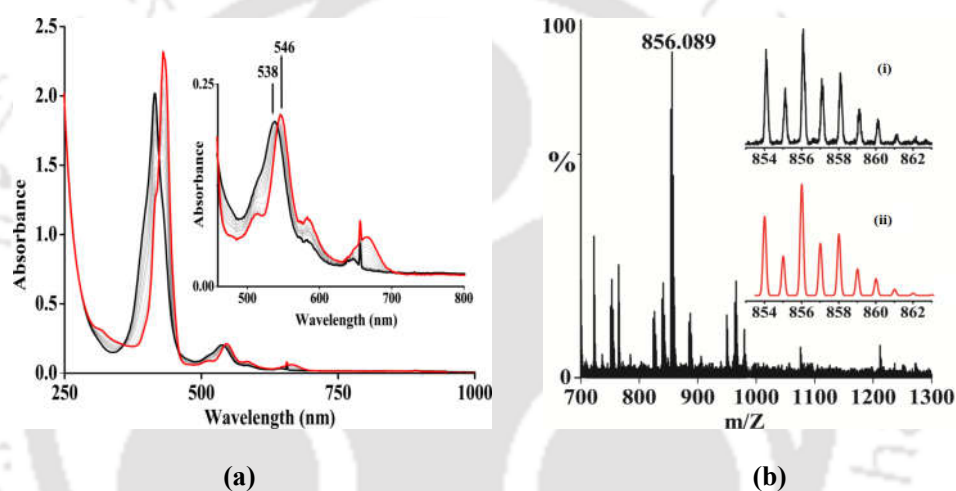


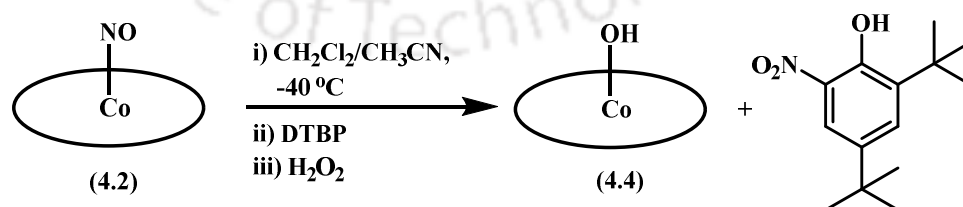
Figure 4.3. UV-visible spectral monitoring of complex **4.2** (black) and after addition of H₂O₂ to result in complex **4.3** (red) at -40 °C. (b) ESI-mass spectrum of complex **4.3** in acetonitrile. Inset: (i) experimental (black) and (ii) simulated (red) isotopic distribution pattern.

In the FT-IR spectrum, the stretching frequencies at 1270 cm⁻¹ is assignable to the nitrite (NO₂⁻) stretching (Appendix III). In cases of earlier reported cobalt porphyrin nitrites, this stretching was observed in the similar range.²¹ Comparing the other reported results of nitrites of metal porphyrinates, it is logical to assume that **4.3** as an N-bound nitrite.²¹ Even after several attempts, we could not get the X-ray quality crystal of **4.3** for structural characterization. The formation of cobalt-nitrito complex is supposed to be accompanied by the release of O₂ (Scheme 4.2). The formation of O₂ in the reaction was confirmed by

its detection in the GC-mass spectral analysis of the headspace gas of the reaction flask and by alkaline pyrogallol test, as well. However, no attempts were made to quantify the amount of O_2 formed in the reaction.

It is to be noted that in case of aqueous peroxyxynitrite chemistry, it is reported earlier that $ONOOH$ and $ONOO^-$ react to result in NO_2^- , O_2 and H^+ .²² On the other hand, Cu-peroxyxynitrite complexes are also known to undergo transformation to Cu(II)-nitrito complexes with the release of O_2 .¹³ Though these observations suggested the formation of Co-peroxyxynitrite intermediate, no hint of it was observed in UV-visible spectroscopic monitoring even at $-80^\circ C$.

While we do not have direct spectroscopic evidence of formation of Co-peroxyxynitrite intermediate, we sought chemical evidence for the postulated species. When the reaction of **4.2** with H_2O_2 is followed by the addition of 2,4-di-*tert*-butylphenol (DTBP), complex **4.3** is formed and unreacted DTBP is recovered. However, effective nitration (*ca.* 50%) is observed when DTBP is added before the addition of one equivalent H_2O_2 (Scheme 4.3). Work-up of the reaction mixture reveals the presence of corresponding Co(III)-hydroxo product, $[(L4)Co(OH)]$, **4.4** (*ca.* 70%) and 2,4-di-*tert*-butyl-6-nitrophenol (*ca.* 50%). A product from oxidative coupled phenol is also observed though in very low yield (*ca.* 10%). It would be worth to mention here that the phenol nitration has been extensively used to provide evidence in support of presence of metal-peroxyxynitrite intermediates.



Scheme 4.3. Phenol ring nitration by complex **4.2** in the presence of H_2O_2 .

4.3 Experimental section

4.3.1 Materials and methods

All reagents and solvents were purchased from commercial sources and were of reagent grade. Acetonitrile was distilled from calcium hydride. Deoxygenation of the solvent and solutions were effected by repeated vacuum/purge cycles or bubbling with argon for 30 minutes. NO gas was purified by passing through KOH and P₂O₅ column. UV-visible spectra were recorded on a Agilent Cary 8454 UV-visible spectrophotometer. FT-IR spectra were taken on a Perkin Elmer spectrophotometer with samples prepared as KBr pellets. ¹H-NMR spectra were obtained with a 600 MHz Varian FT spectrometer. Chemical shifts (ppm) were referenced either with an internal standard (Me₄Si) for organic compounds or to the residual solvent peaks. Elemental analyses were obtained from a Perkin Elmer Series II Analyzer. Mass spectra were recorded on a Waters, Model: Q-ToF Premier instrument with ESI mode of ionization.

The single crystal of the ligand was obtained by slow evaporation from a CHCl₃ solution; whereas the crystals of **4.1** and **4.2** were grown from the respective THF solutions. The intensity data were collected using a Bruker SMART APEX-II CCD diffractometer, equipped with a fine focus 1.75 kW sealed tube MoK_α radiation ($\lambda = 0.71073 \text{ \AA}$) at 273(3) K, with increasing ω (width of 0.3° per frame) at a scan speed of 3 s/frame. The SMART software was used for data acquisition. Data integration and reduction were undertaken with SAINT and XPREP software.²³ Multi-scan empirical absorption corrections were applied to the data using the program SADABS.²⁴ Structures were solved by direct methods using SHELXS-2014 and refined with full-matrix least squares on F^2 using SHELXL-2014/7.²⁵ Structural illustrations have been drawn with ORTEP-3 for Windows.²⁶

4.3.2 Syntheses

4.3.2.1 Synthesis of ligand **L4H₂**, [5,10,15,20-tetrakis(4'-chlorophenyl)porphyrin]

The ligand **L4H₂** was prepared by following earlier reported general procedure of porphyrin synthesis with slight modification. *p*-chlorobenzaldehyde (2.80 g, 20 mmol) and freshly distilled pyrrole (1.34 g, 20 mmol) were added to 37 mL of propionic acid. After refluxing for 2 h the solution was cooled to room temperature. It was then neutralized by aqueous Na₂CO₃. A precipitate appeared and it was filtered off. The crude mass was subjected to purification using column chromatography using CH₂Cl₂ and hexane as solvent to afford the desired ligand as purple solid. Yield: 0.750 g (20%). Elemental analyses for C₄₄H₂₆N₄Cl₄. Calcd. (%): C, 70.23; H, 3.48; N, 7.45, found (%): C, 70.15; H, 3.47; N, 7.58. FT-IR (in KBr): 3444, 2922, 1487, 1469, 1090, 1015, 966, 797, 728, 491 cm⁻¹. ¹H-NMR (600 MHz, CDCl₃): δ_{ppm}, 7.75-7.74 (d, 8H), 8.14-8.13(d, 8H), 8.85 (s, 8H). Mass (m/z): Calcd: 752.52, found: 753.08 (M+1).

4.3.2.2 Syntheses of complexes

(a) **4.1**, [(**L4**)Co]

To a mixture of ligand, **L4H₂** (0.188 g, 0.25 mmol) in CHCl₃ (12 mL) and acetic acid (12 mL), cobalt(II) acetate tetrahydrate (0.622 g, 2.50 mmol) was added. After refluxing at 120 °C for 2 h, the precipitate was filtered and washed with methanol. The crude mass was subjected to column chromatography using silica gel column and CHCl₃: hexane (2:3, v/v) solvent mixture to result in complex **4.1** as violet solid. Yield: 0.141 g (70%). Elemental analyses for C₄₄H₂₄N₄Cl₄Co, Calcd. (%): C, 65.29; H, 2.99; N, 6.92, found (%): C, 65.22; H, 2.98; N, 7.02. UV-visible (CH₂Cl₂): 410 nm (ε/M⁻¹cm⁻¹, 2.24 × 10⁵), 525 nm (ε/M⁻¹cm⁻¹, 2.8 × 10⁴). FT-IR (in KBr): 1541, 1486, 1348, 1090, 1001, 795, 719, 505 cm⁻¹. Mass (m/z): Calcd. 809.00, found: 809.05 (molecular ion peak).

(b) 4.2, [(L4)Co(NO)]

To a dry and degassed CH_2Cl_2 solution of **4.1** (0.8 g, 1 mmol), NO gas was bubbled for 5 min. The violet color of the solution changed to dark red. The excess of NO gas was removed by applying several cycles of vacuum/argon purge. The crude product was isolated by drying under reduced pressure. The pure crystalline complex **4.2** was obtained after recrystallization from THF. Yield: 0.680 g (80%). Elemental analyses for $\text{C}_{44}\text{H}_{24}\text{N}_5\text{OCl}_4\text{Co}$, Calcd. (%): C, 62.96; H, 2.88; N, 8.34, found (%): C, 62.92; H, 2.85; N, 8.41. UV-visible (CH_2Cl_2): 415 nm ($\epsilon/\text{M}^{-1}\text{cm}^{-1}$, 2.21×10^5), 538 nm ($\epsilon/\text{M}^{-1}\text{cm}^{-1}$, 3.1×10^4). FT-IR (in KBr): 1701, 1485, 1346, 1090, 999, 795, 714, 504 cm^{-1} . $^1\text{H-NMR}$ (600 MHz, CDCl_3): δ_{ppm} , 7.64-7.66 (d, 8H), 8.05-8.00 (d, 8H), 8.82 (s, 4H), 8.94 (s, 4H).

(c) 4.3, [(L4)Co(NO₂)]

Complex **4.2** (0.418 g, 0.5 mmol) was dissolved in 20 mL of dried and degassed $\text{CH}_2\text{Cl}_2/\text{CH}_3\text{CN}$ (v/v, 5:1) and the solution was cooled at -40°C . To this cold solution, pre-cooled hydrogen peroxide (37% v/v, 200 μL) was added and stirred for 1/2 h. The red color of the solution changed to yellowish red. The solution was then warmed to room temperature and dried under reduced pressure. Yield: 0.254 g (60%). Elemental analyses for $\text{C}_{44}\text{H}_{24}\text{N}_5\text{O}_2\text{Cl}_4\text{Co}$, Calcd. (%): C, 61.78; H, 2.83; N, 8.19, found (%): C, 61.72; H, 2.80; N, 8.25. UV-visible ($\text{CH}_2\text{Cl}_2/\text{CH}_3\text{CN}$): 430 nm ($\epsilon/\text{M}^{-1}\text{cm}^{-1}$, 2.84×10^5), 546 ($\epsilon/\text{M}^{-1}\text{cm}^{-1}$, 3.3×10^4), 665 nm ($\epsilon/\text{M}^{-1}\text{cm}^{-1}$, 4.2×10^3). FT-IR (in KBr): 1637, 1485, 1390, 1321, 1270, 1090, 1063, 798, 504 cm^{-1} . $^1\text{H-NMR}$ (600 MHz, CDCl_3): δ_{ppm} , 7.71-7.73 (d, 8H), 8.07-8.09 (d, 8H), 8.90 (s, 8H). Mass (m/z): Calcd: 854.99, found: 856.08 (M+1).

(d) 4.4 and 2,4-di-*tert*-butyl-6-nitrophenol

Complex **4.2** (0.837 g, 1 mmol) was dissolved in 20 mL of dried and degassed $\text{CH}_2\text{Cl}_2/\text{CH}_3\text{CN}$ (v/v, 5:1) and the solution was cooled at -40°C . To this cold solution, pre-

cooled 2,4-di-*tert*-butylphenol (1.03 g; 5 mmol) was added and stirred for 5 min. To this, pre-cooled H₂O₂ (37% v/v, 400 μ L) in acetonitrile was added and the resulting mixture was stirred for 30 min at -40 °C. The reaction mixture was then warmed to room temperature and dried under reduce pressure. The solid mass was then subjected to column chromatography using silica gel column and hexane as solvent to obtain 2,4-di-*tert*-butyl-6-nitrophenol. Yield: 0.125 g (50%) and complex **4.4** as solid. Yield: 0.575 g (70%).

Complex 4.4: Elemental analyses for C₄₄H₂₅N₄OCl₄Co, Calcd. (%): C, 63.95; H, 3.05; N, 6.78, found (%): C, 63.91; H, 3.07; N, 6.86. FT-IR (in KBr): 3439, 2958, 1656, 1491, 1369, 1090, 998, 785 cm⁻¹. UV-visible (CH₂Cl₂/CH₃CN): 390 nm (ϵ /M⁻¹cm⁻¹, 1.95 \times 10⁵), 498 nm (ϵ /M⁻¹cm⁻¹, 2.65 \times 10⁴), 621 nm (ϵ /M⁻¹cm⁻¹, 2.58 \times 10²).

4.4 Conclusion

In conclusion, a nitrosyl complex of cobalt porphyrin, [(L4)Co(NO)] having {CoNO}⁸ description was synthesized and characterized structurally. It was found to be inert toward dioxygen. However, in CH₂Cl₂/CH₃CN solution, the {CoNO}⁸ complex reacts with H₂O₂ to result in the corresponding Co-nitrito complex, [(L4)Co(NO₂)] with the release of O₂. The reaction presumably proceeds through the formation of Co-peroxynitrite intermediate. Thus, the present study demonstrates an example of the reaction of a nitrosyl complex of metal-porphyrin with H₂O₂ which led to the formation of the corresponding nitrito complex along with the release of O₂ via a presumed metal-peroxynitrite intermediate.

4.5 References

- (1) Ignarro L. J. *Nitric oxide: Biology and Pathobiology* Ed. Academic press; San Diego, **2000**.
- (2) (a) Moncada, S.; Palmer, R. M. J.; Higgs, E. A. *Pharmacol. Rev.* **1991**, *43*, 109. (b) Butler, A. R.; Williams, D. L. H. *Chem. Soc. Rev.* **1993**, *22*, 233. (c) Feelisch, M.;

- Stamler, J. S. *Methods in Nitric Oxide Research* Ed. John Wiley and Sons, New York **1996**. (d) Jia, L.; Bonaventura, C.; Bonaventura, J.; Stamler, J. S. *Nature* **1996**, *380*, 221. (e) Galdwin, M. T.; Lancaster, J. R. Jr.; Freeman, B. A.; Schechter, A. N. *Nat. Med.* **2003**, *9*, 496.
- (3) (a) Radi, R. *Proc. Natl. Acad. Sci. U. S. A.* **2004**, *101*, 4003. (b) Qiao, L.; Lu, Y.; Liu, B.; Girault, H. H. *J. Am. Chem. Soc.* **2011**, *133*, 19823. (c) Ford, P. C.; Wink, D. A.; Stanbury, D. M. *FEBS Lett.* **1993**, *326*, 1. (d) Tran, N. G.; Kalyvas, H.; Skodje, K. M.; Hayashi, T.; Moëne-Loccoz, P.; Callan, P. E.; Shearer, J.; Kirschenbaum, L. J.; Kim, E. *J. Am. Chem. Soc.* **2011**, *133*, 1184.
- (4) (a) Goldstein, S.; Lind, J.; Merenyi, G. *Chem. Rev.* **2005**, *105*, 2457. (b) Pacher, P.; Beckman, J. S.; Liaudet, L. *Physiol. Rev.* **2007**, *87*, 315. (c) Blough, N. V.; Zafiriou, O. C. *Inorg. Chem.* **1985**, *24*, 3502. (d) Nauser, T.; Koppenol, W. H. *J. Phys. Chem. A* **2002**, *106*, 4084. (e) Speelman, A. L.; Lehnert, N. *Acc. Chem. Res.* **2014**, *47*, 1106. (f) Fry, N. L.; Mascharak, P. K. *Acc. Chem. Res.* **2011**, *44*, 289.
- (5) (a) Doyle, M. P.; Hoekstra, J. W. *Inorg. Biochem.* **1981**, *14*, 351. (b) Cooper, C. E.; Torres, J.; Sharpe, M. A.; Wilson, M. T. *FEBS Lett.* **1997**, *414*, 281. (c) Tocheva, E. I.; Rosell, F. I.; Mauk, A. G.; Murphy, M. E. *Science* **2004**, *304*, 867.
- (6) (a) Gardner, P. R.; Gardner, A. M.; Martin, L. A.; Salzman, A. L. *Proc. Natl. Acad. Sci. U. S. A.* **1998**, *95*, 10378. (b) Ford, P. C.; Lorkovic, I. M. *Chem. Rev.* **2002**, *102*, 993. (c) Schopfer, M. P.; Mondal, B.; Lee, D.-H.; Sarjeant, A. A. N.; Karlin, K. D. *J. Am. Chem. Soc.* **2009**, *131*, 11304.
- (7) Wick, P. K.; Kissner, R.; Koppenol, W. H. *Helv. Chim. Acta* **2000**, *83*, 748.
- (8) (a) Roncaroli, F.; Videla, M.; Slep, L. D.; Olabe, J. A. *Coord. Chem. Rev.* **2007**, *251*, 1903. (b) Maiti, D.; Lee, D.-H.; Sarjeant, A. A. N.; Pau, M. Y. M.; Solomon,

- E. I.; Gaoutchenova, K.; Sundermeyer, J.; Karlin, K. D. *J. Am. Chem. Soc.* **2008**, *130*, 6700.
- (9) (a) Goodwin, J. A.; Coor, J. L.; Kavanagh, D. F.; Sabbagh, M.; Howard, J. W.; Adamec, J. R.; Parmley, D. J.; Tarsis, E. M.; Kurtikyan, T. S.; Hovhannisyan, A. A.; Desrochers, P. J.; Standard, J. M. *Inorg. Chem.* **2008**, *47*, 7852. (b) Kurtikyan, T. S.; Ford, P. C. *Chem. Commun.* **2010**, *46*, 8570. (c) Kurtikyan, T. S.; Eksuzyan, S. R.; Goodwin, J. A.; Hovhannisyan, G. S. *Inorg. Chem.* **2013**, *52*, 12046.
- (10) (a) Yokoyama, A.; Han, J. E.; Cho, J.; Kubo, M.; Ogura, T.; Sieglar, M. A.; Karlin, K. D.; Nam, W. *J. Am. Chem. Soc.* **2012**, *134*, 15269. (b) Yokoyama, A.; Cho, K.-B.; Karlin, K. D.; Nam, W. *J. Am. Chem. Soc.* **2013**, *135*, 14900.
- (11) (a) Clarkson, S. G.; Basolo F. *J. Chem. Soc. Chem. Commun.* **1972**, *119*, 670. (b) Clarkson, S. G.; Basolo F. *Inorg. Chem.* **1973**, *12*, 1528.
- (12) Skodje, K. M.; Williard, P. G.; Kim, E. *Dalton Trans.* **2012**, *41*, 7849.
- (13) Park, G. Y.; Deepalatha, S.; Puiiu, S. C.; Lee, D.-H.; Mondal, B.; Sarjeant, A. A. N.; del Rio, D.; Pau, M. Y. M.; Solomon, E. I.; Karlin, K. D. *J. Biol. Inorg. Chem.* **2009**, *14*, 1301.
- (14) (a) Kalita, A.; Kumar, P.; Mondal, B. *Chem. Commun.* **2012**, *48*, 4636. (b) Kalita, A.; Deka, R. C.; Mondal, B. *Inorg. Chem.* **2013**, *52*, 10897.
- (15) (a) Li, C.; Wang, Q.; Shen, B.; Xiong, Z.; Chen, C. *J. Chem. Eng. Data* **2014**, *59*, 3953. (b) Walker, F. A.; Beroiz, D.; Kadish, K. M. *J. Am. Chem. Soc.* **1976**, *98*, 3484.
- (16) (a) Dey, S.; Rath, S. P. *Dalton Trans.* **2014**, *43*, 2301. (b) Smirnov, V. V.; Woller, E. K.; DiMagno, S. G. *Inorg. Chem.* **1998**, *37*, 4971. (c) Cheng, R. J.; Chen, Y. H.; Chen, C. C.; Lee, G. H.; Peng, S. M.; Chen, P. P. Y. *Inorg. Chem.* **2008**, *53*, 8848. (d) Dey, S.; Sil, D.; Rath, S. P. *Angew. Chem. Int. Ed.* **2016**, *55*, 996.

- (17) (a) Enemark, J. H.; Feltham, R. D. *Coord. Chem. Rev.* **1974**, *13*, 339. (b) Richter-Addo, G. B.; Legzdins, P. *Metal Nitrosyls*: Oxford University Press: New York **1992**. (c) McCleverty, J. A. *Chem. Rev.* **2004**, *104*, 403. (d) Berto, T. C.; Speelman, A. L.; Zheng, S.; Lehnert, N. *Coord. Chem. Rev.* **2013**, *257*, 244.
- (18) (a) Scheidt, W. R.; Hoard, J. L. *J. Am. Chem. Soc.* **1973**, *95*, 8281. (b) Wayland, B. B.; Minkiewicz, J. V.; Abd-Elmageed, M. E. *J. Am. Chem. Soc.* **1974**, *96*, 2795. (c) Fujita, E.; Chang, C. K.; Fazer, J. *J. Am. Chem. Soc.* **1985**, *107*, 7665. (d) Fujita, E.; Fazer, J. *J. Am. Chem. Soc.* **1983**, *105*, 6743.
- (19) Addo, G. B. R.; Hodge, S. J.; Yi, G. B.; Khan, M. A.; Ma, T.; Caemelbecke, E. V.; Guo, N.; Kadish, K. M. *Inorg. Chem.* **1996**, *35*, 6530.
- (20) Kumar, P.; Lee, Y.-M.; Park, Y. J.; Siegler, M. A.; Karlin, K. D.; Nam, W. *J. Am. Chem. Soc.* **2015**, *137*, 4284.
- (21) (a) Goodwin, J.; Kurtikyan, T.; Standard, J.; Walsh, R.; Zheng, B.; Parmley, D.; Howard, J.; Green, S.; Mardyukov, A.; Przybyla, D. E. *Inorg. Chem.* **2005**, *44*, 2215. (b) Wyllie, G. R. A.; Scheidt, W. R. *Chem. Rev.* **2002**, *102*, 1067.
- (22) (a) Pfeiffer, S.; Gorren, A. C. F.; Schmidt, K.; Werner, E. R.; Hansert, B.; Bohle, D. S.; Mayer, B. *J. Biol. Chem.* **1997**, *272*, 3465. (b) Coddington, J. W.; Hurst, J. K.; Lyman, S. V. *J. Am. Chem. Soc.* **1999**, *121*, 2438. (c) Koppenol, W. H.; Bounds, P. L.; Nauser, T.; Kissner, R.; Rügger, H. *Dalton Trans.* **2012**, *41*, 13779.
- (23) *SMART, SAINT and XPREP*, Siemens Analytical X-ray Instruments Inc., Madison, Wisconsin, U. S. A. **1995**.
- (24) Sheldrick, G. M. *SADABS: software for Empirical Absorption Correction*, University of Gottingen, Institut für Anorganische Chemie der Universität, Tammanstrasse 4, D-3400 Gottingen, Germany **1999**.
- (25) Sheldrick, G. M. *SHELXS-2014*, University of Gottingen, Germany.

- (26) Farrugia, L. J. ORTEP-3 for Windows - a version of ORTEP-III with a Graphical User Interface (GUI) *J. Appl. Crystallogr.* **1997**, *30*, 565.



Chapter 5

Reaction of a Co(III)-Peroxo Complex and NO: Formation of a Putative Peroxynitrite Intermediate

Abstract

The complex, $[(L1)_2Co]Cl_2$, **2.1** of the ligand **L1** {**L1** = *bis*(2-ethyl-4-methylimidazol-5-yl)methane} upon reaction with H_2O_2 in methanol solution at $-40\text{ }^\circ\text{C}$ resulted in the formation of the corresponding Co(III)-peroxo complex, $[(L1)_2Co(O_2)]^+$, **5.1**. The addition of NO gas to the freshly generated solution of the complex **5.1** led to the formation of the Co(II)-nitrate complex, **5.2** through the putative formation of a Co(II)-peroxynitrite intermediate, **5.1a**. The intermediate **5.1a** was found to mediate the nitration of the externally added phenol resembling the nitration of tyrosine in biological systems.

5.1 Introduction

Nitric oxide (NO) is an important small molecule that is involved in various physiological processes such as neurotransmission, vasodilation, immune response, etc.¹⁻⁴ Under normal conditions, NO is produced by the nitric oxide synthases (NOS) at low concentration.⁵ However, an excess production of NO can have detrimental effects *via* the formation of secondary reactive nitrogen species (RNS) such as nitrogen dioxide (NO₂) and peroxynitrite (ONOO⁻).⁶ Both of these RNS are known to play important roles in biomolecule oxidation leading to the oxidative and nitrosative stress.⁷ The nitric oxide dioxygenases (NODs) are known to control the *in vivo* level of NO by converting it into the biologically benign nitrate (NO₃⁻) and thereby removing the excess of it.⁸ The conversion of NO to NO₃⁻ by NODs is believed to proceed through the formation of a peroxynitrite intermediate.^{8,9} Peroxynitrite is proposed to form *in vivo* in a diffusion controlled reaction of NO and O₂⁻ anion or H₂O₂ and nitrite (NO₂⁻) in the presence of the peroxidase enzymes.^{10,11} An aqueous peroxynitrite is known to isomerize to the nitrate (NO₃⁻) very easily.⁸ In the literature, peroxynitrites are exemplified to form either in the reaction of oxy-heme (formally, Fe^{III} - O₂⁻) proteins with NO or metal-nitrosyls with O₂ or O₂⁻.^{9,12} Recently, the peroxynitrite intermediates have been shown to form in the reaction of NO with Cr-superoxo or peroxo species. A Cr(IV)-peroxo complex {[12-TMC)Cr(O₂)(Cl)]⁺} {12-TMC = 1,4,8,11-tetramethyl-1,4,8,11-tetraazacyclotetradecane} is reported to react with NO to result in a Cr(III)-nitrate complex, {[12-TMC)Cr(NO₃)(Cl)]⁺}; whereas the reaction of Cr(III)-superoxo complex, {[14-TMC)Cr(O₂)(Cl)]⁺} and NO resulted in the corresponding Cr(IV)-oxo complex, {[14-TMC)Cr(O)(Cl)]⁺} and NO₂ presumably *via* the formation of a Cr(III)-peroxynitrite intermediate, [(14-TMC)Cr(OONO)(Cl)]⁺.¹³⁻¹⁵ Nam *et al.* reported the reactivity of an Fe(III)-peroxo complex, [(14-TMC)Fe(O₂)]⁺ with NO⁺ as an approach for generating the

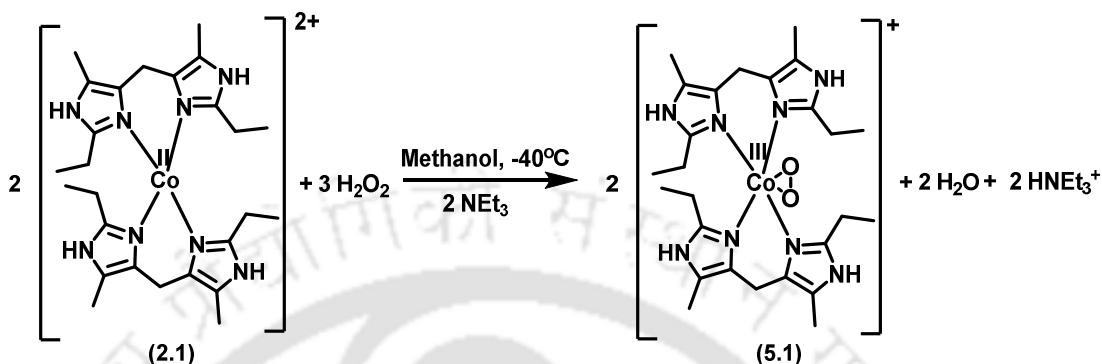
peroxynitrite intermediate which led to the formation of an Fe(III)-nitrate complex, [(14-TMC)Fe(NO₃)(F)]⁺.¹⁶ On the other hand, Basalo *et al.* reported the reaction of a Co-nitrosyl with O₂ to result in the Co-nitrite where the intermediate formation of a peroxynitrite is presumed.¹⁷ Similarly, a non-heme dinitrosyliron complex has been shown to result in the corresponding nitrite in its reaction with O₂.¹⁸ Recently, Karlin and coworkers reported the reaction of a mixed-valent nitrosyl complex of Cu(I)Cu(II), [Cu₂(UN-O⁻)(NO)]²⁺ with O₂ to result in the superoxide and nitrosyl adduct, [Cu₂(UN-O⁻)(NO)(O₂⁻)]²⁺ which was subsequently converted to the corresponding peroxynitrite complex.¹⁹

In our laboratory, we have been working on the reactivity of the metal nitrosyls with O₂⁻ anion and H₂O₂ with an aim to generate a peroxynitrite species. For example, {CuNO}¹⁰ complex of the *bis*(2-ethyl-4-methylimidazol-5-yl)methane ligand was found to react with H₂O₂ to afford the corresponding Cu(I)-nitrite and the formation of a Cu(I)-peroxynitrite intermediate is presumed.²⁰ The same nitrosyl complex, upon reaction with O₂⁻ anion was observed to result in Cu(II)-nitrite.²⁰ In another example, the {CuNO}¹⁰ complex in the presence of H₂O₂ was shown to form Cu(II)-nitrite *via* a presumed peroxynitrite intermediate.²¹ Cobalt-nitrosyls, both with porphyrin and non-porphyrin ligands, were reported to react with O₂ and O₂⁻ to afford cobalt-nitrate/nitrite complexes.^{17,22} The involvement of a peroxynitrite intermediate in these reactions was implicated. However, the examples involving the reactions of the cobalt-peroxo complexes of non-porphyrinate ligands with NO are limited.

5.2 Results and discussion

The addition of 5 equivalents amount of H₂O₂ in presence of 2 equivalents of NEt₃ to the methanol solution of **2.1** at -40 °C afforded a pink color intermediate which was thermally

unstable and decomposed readily at room temperature (Scheme 5.1). In the visible region of the spectrum, the intermediate displayed a new absorption band at 452 nm ($\epsilon/M^{-1}cm^{-1}$, 890) (Figure 5.1a). This was attributed to the formation of corresponding Co(III)-peroxo complex, **5.1**.



Scheme 5.1 Reaction of complex **2.1** with H_2O_2 in methanol at -40°C .

The Nam group has reported a number of transition metal side-on peroxo complexes where the absorption band in the visible region appeared in the range of 340 nm to 470 nm.²³ For example, the side-on peroxo complexes $[(\text{TMC})\text{Co}(\text{O}_2)]^+$, $[(15\text{-TMC})\text{Co}(\text{O}_2)]^+$ and $[(12\text{-TMC})\text{Co}(\text{O}_2)]^+$ (TMC = 1,4,8,11-tetramethyl-1,4,8,11-tetraazacyclotetradecane) were reported to absorb at 436 nm ($\epsilon/M^{-1}cm^{-1}$, 254), 464 nm ($\epsilon/M^{-1}cm^{-1}$, 120) and 350 nm ($\epsilon/M^{-1}cm^{-1}$, 450), respectively.^{23,24} On the other hand, the end-on peroxo complexes of Co(III) displayed absorption bands in the range of 485 to 580 nm.²⁵ The addition of 5 equivalents of H_2O_2 and 2 equivalents of NEt_3 in methanol solution of **2.1** resulted in the appearance of a new stretching band at 874 cm^{-1} in the FT-IR spectrum (Figure 5.1b). The intensity of the band was found to diminish with time suggesting the unstable nature of the intermediate (Figure 5.1b). The band appeared to be sensitive to ^{18}O -labelling and shifted to 826 cm^{-1} when $\text{H}_2^{18}\text{O}_2$ was used. Thus, it was assigned to the O-O stretching frequency in the Co(III)-peroxo intermediate. It is to be noted that in cases of transition metal peroxo complexes, the O-O stretching frequency which appeared in the range of $830\text{-}900\text{ cm}^{-1}$ are

designated for side-on (η^2) peroxo mode for 1:1 metal/ O_2 species.²⁶ In case of structurally characterized side-on $[(TMEN)_2Co(O_2^{2-})]^+$ (TMEN = tetramethylethylenediamine), the O-O stretching appeared at 861 cm^{-1} in KBr disc.^{30b} In addition, the O-O stretching in side-on $[(Ph_2PCH=CHPh)_2Co(O_2)]^+$ and $[(PhP(CH_2CH_2CH_2PPh_2)_2Rh)Cl(O_2)]$ appeared at 909 cm^{-1} and 862 cm^{-1} , respectively.²⁷ Thus, it is logical to believe that addition of H_2O_2 to the methanol solution of **2.1** at $-40\text{ }^\circ\text{C}$ resulted in the formation of the corresponding Co(III)-peroxo intermediate where the peroxo group is bonded to the metal ion in a side-on fashion. Though, the resonance Raman study of the oxygenated intermediate gives a more accurate picture of peroxo binding mode in metal-peroxo complexes, the photo-decomposition of the intermediate in the present case precluded its study.

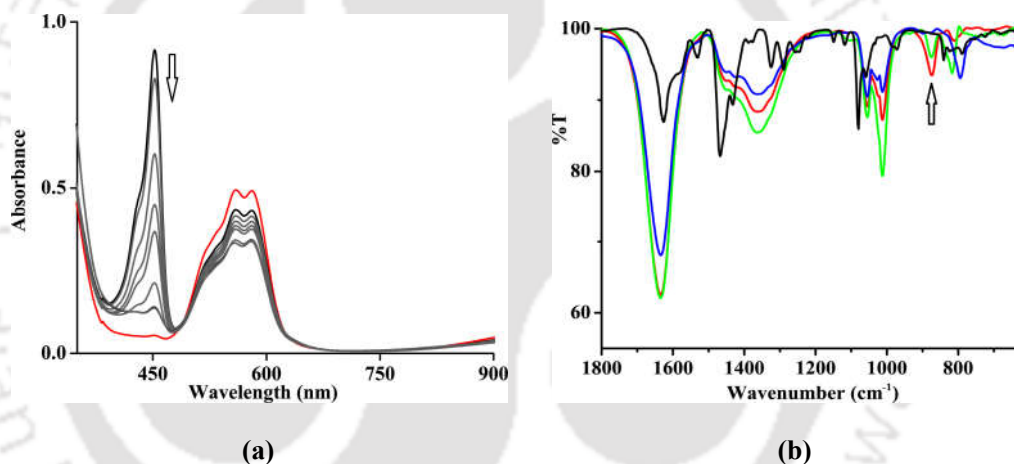


Figure 5.1. (a) UV-visible spectra of complex **2.1** (red), after addition of H_2O_2 {complex **5.1**} (grey), in methanol at $-40\text{ }^\circ\text{C}$. (b) Solution FT-IR spectra of complexes **2.1** (black), **5.1** (red) in methanol. Green and blue traces represent the gradual decomposition of **5.1** at room temperature.

As expected for a Co(III)-peroxo species, the intermediate was silent in X-band EPR study (Figure 5.3a).^{23,24} The ESI-mass spectrum of the intermediate was populated by a peak at m/z 555.28 which is assignable to the mass of $[(L1)_2Co(O_2)]^+$, **5.1** (calculated m/z 555.26) (Figure 5.3b). The peak was sensitive towards ^{18}O -labelling and found to appear at m/z 559.41 when $H_2^{18}O_2$ was used (Figures 5.3b and Appendix IV). The upshift of mass by 4 units upon substitution of ^{16}O by ^{18}O suggests the presence of O_2 unit in complex **5.1**. The

observed isotopic distribution pattern was in good agreement with the simulated one (Appendix IV). Thermal instability of the intermediate precluded its isolation as solid and further characterization.

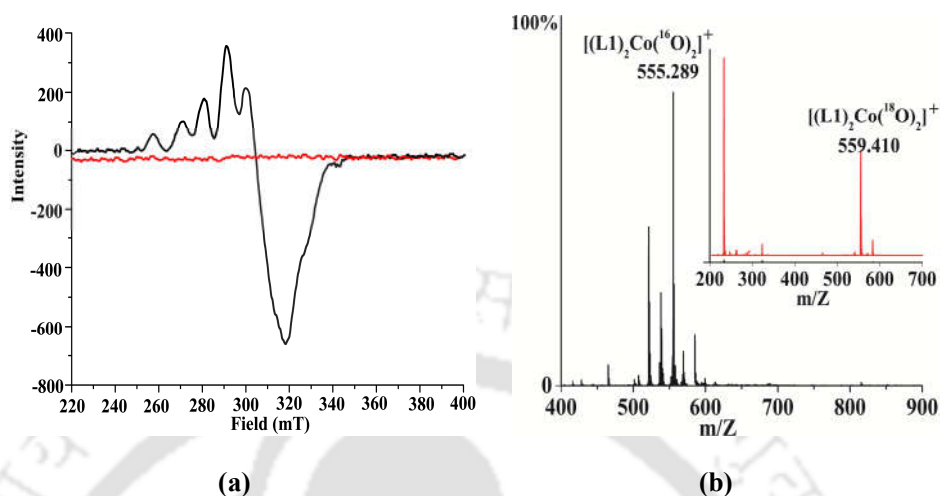


Figure 5.3. (a) X-band EPR spectra of complexes **2.1** (black) and **5.1** (red) in methanol at 77 K. (b) ESI-Mass spectra of complex **5.1** obtained from the reaction of **2.1** and $\text{H}_2^{16}\text{O}_2$ in methanol. Inset shows the same when the reaction was carried out with $\text{H}_2^{18}\text{O}_2$.

NO reactivity of the Co(III)-peroxo intermediate

The addition of NO gas to the freshly generated complex, $[(\text{L}1)_2\text{Co}(\text{O}_2)]^+$, **5.1** in methanol at $-40\text{ }^\circ\text{C}$ followed by warming up at room temperature resulted in the formation of complex, $\{[(\text{L}1)_2\text{Co}(\text{NO}_3)]\text{Cl}\}$, **5.2**. It was isolated and characterized by elemental and spectroscopic analyses (Experimental section and Appendix IV). It was further characterized by the single crystal X-ray structure determination. The crystallographic data, important bond angles and distances are listed in tables A5.1, A5.2 and A5.3, respectively, in the appendix IV. The ORTEP diagram of **5.2** is shown in figure 5.5. The crystal structure revealed that the Co(II) center is bonded with two units of the ligand and a nitrate (NO_3^-) anion in a distorted octahedral geometry. An κ^2 -O coordination mode of NO_3^- to the Co(II) center was observed. The $\text{Co-O}_{\text{nitrate}}$ bond distance is $2.287(4)\text{ \AA}$ and Co-O-N bond angle is 94.08° . The N-O bond distances are $1.273(5)\text{ \AA}$ and $1.15(1)\text{ \AA}$. In

the FT-IR spectrum, **5.2** displayed a strong band at 1384 cm^{-1} which is assignable to the NO_3^- stretching frequency.²⁰ It is to be noted that the **5.2** with NO_3^- as counter anion was reported earlier by Sun and coworkers.²⁸

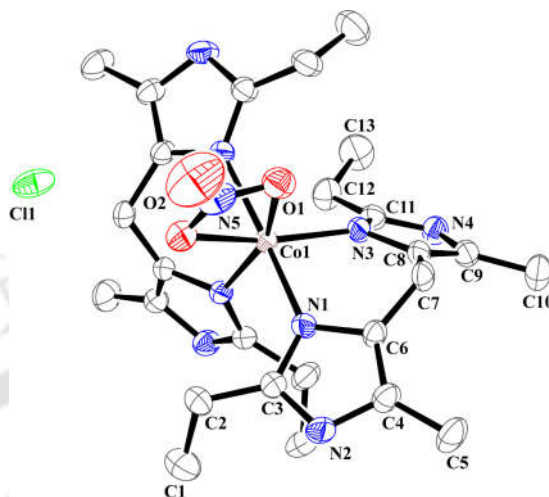
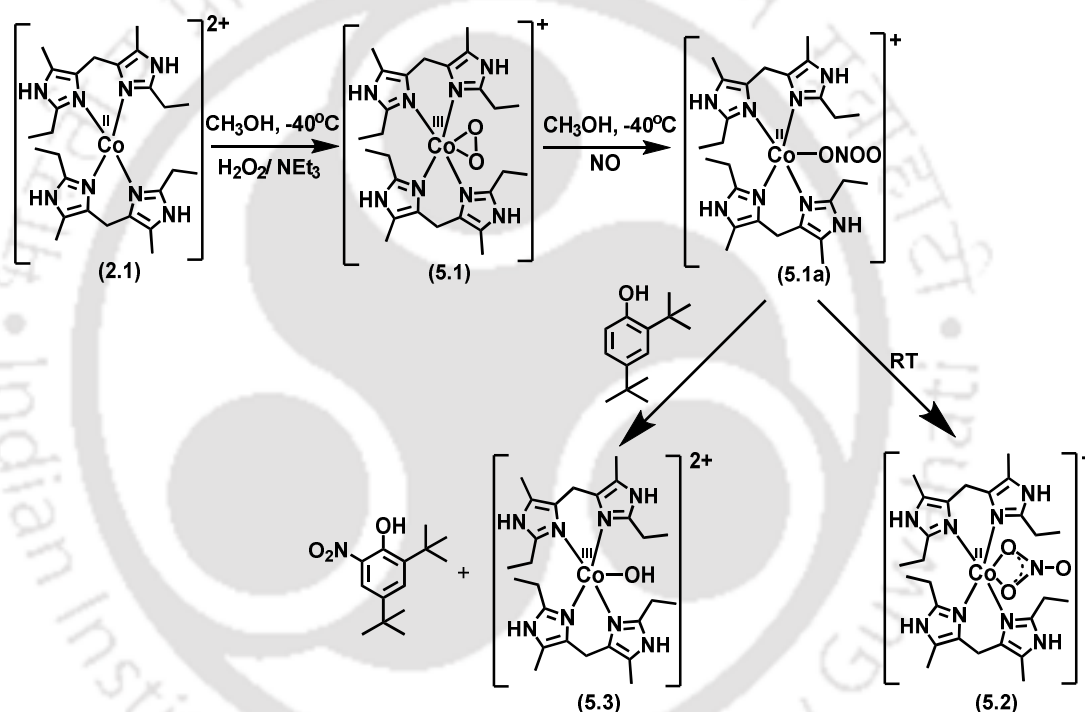


Figure 5.5. ORTEP diagram of complex **5.2**. (30% thermal ellipsoid plot, H-atoms and solvent molecule are not shown for clarity).

The formation of **5.2** can be envisaged through the formation of a putative peroxyxynitrite intermediate (complex **5.1a**) in the course of the reaction (Scheme 5.2). It is to be noted that NO_3^- is the common decomposition or isomerization product of the peroxyxynitrite anion.⁸ Since direct spectroscopic evidence of the peroxyxynitrite intermediate was not obtained owing to its unstable nature, we sought chemical evidence for the proposed intermediate. When the reaction of the peroxo complex, **5.1** with NO was followed by the addition of 2,4-di-tert-butylphenol (DTBP), the exclusive formation of the complex **5.2** was observed and unreacted DTBP (ca. 95%) was recovered. However, when DTBP was added before the addition of NO (Scheme 5.2), an appreciable nitration (ca. 60%) was observed. Work-up of the reaction mixture revealed the formation of the corresponding Co(III)-hydroxo product, **5.3** (ca. 70%) along with 2,4-di-tert-butyl-6-nitrophenol. The nitration of phenol ring by Co(II)-peroxyxynitrite intermediate is expected to result in the formation of corresponding Co(II)-hydroxide (Scheme 5.2). However, only Co(III)-

hydroxide was isolated. This is perhaps because of the air sensitivity of the Co(II)-hydroxide. It has been found in a separate control experiment that in the reaction condition 5.2 does not induce phenol ring nitration and this excludes the possibility of the formation of nitro-phenol from the reaction of 5.2 with externally added phenol. It is to be noted that the phenol nitration has been used extensively as an evidence of the formation of metal-peroxynitrite intermediates.^{9a,13,15} It would be worth mentioning that even at -80 °C temperature, no indication of formation of a new species was observed in the UV-visible spectroscopy.



Scheme 5.2. Formation of peroxynitrite intermediate.

5.3 Experimental section

5.3.1 Materials and methods

All reagents and solvents were purchased from commercial sources and were of reagent grade. HPLC grade methanol was used and dried by heating with iodine-activated

magnesium with magnesium loading of *ca.* 5 g/L. The dried methanol was stored over 20% (m/v) molecular sieves (3 Å) for 3 days before use. Deoxygenation of the solvent and solutions was effected by repeated vacuum/purge cycles or bubbling with nitrogen or argon for 30 minutes. NO gas was purified by passing through KOH and P₂O₅ column. The dilution of NO was effected with argon gas using Environics Series 4040 computerized gas dilution system. UV-visible spectra were recorded on an Agilent HP 8454 spectrophotometer. FT-IR spectra were taken on a Perkin-Elmer spectrophotometer with either sample prepared as KBr pellets or in solution in a KBr cell. ¹H-NMR spectra were obtained with a 400 MHz Varian FT spectrometer. Chemical shifts (ppm) were referenced either with an internal standard (Me₄Si) for organic compounds or to the residual solvent peaks. The X-band Electron Paramagnetic Resonance (EPR) spectra were recorded on a JES-FA200 ESR spectrometer, at room temperature or at 77 K. Spectra were recorded with all the samples prepared in methanol solution at 77 K. The experimental conditions [Frequency, 9.136 GHz; Power, 0.995 mW; Field center, 336.00 mT, Width, ± 250.00 mT; Sweep time, 30.0 s; Modulation frequency, 100.00 kHz, Width, 1.000 mT; Amplitude, 1.0 and Time constant, 0.03 s] kept same for all the samples. Mass spectra of the compounds were recorded in a Waters Q-ToF Premier and Aquity instrument. Solution electrical conductivity was checked using a Systronic 305 conductivity bridge. The magnetic moment of complexes were measured on a Cambridge Magnetic Balance. Elemental analyses were obtained from a Perkin Elmer Series II Analyzer.

Single crystals of **5.2** were grown by slow evaporation technique from methanol. The intensity data were collected using a Bruker SMART APEX-II CCD diffractometer, equipped with a fine focus 1.75 kW sealed tube Mo K α radiation ($\lambda = 0.71073$ Å) at 273(3) K, with increasing ω (width of 0.3° per frame) at a scan speed of 3 s/frame. The SMART software was used for data acquisition.²⁹ Data integration and reduction was undertaken

with SAINT and XPREP software. Structures were solved by direct methods using SHELXS-97 and refined with full-matrix least squares on F^2 using SHELXL-97.³⁰ Structural illustrations have been drawn with ORTEP-3 for Windows.³¹

5.3.2 Syntheses of complexes

(a) **5.1**, $[(L1)_2Co(O_2)]^+$

Complex **2.1** (1.18 g, 2 mmol) was dissolved in 20 mL of dried and degassed methanol in a 50 mL Schlenk flask fitted with a rubber septum and connected to the Schlenk line. The solution was cooled at $-40\text{ }^\circ\text{C}$. To this cold solution, pre-cooled 5 equivalents of hydrogen peroxide (37% v/v, 0.8 mL) and 2 equivalents amount of NEt_3 were added and the solution turned pink. It was then stirred for 10 minutes at $-40\text{ }^\circ\text{C}$ to afford complex **5.1**. The complex was found to be thermally unstable. So attempts were not made to isolate it. All the spectral characterization have been done using freshly prepared complex **5.1** in methanol at $-40\text{ }^\circ\text{C}$. UV-visible (CH_3OH): 452 nm ($\epsilon/M^{-1}cm^{-1}$, 890), 559 nm ($\epsilon/M^{-1}cm^{-1}$, 419). FT-IR (CH_3OH/KBr): 1637, 1054, 874, 817 cm^{-1} . ESI-Mass (m/z): Calcd: 555.28, found: 555.26 (molecular ion peak).

(b) **5.2**, $[(L1)_2Co(NO_3)]^+$

The peroxo complex **5.1** was prepared freshly in a 50 mL Schlenk flask under Ar atmosphere as stated above. To this freshly generated **5.1** in methanol at $-40\text{ }^\circ\text{C}$, NO gas was added through a gas-tight syringe fitted in the Schlenk line. The resulting solution was stirred for 10 min; then warmed up to room temperature and the excess of NO gas was removed by applying several cycles of vacuum and Ar purge. Then the solution was kept for slow evaporation in air. After a few days, crystals of **5.2** were obtained. Elemental analyses for $C_{26}H_{40}ClCoN_9O_3$, Calcd. (%): C, 50.28; H, 6.43; N, 20.29, found (%): C,

50.40; H, 6.44; N, 20.41. UV-visible (CH₃OH): 532 nm ($\epsilon/M^{-1}cm^{-1}$, 190). FT-IR (in KBr): 2975, 1634, 1580, 1470, 1384, 1319, 1086 cm⁻¹. Conductivity (CH₃OH): 124 Scm²mol⁻¹. X-band EPR: g_{av} , 2.16. Observed magnetic moment: 1.81 μ_B .

(d) **5.3 and 2,4-di-*tert*-butyl-6-nitrophenol**

Complex **2.1** (1.18 g, 2 mmol) was dissolved in 20 mL of dried and degassed methanol under Ar atmosphere in a 50 mL Schlenk flask with a rubber septum and fitted in the Schlenk line and the solution was cooled at -40 °C. To this cold solution, pre-cooled hydrogen peroxide (37% v/v, 0.8 mL, 5 equivalent) was added and stirred for 10 min at -40 °C to result in the formation of **5.1**. To this solution, the NO gas was added through a gas-tight syringe fitted in the Schlenk line followed by a methanol (5 mL) solution containing 2,4-di-*tert*-butylphenol (2.06 g; 10 mmol) pre-cooled at -40 °C and the mixture was stirred for 30 min at -40 °C. The reaction mixture was then warmed up to room temperature and the excess of NO gas was removed by applying several cycles of vacuum and Ar purge. Then the solution was dried using rotavapor. The solid mass was then subjected to column chromatography using silica gel column. Pure 2, 4-di-*tert*-butyl-6-nitrophenol {Yield: 0.305 g (60 %)} was eluted with 100% hexane and complex **5.3** was eluted with methanol.

Complex 5.3: Yield: 0.800 g (65 %). Elemental analyses for C₂₆H₄₁Cl₂CoN₈O, Calcd. (%): C, 51.07; H, 6.76; N, 18.32, found (%): C, 51.01; H, 6.80; N, 18.38. UV-visible (MeOH): 507 nm ($\epsilon/M^{-1}cm^{-1}$, 67), 565 nm ($\epsilon/M^{-1}cm^{-1}$, 107) and 615 nm ($\epsilon/M^{-1}cm^{-1}$, 90). FT-IR (in KBr): 3450, 2977, 1636, 1452, 1078, 920, 838 cm⁻¹.

5.4 Conclusion

In conclusion, the present study demonstrate an example of a Co(II) complex, **2.1** which in methanol solution reacted with H₂O₂ at -40 °C to result in the corresponding Co(III)-

peroxo complex, **5.1**. It was characterized by spectroscopic analyses. The peroxo intermediate, **5.1** upon reaction with NO, resulted a Co(II)-nitrate complex, **5.2** presumably through the formation of Co(II)-peroxynitrite intermediate. It was evidenced by the external phenol ring nitration reaction.

5.5 References

- (1) Goyal, R. K.; Hirano, I. N. *Engl. J. Med.* **1996**, *334*, 1106.
- (2) Stark, M. E.; Szurszewski, J. H. *Gastroenterology* **1992**, *103*, 1928.
- (3) Jaffrey, S. R.; Snyder, S. H. *Annu. Rev. Cell Dev. Biol.* **1995**, *11*, 417.
- (4) Bogdan, C. *Nature Immunology* **2001**, *2*, 907.
- (5) (a) Moreno, V. R.; Beddell, C.; Moncada, S. *Eur. J. Biochem.* **1993**, *215*, 801. (b) Ignarro, L. J. *Annu. Rev. Pharmacol. Toxicol.* **1990**, *30*, 535. (c) Radi, R. *Proc. Natl. Acad. Sci. U. S. A.* **2004**, *101*, 4003.
- (6) Liaudet, L.; Soriano, F. G.; Szabo, C. *Crit. Care Med.* **2000**, *28*, 169.
- (7) (a) Pacher, P.; Beckman, J. S.; Liaudet, L. *Physiol. Rev.* **2007**, *87*, 315. (b) Beckman J. S.; Koppenol, W. H. *Am. J. Physiol.* **1996**, *271*, 1424.
- (8) (a) Pfeiffer, S.; Gorren, A. C. F.; Schmidt, K.; Werner, E. R.; Hansert, B.; Bohle, D. S.; Mayer, B. *J. Biol. Chem.* **1997**, *272*, 3465. (b) Coddington, J. W.; Hurst, J. K.; Lyman, S. V. *J. Am. Chem. Soc.* **1999**, *121*, 2438. (c) Koppenol, W. H.; Bounds, P. L.; Nauser, T.; Kissner, R.; Rügger, H. *Dalton Trans.* **2012**, *41*, 13779. (d) Lyman, S. V.; Khairutdinov, R. F.; Hurst, J. K. *Inorg. Chem.* **2003**, *42*, 5259. (e) Goldstein, S.; Lind, J.; Merényi, G. *Chem. Rev.* **2005**, *105*, 2457. (f) Molina, C.; Kissner, R.; Koppenol, W. H. *Dalton Trans.* **2013**, *42*, 9898.
- (9) (a) Schopfer, M. P.; Wang, J.; Karlin, K. *Inorg. Chem.* **2010**, *49*, 6267. (b) Ouellet, H.; Ouellet, Y.; Richard, C.; Labarre, M.; Wittenberg, B.; Wittenberg, J.; Guertin, M. *Proc. Natl. Acad. Sci. U. S. A.* **2002**, *99*, 5902. (c) Gardner, P. R.; Gardner, A.

- M.; Martin, L. A.; Salzman, A. L. *Proc. Natl. Acad. Sci. U. S. A.* **1998**, *95*, 10378.
- (d) Ford, P. C.; Lorkovic, I. M. *Chem. Rev.* **2002**, *102*, 993. (e) Gardner, P. R.; Gardner, A. M.; Brashear, W. T.; Suzuki, T.; Hvitved, A. N.; Setchell, K. D. R.; Olson, J. S. *J. Inorg. Biochem.* **2006**, *100*, 542.
- (10) Qiao, L.; Lu, Y.; Liu, B.; Girault, H. H. *J. Am. Chem. Soc.* **2011**, *133*, 19823.
- (11) Vilet, A.; Eiserich, J. P.; Halliwell, B.; Cross, C. E. *J. Biol. Chem.* **1997**, *272*, 7617.
- (12) Kurtikyan, T. S.; Ford, P. C. *Chem. Commun.* **2010**, *46*, 8570.
- (13) (a) Hughes, M. N.; Nicklin, H. G.; Sackrile, W. A. C. *J. Chem. Soc.* **1971**, 3722. (b) Babich, O. A.; Gould, E. S. *Res. Chem. Intermed.* **2002**, *28*, 575.
- (14) (a) Herold, S.; Koppenol, W. H. *Coord. Chem. Rev.* **2005**, *249*, 499. (b) Roncaroli, F.; Videla, M.; Slep, L. D.; Olabe, J. A. *Coord. Chem. Rev.* **2007**, *251*, 1903.
- (15) (a) Maiti, D.; Lee, D.-H.; Sarjeant, A. A. N.; Pau, M. Y. M.; Solomon, E. I.; Gaoutchenova, K.; Sundermeyer, J.; Karlin, K. D. *J. Am. Chem. Soc.* **2008**, *130*, 6700. (b) Yokoyama, A.; Cho, K. B.; Karlin, K. D.; Nam, W. *J. Am. Chem. Soc.* **2013**, *135*, 14900.
- (16) Yokoyama, A.; Han, J. E.; Karlin, K. D.; Nam, W. *Chem. Commun.* **2014**, *50*, 1742.
- (17) (a) Clarkson, S. G.; Basolo, F. *J. Chem. Soc. Chem. Commun.* **1972**, *119*, 670. (b) Clarkson, S. G.; Basolo, F. *Inorg. Chem.* **1973**, *12*, 1528.
- (18) Skodje, K. M.; Williard, P. G.; Kim, E. *Dalton Trans.* **2012**, *41*, 7849.
- (19) Cao, R.; Elrod, L. T.; Lehane, R. L.; Kim, E.; Karlin, K. D. *J. Am. Chem. Soc.* **2016**, *138*, 16148.
- (20) Kalita, A.; Kumar, P.; Mondal, B. *Chem. Commun.* **2012**, *48*, 4636.
- (21) Kalita, A.; Deka, R. C.; Mondal, B. *Inorg. Chem.* **2013**, *52*, 10897.

- (22) (a) Roncaroli, F.; Videla, M.; Slep, L. D.; Olabe, J. A. *Coord. Chem. Rev.* **2007**, *251*, 1903. (b) Goodwin, J. A.; Coor, J. L.; Kavanagh, D. F.; Sabbagh, M.; Howard, J. W.; Adamec, J. R.; Parmley, D. J.; Tarsis, E. M.; Kurtikyan, T. S.; Hovhannisyanyan, A. A.; Desrochers, P. J.; Standard, J. M. *Inorg. Chem.* **2008**, *47*, 7852. (c) Kurtikyan, T. S.; Eksuzyan, S. R.; Goodwin, J. A.; Hovhannisyanyan, G. S. *Inorg. Chem.* **2013**, *52*, 12046.
- (23) Kim, D.; Cho, J.; Lee, Y. M.; Sarangi, R.; Nam, W. *Chem. Eur. J.* **2013**, *19*, 14112.
- (24) (a) Jo, Y.; Annaraj, J.; Seo, M. S.; Lee, Y. M.; Kim, S. Y.; Cho, J.; Nam, W. *J. Inorg. Biochem.* **2008**, *102*, 2155. (b) Cho, J.; Sarangi, R.; Kang, H. Y.; Lee, J. Y.; Kubo, M.; Ogura, T.; Solomon, E. I.; Nam, W. *J. Am. Chem. Soc.* **2010**, *132*, 16977.
- (25) Wang, C. C.; Chang, H. C.; Lai, Y. C.; Fang, H.; Li, C. C.; Hsu, H. K.; Li, Z. Y.; Lin, T. S.; Kuo, T. S.; Neese, F.; Ye, S.; Chiang, Y. W.; Tsai, M. L.; Liaw, W. F.; Lee, W. Z. *J. Am. Chem. Soc.* **2016**, *138*, 14186.
- (26) (a) Cramer, C. J.; Tolman, W.B.; Theopold, K. H.; Rheingold, A. L. *Proc. Natl. Acad. Sci. U. S. A.* **2003**, *100*, 3635. (b) Rahman, A. F. M. M.; Jackson, W. G.; Wills, A. C. *Inorg. Chem.* **2004**, *43*, 7558.
- (27) Valentine, J. S. *Chem. Rev.* **1973**, *73*, 235.
- (28) Luo, Y.-H.; Wu, G.-G.; Mao, S.-L.; Sun, B.-W. *Inorg. Chim. Acta.* **2013**, *397*, 1.
- (29) SMART, SAINT and XPREP, Siemens Analytical X-ray Instruments Inc., Madison, Wisconsin, USA, **1995**.
- (30) (a) Sheldrick, G. M.; SADABS: software for Empirical Absorption Correction, University of Gottingen, Institute for Anorganische Chemieder Universitat,

- Tammanstrasse 4, D-3400 Gottingen, Germany **1999**. (b) Sheldrick, G. M. SHELXS-97, University of Gottingen, Germany **1997**.
- (31) Farrugia, L. J. ORTEP-3 for windows-a version of ORTEP-III with a graphical user interface (GUI). *J. Appl. Crystallogr.* **1997**, 30, 565.



Appendix I

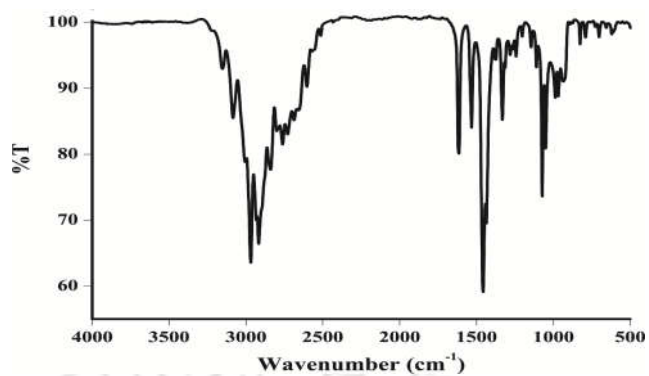


Figure A1.1. FT-IR spectrum of L1 in KBr pellet.

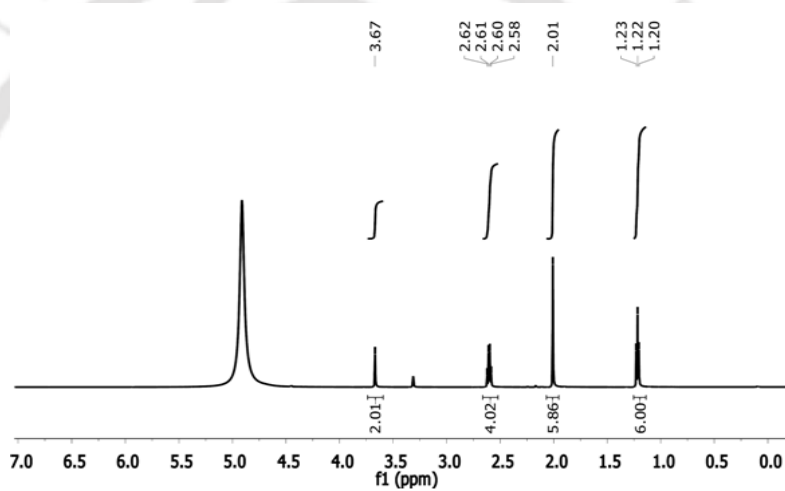


Figure A1.2. ¹H-NMR spectrum of L1 in CD₃OD.

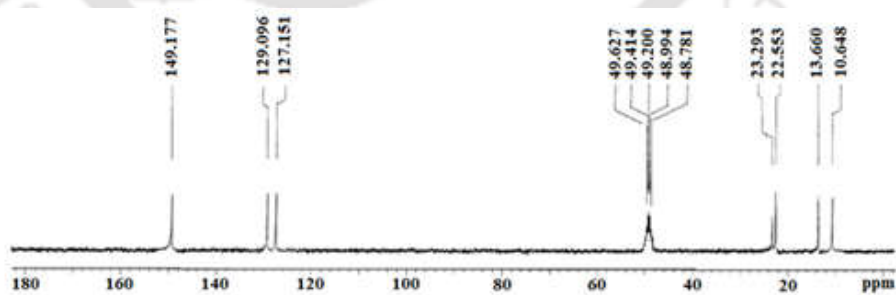


Figure A1.3. ¹³C-NMR spectrum of L1 in CD₃OD.

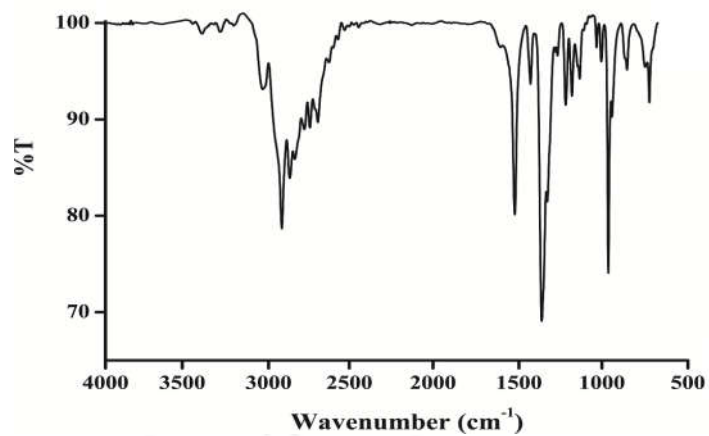


Figure A1.4. FT- IR spectrum of complex 2.1 in KBr pellet.

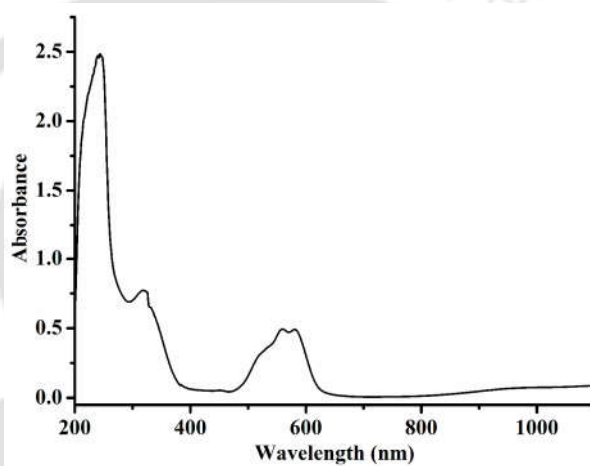


Figure A1.5. UV-visible spectrum of complex 2.1 in methanol.

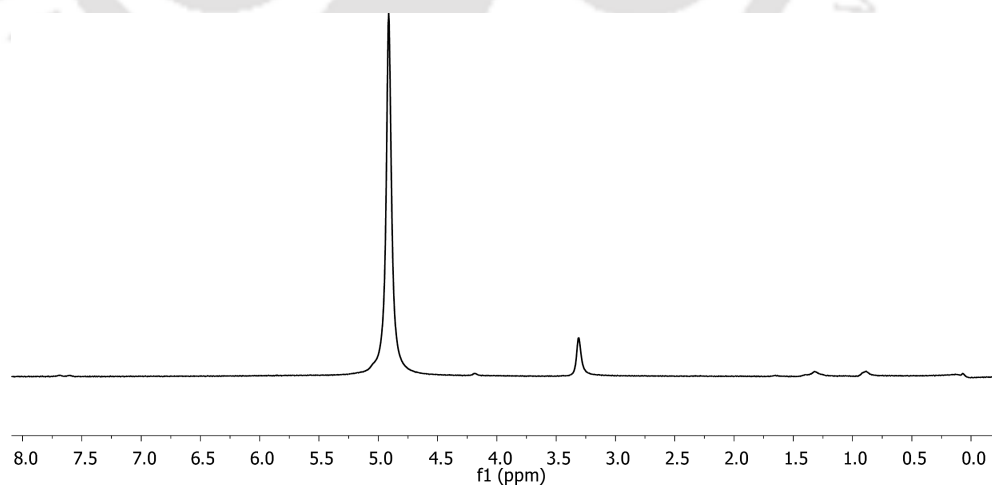


Figure A1.6. ¹H-NMR spectrum of complex 2.3 in CD₃OD.

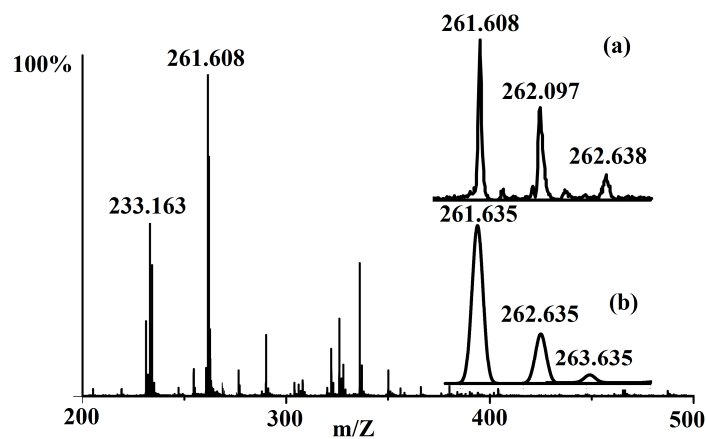


Figure A1.7. ESI Mass spectrum of complex **2.1** in methanol. Inset shows the (a) experimental and (b) simulated isotopic distribution pattern.

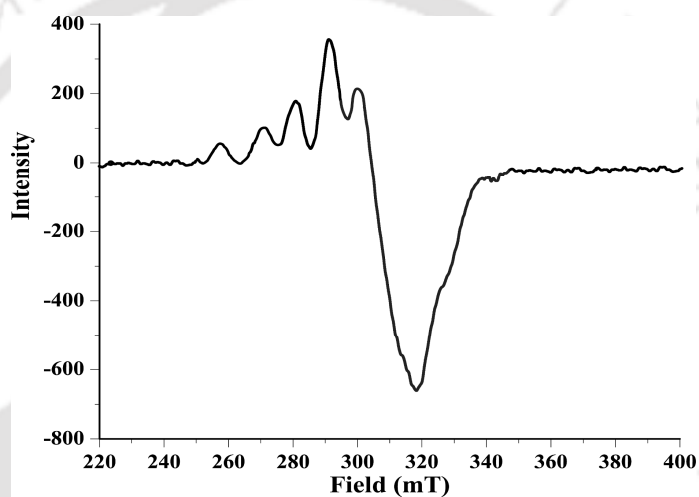


Figure A1.8. X-band EPR spectrum of complex **2.1** in methanol at 77 K.

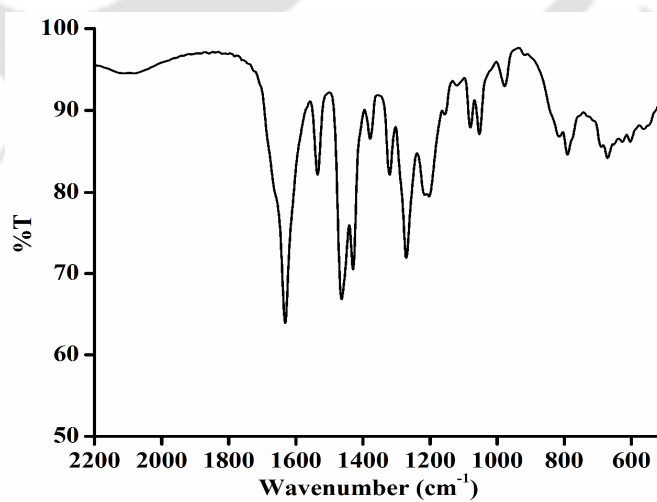


Figure A1.9. FT-IR spectrum of complex **2.3** in KBr.

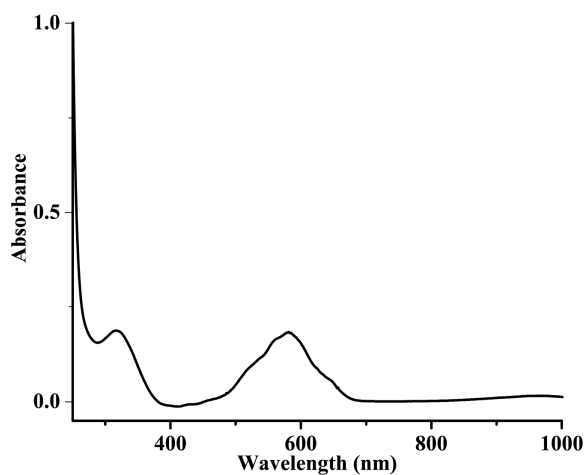


Figure A1.10. UV-visible spectrum of complex **2.3** in methanol.

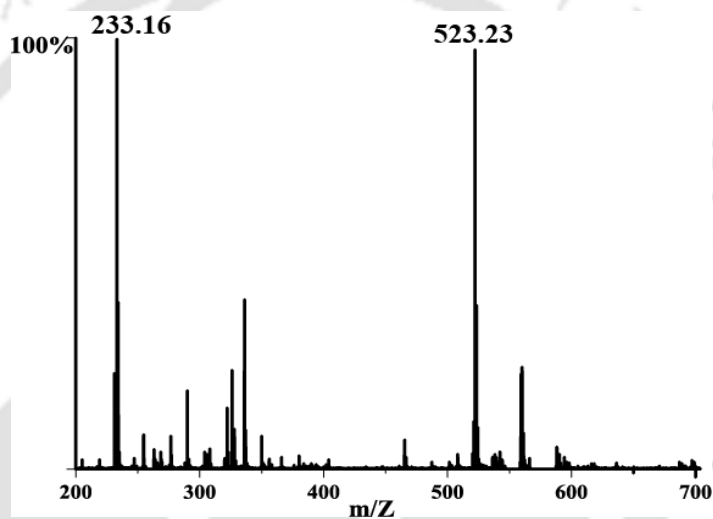


Figure A1.11. ESI Mass spectrum of complex **2.3** in methanol.

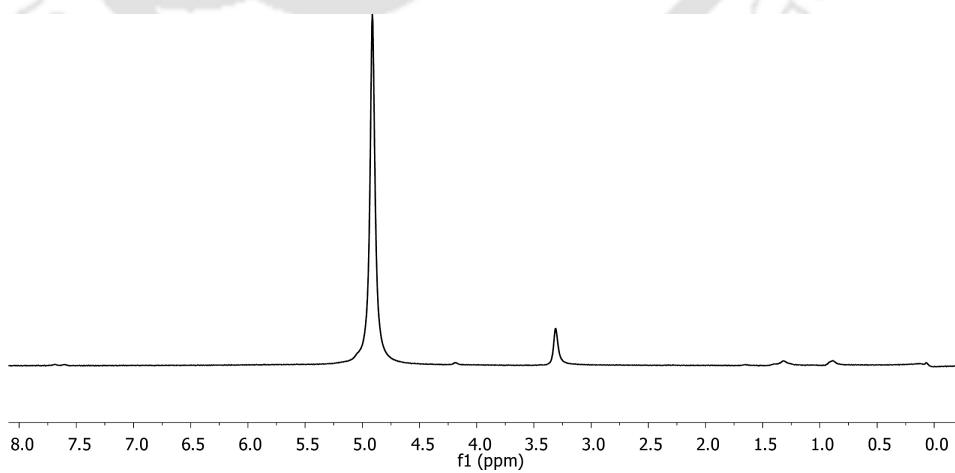


Figure A1.12. ¹H-NMR spectrum of complex **2.3** in CD₃OD.

Table A1.1. Crystallographic data for complexes **2.1** and **2.3**.

	2.1	2.3
Formulae	C ₅₂ H ₉₀ Cl ₄ Co ₂ N ₁₆ O ₅	C ₂₆ H ₃₈ ClCoN ₉ O ₄
Mol. wt.	1279.06	635.03
Crystal system	Monoclinic	Monoclinic
Space group	P21/n	P 2/c
Temperature /K	293(2)	296(2)
Wavelength /Å	0.71073	0.71073
<i>a</i> /Å	14.2005(9)	9.4404(6)
<i>b</i> /Å	14.2147(10)	9.3883(9)
<i>c</i> /Å	32.3238(18)	18.5255(11)
α /°	90.00	90.00
β /°	96.555(6)	91.110(6)
γ /°	90.00	90.00
V/ Å ³	6482.1(7)	1641.6(2)
Z	4	2
Density/Mgm ⁻³	1.311	1.285
Abs. Coeff. /mm ⁻¹	0.732	0.648
Abs. correction	Multi-scan	Multi-scan
F(000)	2704	666
Total no. of reflections	11364	2886
Reflections, <i>I</i> > 2σ(<i>I</i>)	7638	2474
Max. 2θ/°	25.00	25.00
Ranges (h, k, l)	-16 ≤ h ≤ 16 -16 ≤ k ≤ 12 -27 ≤ l ≤ 38	-11 ≤ h ≤ 11 -11 ≤ k ≤ 5 -22 ≤ l ≤ 13
Complete to 2θ (%)	99.7	99.8
Refinement method	Full-matrix least-squares on <i>F</i> ²	Full-matrix least-squares on <i>F</i> ²
Goof (<i>F</i> ²)	1.163	0.989
R indices [<i>I</i> > 2σ(<i>I</i>)]	0.086	0.0674
R indices (all data)	0.1190	0.0755

Table A1.2. Selected bond lengths (Å) for complexes **2.1** and **2.3**.

Atoms	2.1	2.3
Co(1)-N(1)	1.999(5)	2.100(3)
Co(1)-N(3)	1.972(5)	2.100(3)
N(1)-C(3)	1.330(9)	1.340(5)
N(1)-C(6)	1.389(7)	1.400(4)
N(2)-C(3)	1.322(8)	1.3450(5)
N(2)-C(4)	1.368(8)	1.390(5)
N(3)-C(8)	1.399(7)	1.390(4)

N(3)-C(11)	1.326(9)	1.330(5)
Co(1)-O(1)	-	2.230(3)
O(1)-N(5)	-	1.29(4)

Table A1.3. Selected bond angles (°) for complexes **2.1** and **2.3**.

Atoms	2.1	2.3
N(3)-Co(1)-N(1)	95.8(2)	89.0(1)
Co(1)-N(1)-C(3)	128.0(4)	131.0(2)
Co(1)-N(1)-C(6)	123.4(4)	121.0(2)
Co(1)-N(3)-C(8)	125.2(4)	123.0(2)
Co(1)-N(3)-C(11)	127.8(4)	131.0(2)
C(3)-N(2)-C(4)	109.6(5)	109.0(3)
C(8)-N(3)-C(11)	106.7(5)	106.0(3)
N(1)-C(3)-C(2)	126.4(6)	126.0(3)
N(2)-C(4)-C(6)	105.9(5)	106.0(3)
N(1)-C(3)-N(2)	109.3(5)	110.0(3)
N(3)-Co(1)-O(1)	-	85.0(1)
O(1)-N(5)-O(1)	-	108.0(4)
Co(1)-N(5)-O(1)	-	98.0(3)

Appendix II

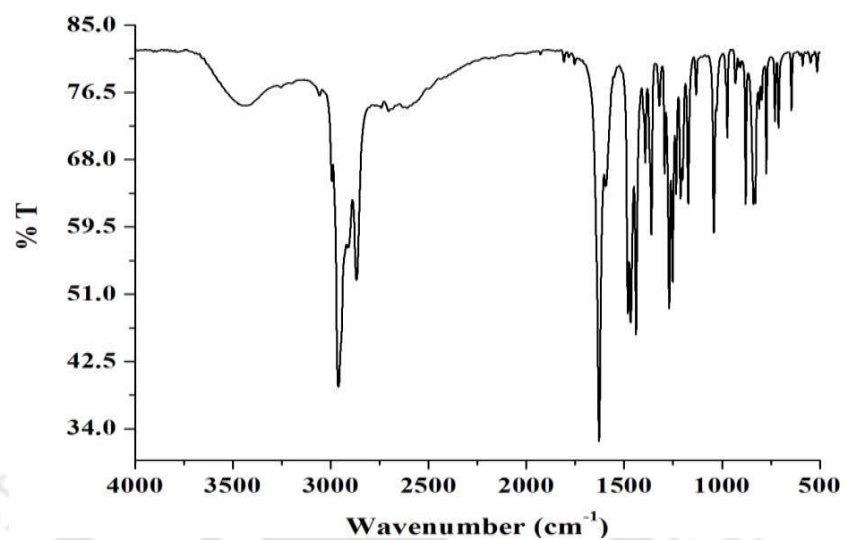


Figure A2.1. FT-IR spectrum of ligand $L2H_2$ in KBr.

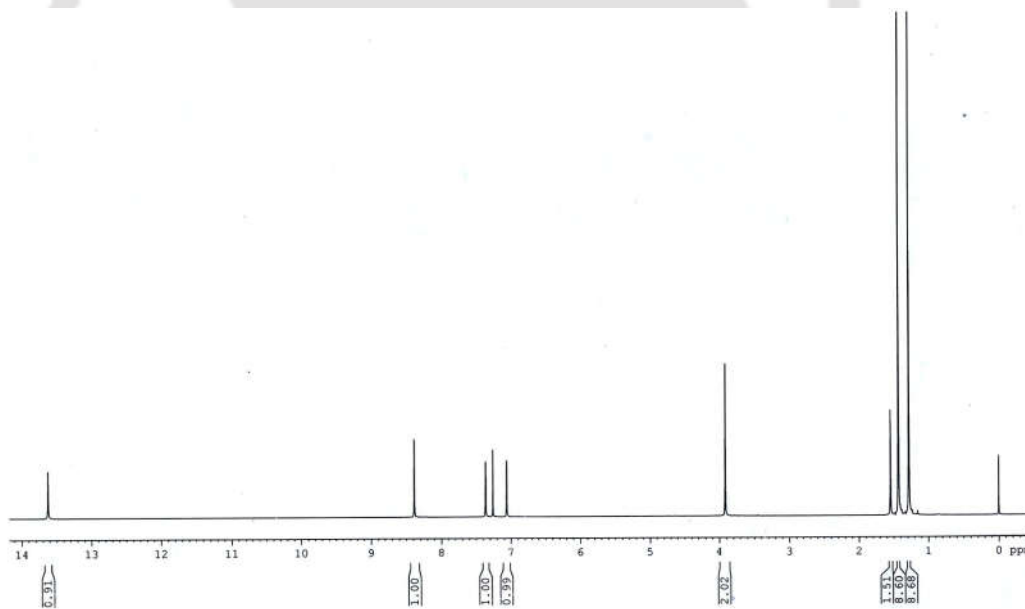


Figure A2.2. 1H -NMR spectrum of ligand $L2H_2$ in $CDCl_3$.

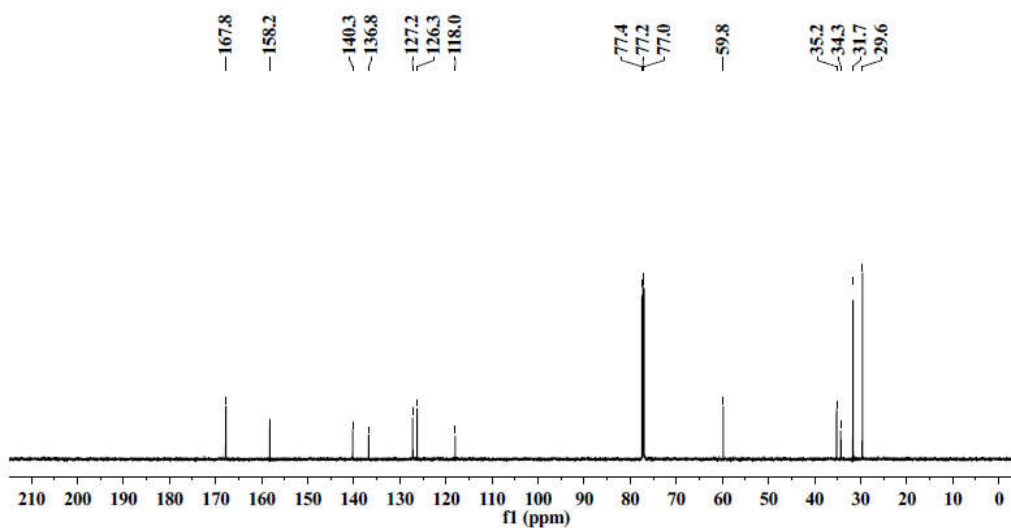


Figure A2.3. ^{13}C -NMR spectrum of ligand **L2H₂** in CDCl_3 .

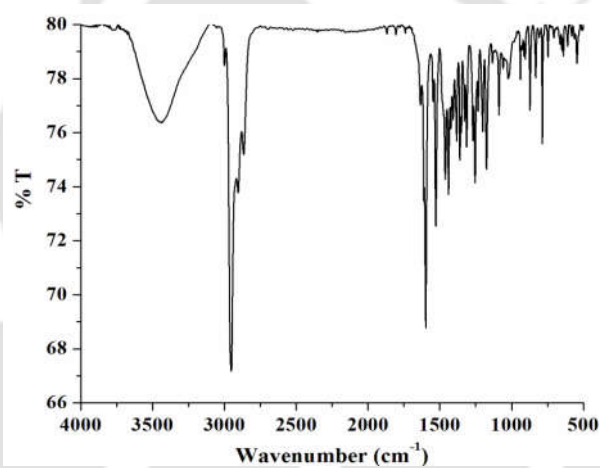


Figure A2.4. FT-IR spectrum of complex **3.1** in KBr.

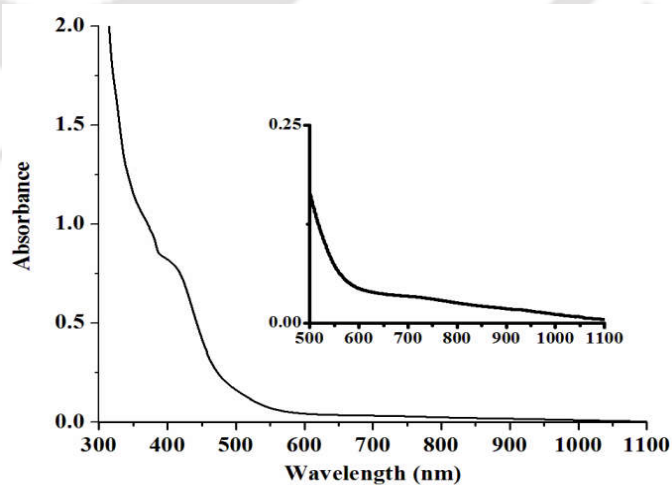


Figure A2.5. UV-visible spectrum of complex **3.1** in dry THF.

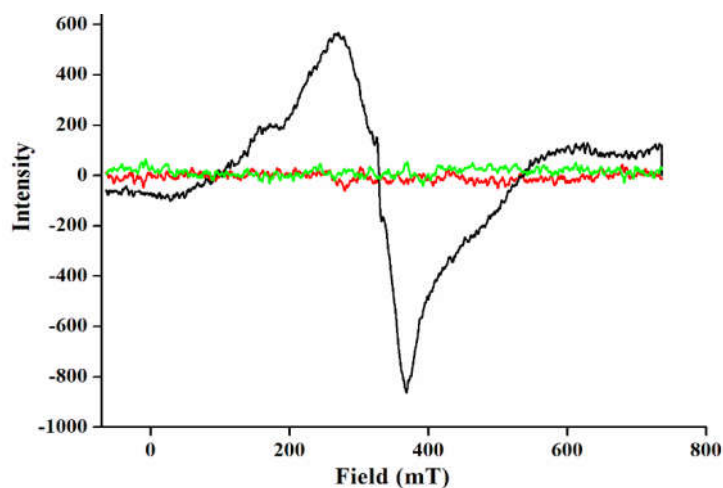


Figure A2.6. X-band EPR spectra of complexes **3.1** (black), **3.2** (red) and **3.3** (green) in dry THF at 77 K.

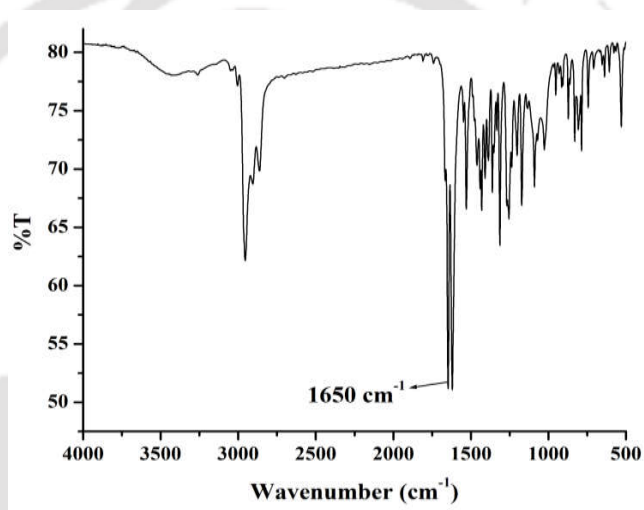


Figure A2.7. FT-IR spectrum of complex **3.2** in KBr.

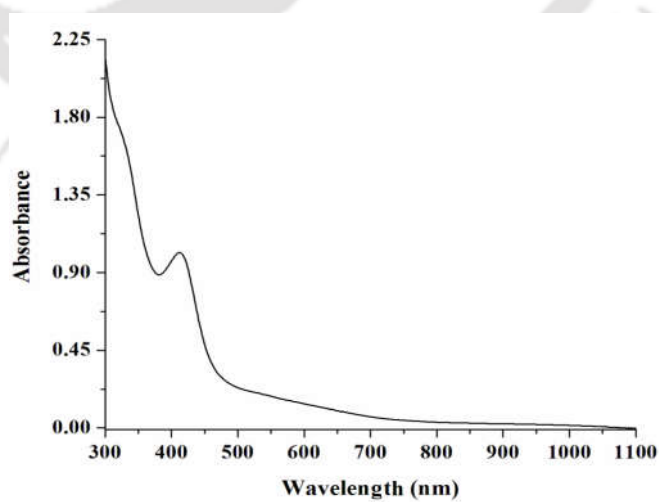


Figure A2.8. UV-visible spectrum of complex **3.2** in dry THF.

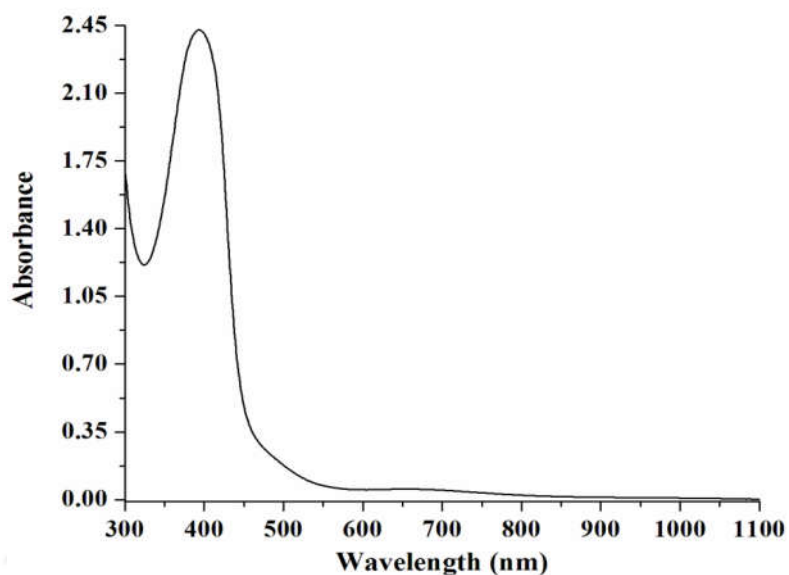


Figure A2.9. UV-visible spectrum of complex **3.3** in dry THF.

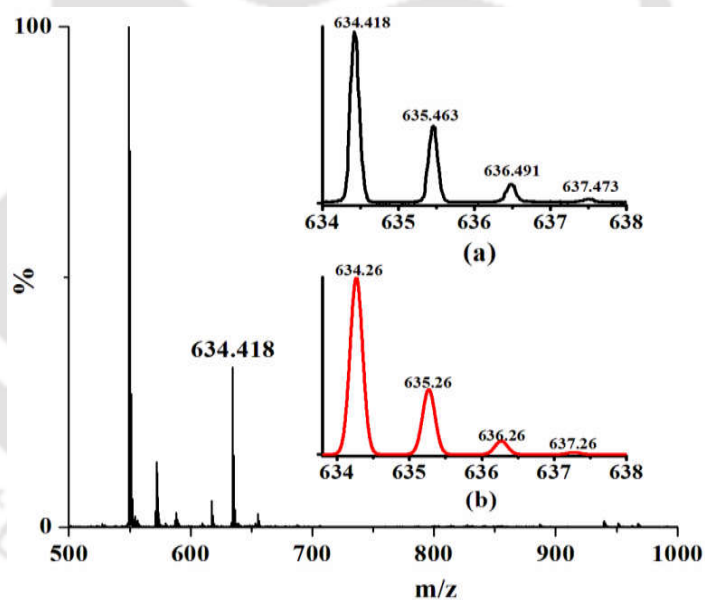


Figure A2.10. ESI-mass spectrum of complex **3.3** with isotopic distribution (a) experimental (b) simulated in methanol $[(L2)Co(NO_3) + Na]^+$.

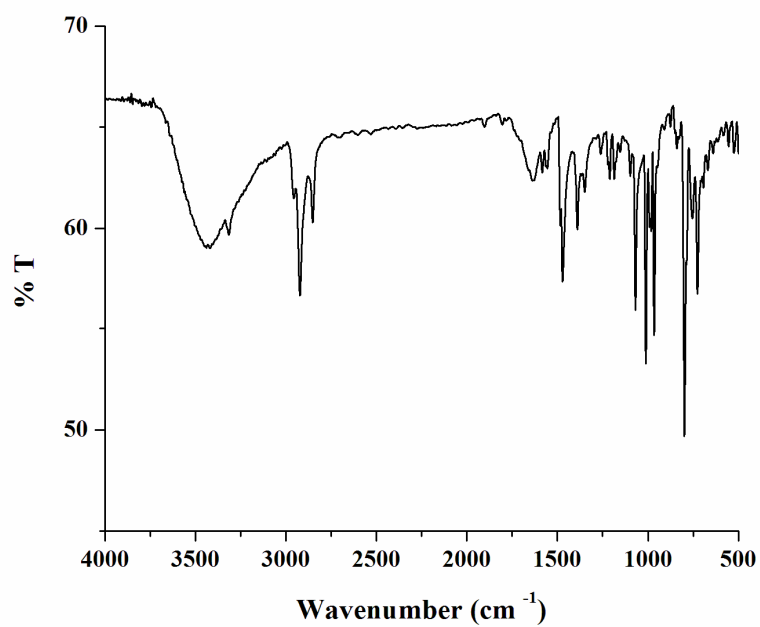


Figure A2.11. FT-IR spectrum of ligand $L3H_2$ in KBr.

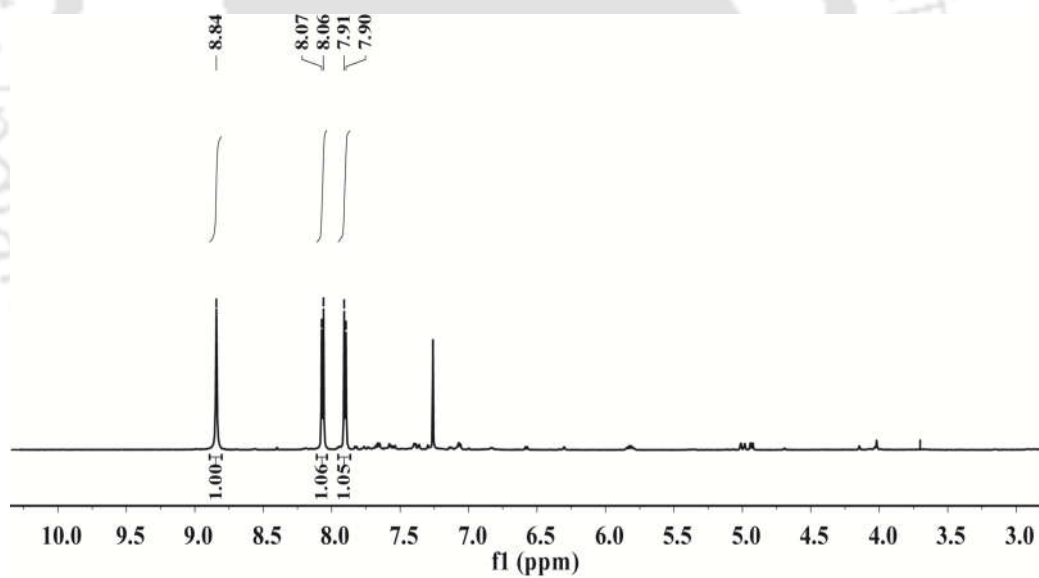


Figure A2.12. 1H -NMR spectrum of ligand $L3H_2$ in $CDCl_3$.

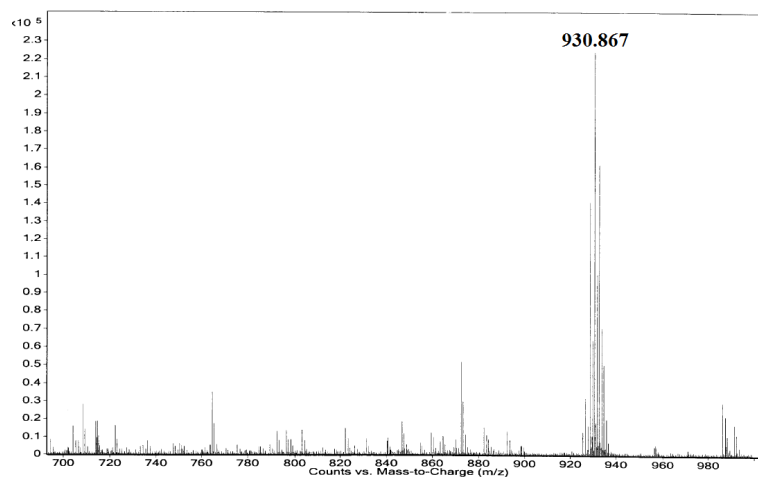


Figure A2.13. ESI-mass spectrum of ligand $L3H_2$ in acetonitrile.

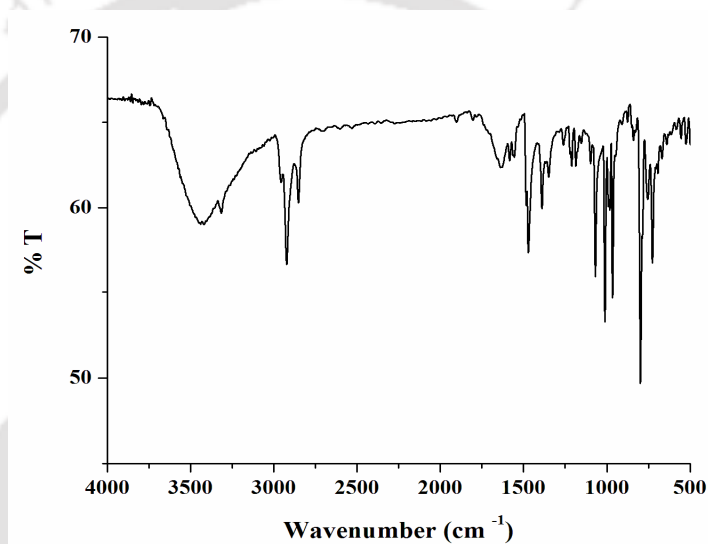


Figure A2.14. FT-IR spectrum of complex **3.4** in KBr.

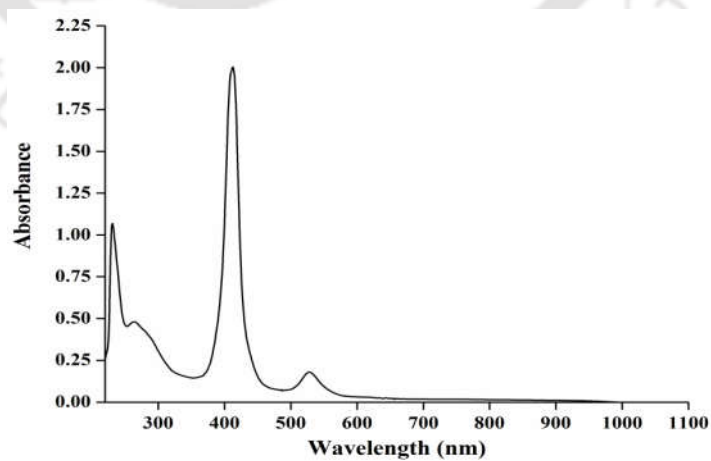


Figure A2.15. UV-visible spectrum of complex **3.4** in dry THF.

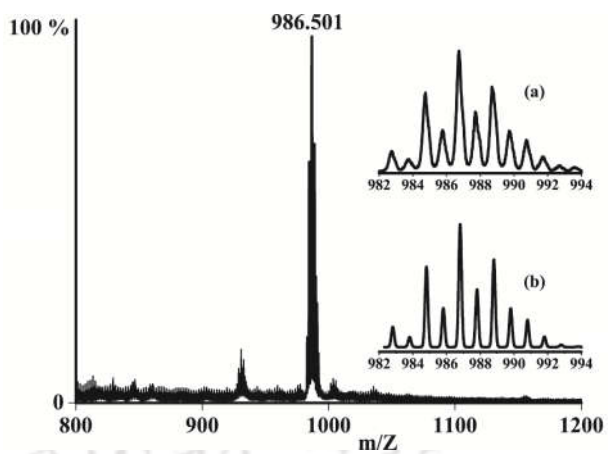


Figure A2.16. ESI-mass spectrum of complex 3.4 with isotopic distribution (a) experimental (b) simulated in methanol.

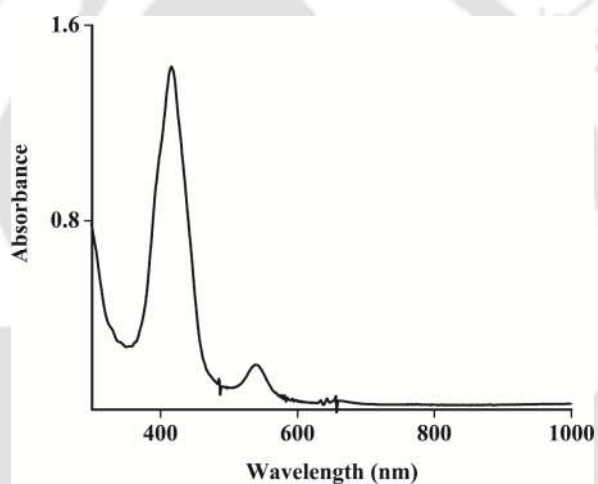


Figure A2.17. UV-visible spectrum of complex 3.5 in dry THF.

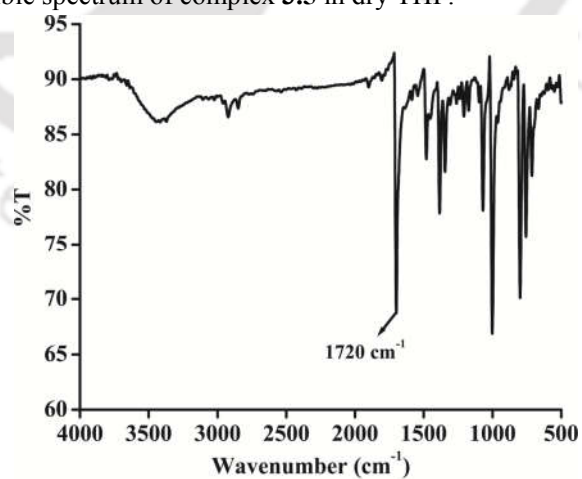


Figure A2.18. FT-IR spectrum of complex 3.4 in KBr.

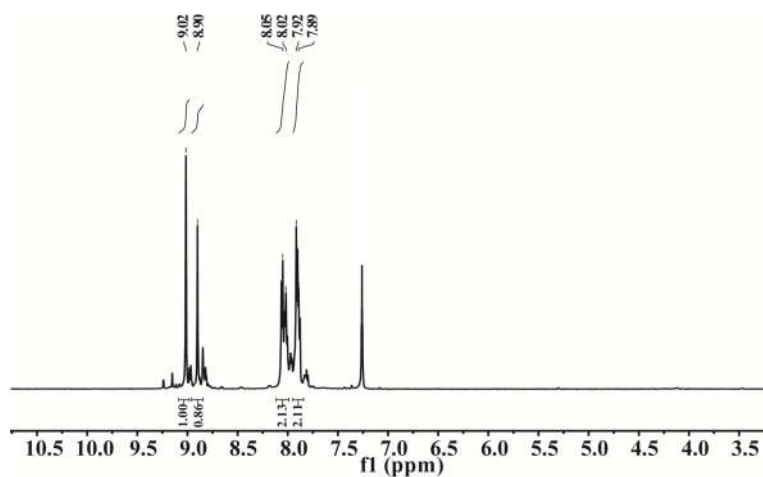


Figure A2.19. ^1H -NMR spectrum of complex 3.5 in CDCl_3 .

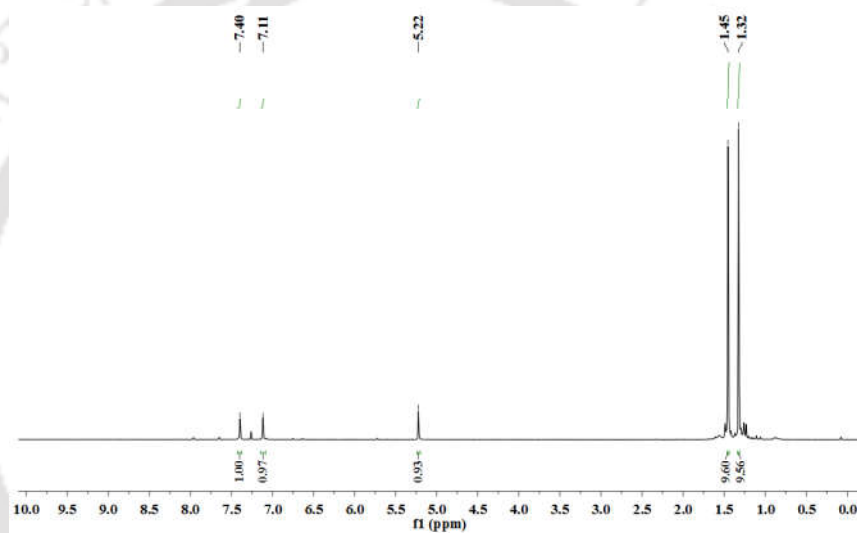


Figure A2.20. ^1H -NMR spectrum of 2,4-di-*tert*-butyl-6-nitrophenol in CDCl_3 .

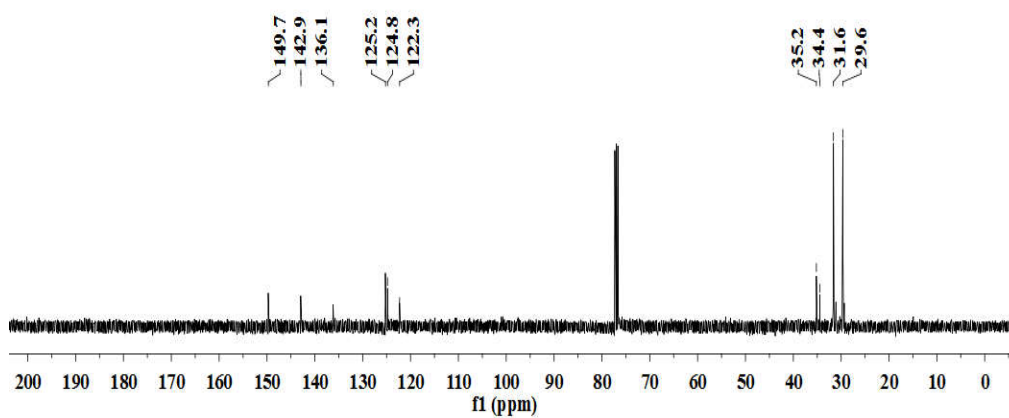


Figure A2.21. ^{13}C -NMR spectrum of 2,4-di-*tert*-butyl-6-nitrophenol in CDCl_3 .

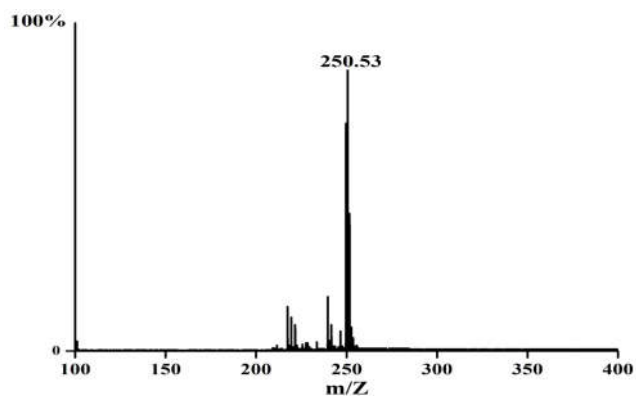


Figure A2.22. ESI-mass spectrum of 2,4-di-*tert*-butyl-6-nitrophenol in methanol.

Table A2.1. Crystallographic data for complexes 3.1, 3.2, 3.4 and 3.5.

	3.1	3.2	3.4	3.5
Formulae	C ₃₂ H ₄₆ CoN ₂ O ₂	C ₃₂ H ₄₆ CoN ₃ O ₃	C ₅₆ H ₄₈ Br ₄ CoN ₄ O ₃	C ₄₈ H ₃₂ Br ₄ CoN ₅ O ₂
Mol. wt.	549.64	579.65	1203.55	1089.32
Crystal system	Orthorhombic	Monoclinic	Monoclinic	Monoclinic
Space group	P b c n	P2(1)/c	C 1 2/c 1	Cc
Temperature /K	296(2)	296(2)	296(2)	296(2)
Wavelength /Å	0.71073	0.71073	0.71073	0.71073
<i>a</i> /Å	26.7490(14)	15.141(3)	24.765(3)	32.6508(19)
<i>b</i> /Å	11.0089(4)	19.113(3)	9.5985(5)	9.0163(7)
<i>c</i> /Å	10.3143(5)	11.689(2)	24.578(4)	15.6113(9)
α /°	90.00	90.00	90.00	90.00
β /°	90.0	105.886(6)	120.213(16)	114.564(5)
γ /°	90.00	90.00	90.00	90.00
<i>V</i> / Å ³	3037.3(2)	3253.4(10)	5048.8(9)	4179.9(5)
<i>Z</i>	8	4	4	4
Density/Mgm ⁻³	1.2020	1.183	1.583	1.928
Abs. Coeff. /mm ⁻¹	0.594	0.561	3.554	6.390
Abs. correction	Multi-scan	None	Multi-scan	Multi-scan
<i>F</i> (000)	1180.0	1240	2412	2152.0
Total no. of reflections	2037	48481	3375	5886
Reflections, <i>I</i> > 2σ(<i>I</i>)	3525	5610	2610	4379
Max. 2θ/°	26.32	25.00	24.50	25.25
Ranges (h, k, l)	-35 ≤ h ≤ 31 -14 ≤ k ≤ 14 -13 ≤ l ≤ 13	-18 ≤ h ≤ 16 -22 ≤ k ≤ 22 -13 ≤ l ≤ 13	-28 ≤ h ≤ 26 -11 ≤ k ≤ 7 -25 ≤ l ≤ 19	-39 ≤ h ≤ 38 -10 ≤ k ≤ 8 -18 ≤ l ≤ 18
Complete to 2θ (%)	99.66	98.1	80.1	99.8
Goof (<i>F</i> ²)	0.792277	1.045	0.955	1.069

R indices [$I > 2\sigma(I)$]	0.049337	0.0550	0.0604	0.0515
R indices (all data)	0.082334	0.0903	0.0813	0.0755

Table A2.2. Selected bond lengths (Å) for complexes **3.1**, **3.2**, **3.4** and **3.5**.

Atoms	3.1	3.2	3.4	3.5
Co(1)-N(1)	1.848(2)	1.880(3)	1.992(6)	1.97(1)
Co(1)-N(3)	-	1.799(4)	-	1.98(1)
Co(1)-O(1)	1.845(2)	1.904(2)	2.382(7)	
O(1)-C(1)	1.315(3)	1.317(3)	-	
N(3)-O(3)		1.155(6)	-	1.330(6)
Co(1)-N(5)		-	-	1.853(6)
N(1)-C(15)	1.293(4)	1.295(5)	-	
N(5)-O(1)		-	-	1.19(2)

Table A2.3. Selected bond angles (°) for complexes **3.1**, **3.2**, **3.4** and **3.5**.

Atoms	3.1	3.2	3.4	3.5
O(1)-Co(1)-N(1)	93.38(9)	92.7(1)	92.8(2)	-
O(1)-Co(1)-N(2)	-	167.8(1)	88.6(2)	-
N(3)-Co(1)-N(1)	-	99.9(2)	-	172.0(5)
Co(1)-N(1)-C(1)	112.7(2)	-	128.1(5)	128.7(9)
N(1)-Co(1)-N(2)	-	-	89.6(2)	89.7(5)
Co(1)-N(5)-O(1)	-	-	-	119(1)
Co(1)-N(3)-O(3)	-	126.5(4)	-	121.9(3)
C(1)-O(1)-Co(1)	129.23(17)	127.5(2)	-	-

Appendix III

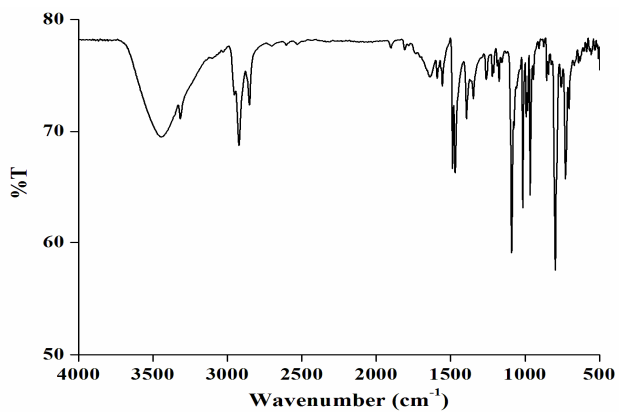


Figure A3.1. FT-IR spectrum of ligand **L4H₂** in KBr.

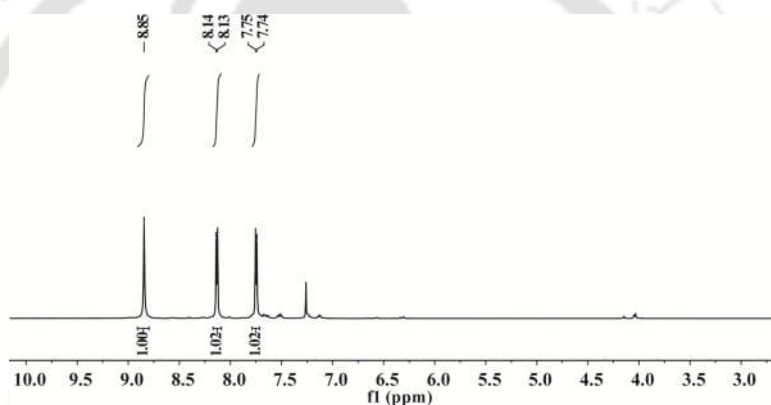


Figure A3.2. ¹H-NMR spectrum of ligand **L4H₂** in CDCl₃.

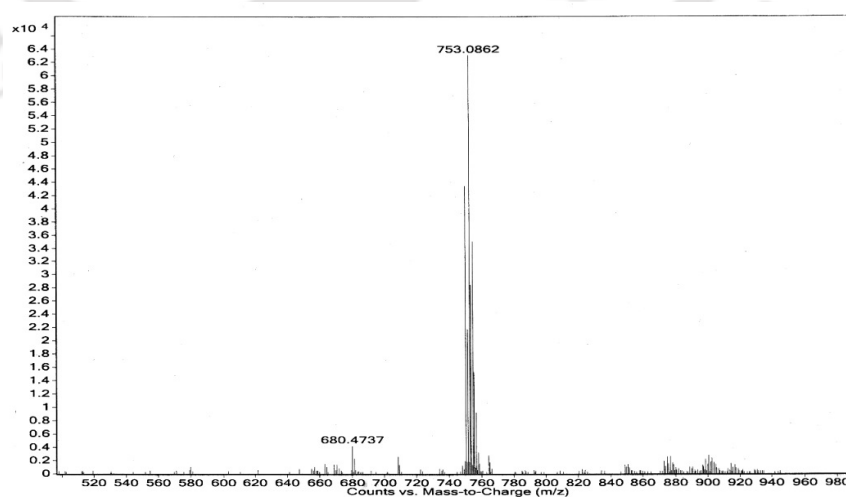


Figure A3.3. ESI mass spectrum of **L4H₂** in acetonitrile.

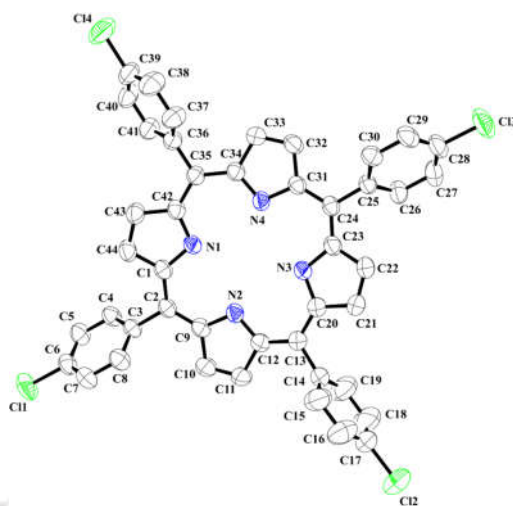


Figure A3.4. ORTEP diagram of ligand **L4H₂** (30% thermal ellipsoid plot; H-atoms and solvent molecules are omitted for clarity).

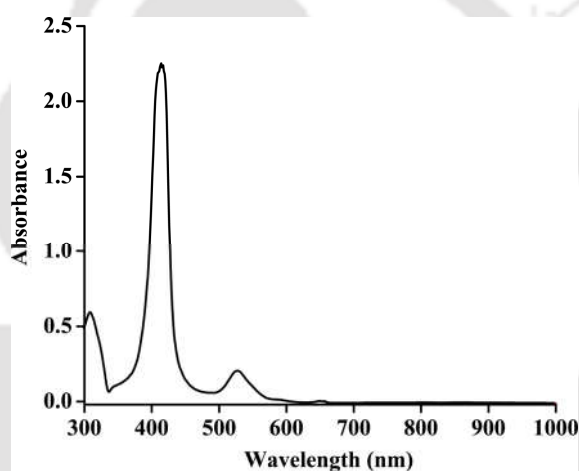


Figure A3.5. UV-visible spectrum of complex **4.1** in dichloromethane.

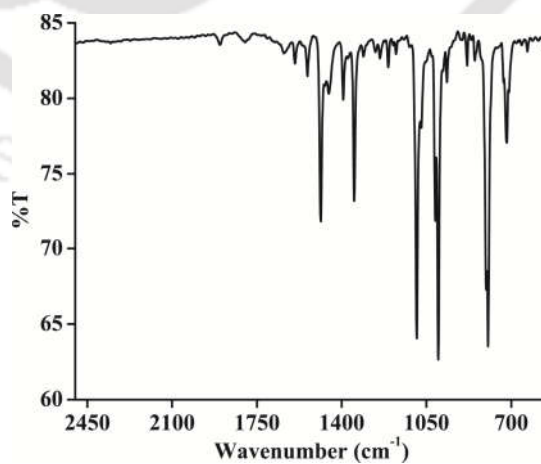


Figure A3.6. FT-IR spectrum of complex **4.1** in KBr.

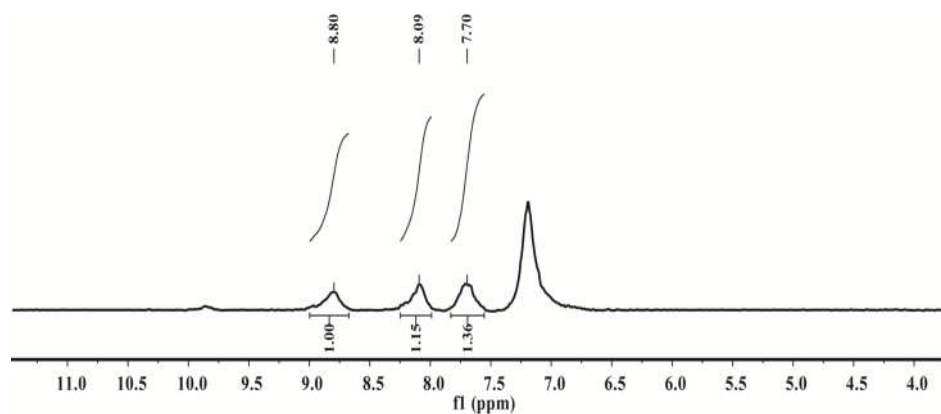


Figure A3.7. $^1\text{H-NMR}$ spectrum of complex **4.1** in CDCl_3 .

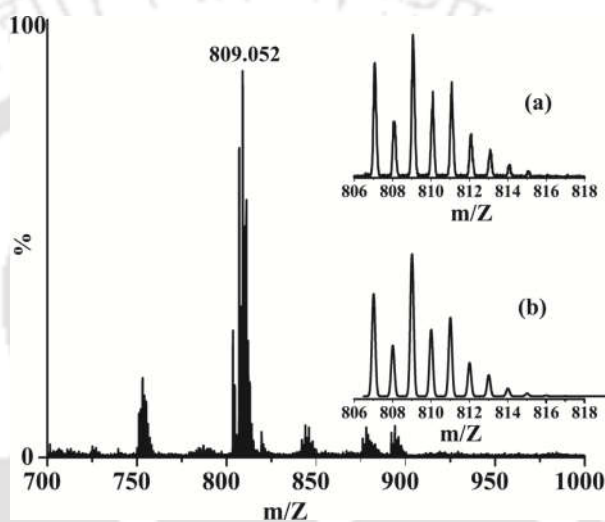


Figure A3.8. ESI-mass spectrum of complex **4.1** in acetonitrile. Inset: (a) experimental and (b) simulated isotopic distribution pattern.

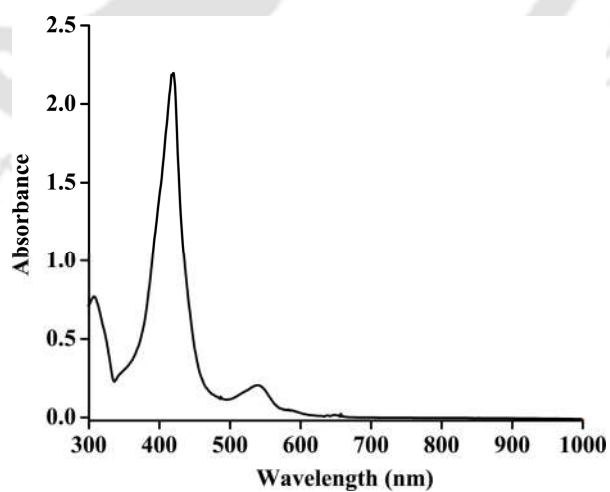


Figure A3.9. UV-visible spectrum of complex **4.2** in dichloromethane.

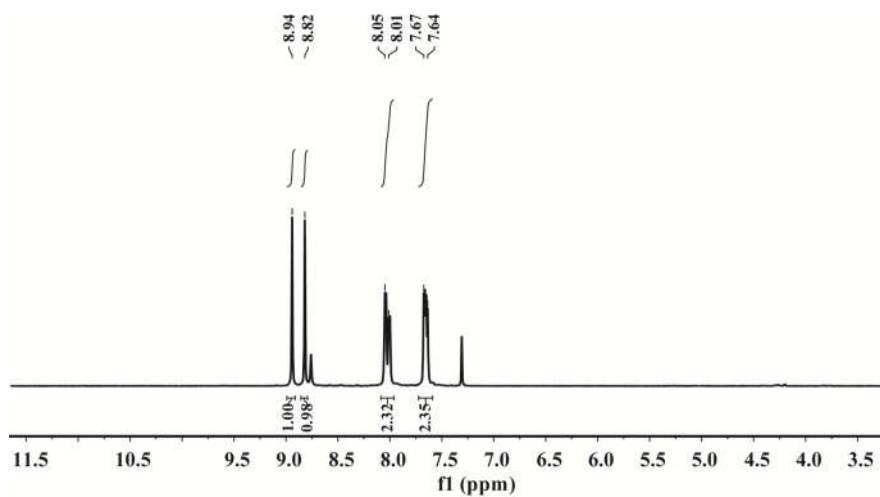


Figure A3.10. $^1\text{H-NMR}$ spectrum of complex 4.2 in CDCl_3 .

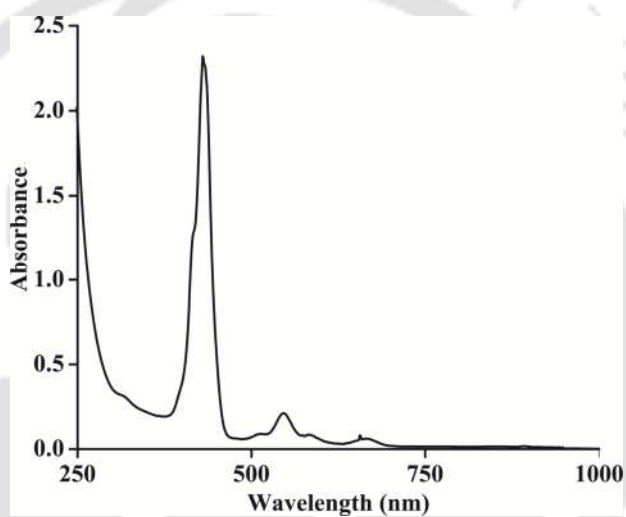


Figure A3.11. UV-visible spectrum of complex 4.3 in acetonitrile.

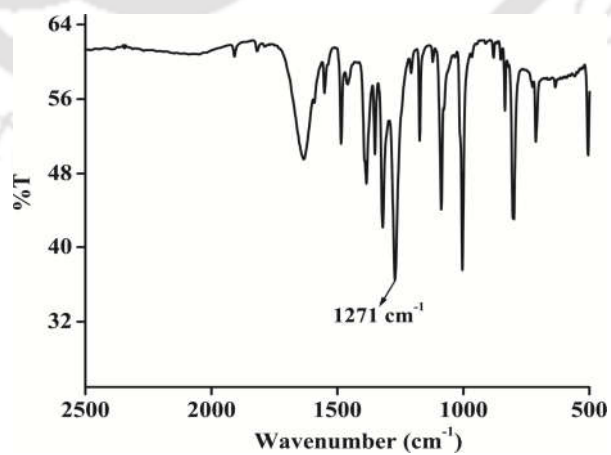


Figure A3.12. FT-IR spectrum of complex 4.3 in KBr.

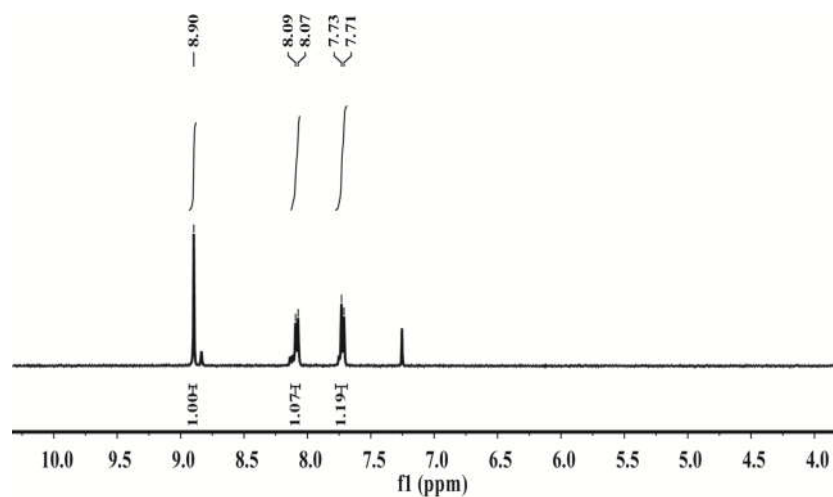


Figure A3.13. ^1H -NMR spectrum of complex 4.3 in CDCl_3 .

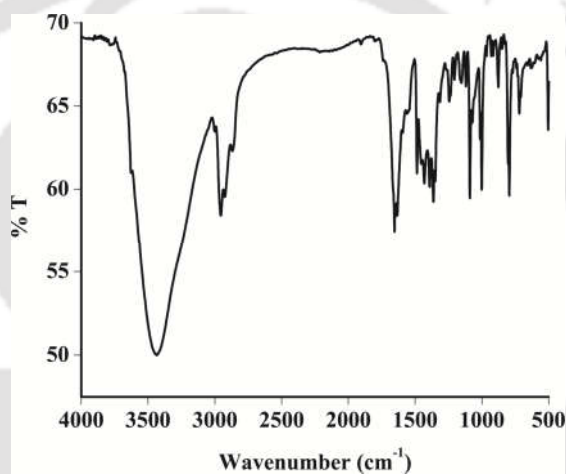


Figure A3.14. FT-IR spectrum of complex 4.4 in KBr.

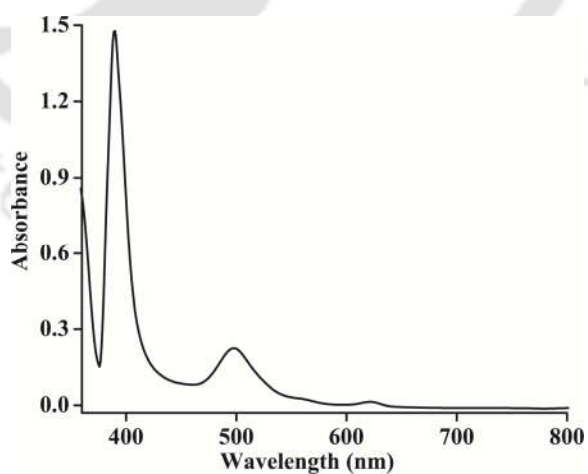


Figure A3.15. UV-visible spectrum of complex 4.4 in acetonitrile.

Table A3.1. Crystallographic data of ligand **L4H₂**, complexes **4.1** and **4.2**.

	L4H₂	4.1	4.2
Formulae	C ₄₄ H ₂₆ Cl ₄ N ₄ O ₃	C ₅₆ H ₄₈ Cl ₄ N ₄ Co O ₃	C ₄₈ H ₃₂ Cl ₄ N ₅ Co O ₂
Mol. wt.	800.49	1025.71	911.52
Crystal system	Triclinic	Monoclinic	Monoclinic
Space group	P -1	C 1 2/c 1	P 121/c1
Temperature /K	296(2)	296(2)	100(2)
Wavelength /Å	0.71073	0.71073	0.71073
<i>a</i> /Å	10.0674(5)	24.482(3)	15.2052(14)
<i>b</i> /Å	13.1785(11)	9.5254(6)	15.4115(12)
<i>c</i> /Å	15.4982(12)	24.225(3)	17.6398(16)
α /°	85.437(7)°	90.00	90.00
β /°	80.873(5)°	119.561(14)	103.442(10)
γ /°	88.471(5)°	90.00	90.00
V/ Å ³	2023.5(3)	4913.8(8)	4020.4(6)
Z	2	4	4
Density/Mgm ⁻³	1.314	1.386	1.506
Abs. Coeff. /mm ⁻¹	0.337	0.616	0.742
Abs. correction	Multi-scan	Multi-scan	Multi-scan
F(000)	820	2124	1864
Total no. of reflections	7104	4320	7257
Reflections, <i>I</i> > 2σ(<i>I</i>)	4624	3541	4976
Max. 2θ/°	25.00	25.00	25.25
Ranges (h, k, l)	-11 ≤ h ≤ 11 -15 ≤ k ≤ 13 -18 ≤ l ≤ 18	-25 ≤ h ≤ 29 -11 ≤ k ≤ 10 -26 ≤ l ≤ 28	-18 ≤ h ≤ 9 -18 ≤ k ≤ 11 -21 ≤ l ≤ 21
Complete to 2θ (%)	99.8	99.8	99.7
Refinement method	Full-matrix least-squares on <i>F</i> ²	Full-matrix least-squares on <i>F</i> ²	Full-matrix least-squares on <i>F</i> ²
Goof (<i>F</i> ²)	1.014	0.802	0.0992
R indices [<i>I</i> > 2σ(<i>I</i>)]	0.1096	0.0471	0.0695
R indices (all data)	0.1438	0.0587	0.1321

Table A3.2. Selected bond lengths (Å) of ligand **L4H₂**, complexes **4.1** and **4.2**.

Atoms	L4H₂	4.1	4.2
Co(1)-N(1)	-	1.991(2)	1.974(6)
Co(1)-N(2)	-	1.987(2)	1.990(6)
Co(1)-N(3)	-	-	1.979(6)
Co(1)-N(4)	-	-	1.982(6)
Co(1)-N(5)	-	-	1.846(7)
C(1)-N(1)	1.373(9)	1.381(4)	1.380(1)
C(1)-C(2)	1.410(1)	1.393(4)	1.40(1)
C(3)-C(4)	1.390(1)	1.385(4)	1.398(9)

C(4)-C(5)	1.370(1)	1.395(5)	1.380(1)
C(5)-C(6)	1.380(1)	1.373(6)	1.390(1)
C(6)-Cl(1)	1.749(8)	1.751(4)	1.747(7)
N(5)-O(1)	-	-	1.230(1)

Table A3.3. Selected bond angles (°) of ligand **L4H₂**, complexes **4.1** and **4.2**.

Atoms	L4H₂	4.1	4.2
N1-Co1-N2	-	89.9(9)	89.4(2)
N1-Co1-N3	-	-	171.6(2)
N2-Co1-N3	-	-	89.9(2)
N3-Co1-N4	-	-	89.7(2)
N2-Co1-N4	-	-	170.2(2)
N1-Co1-N5	-	-	94.2(3)
N2-Co1-N5	-	-	92.8(3)
Co1-N5-O1	-	-	118.4(6)
N1-C1-C2	125.9(7)	125.8(3)	125.4(7)
C1-C2-C3	116.5(6)	117.8(3)	116.5(6)

Appendix IV

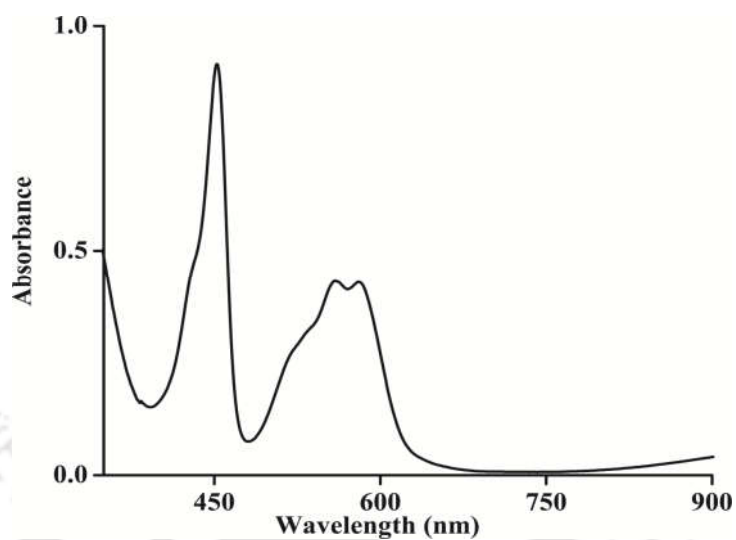


Figure A4.1. UV-visible spectrum of complex **5.1** in methanol at $-40\text{ }^{\circ}\text{C}$.

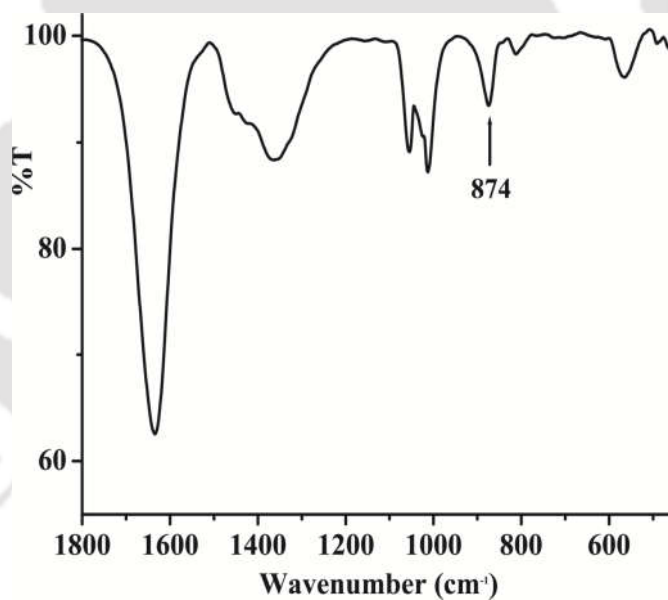


Figure A4.2. FT-IR spectrum of complex **5.1** in KBr.

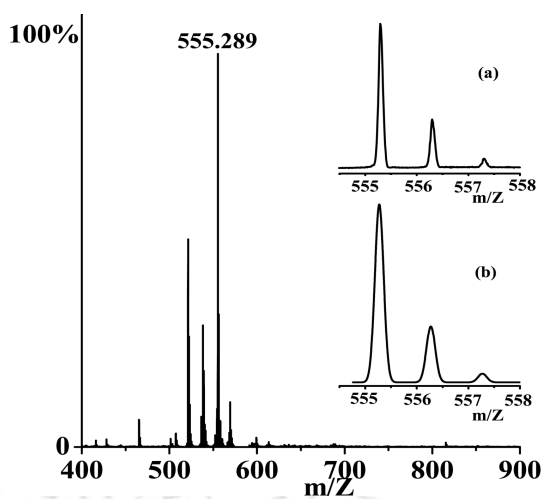


Figure A4.3. ESI-mass spectrum of complex 5.1 in methanol. Inset: (a) experimental and (b) simulated isotopic distribution pattern.

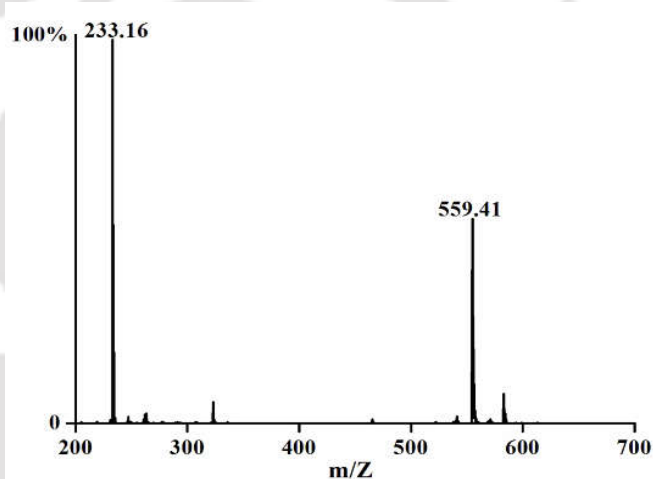


Figure A4.4. ESI-Mass spectrum of complex 5.1 obtained from the reaction of 2.1 and H₂¹⁸O₂ in methanol.

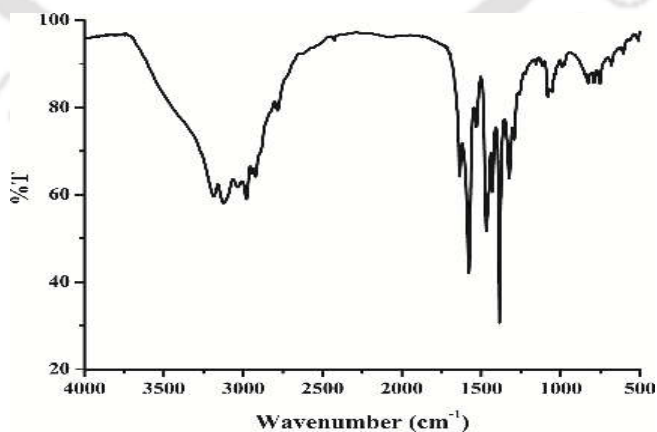


Figure A4.5. FT-IR spectrum of complex 5.2 in KBr.

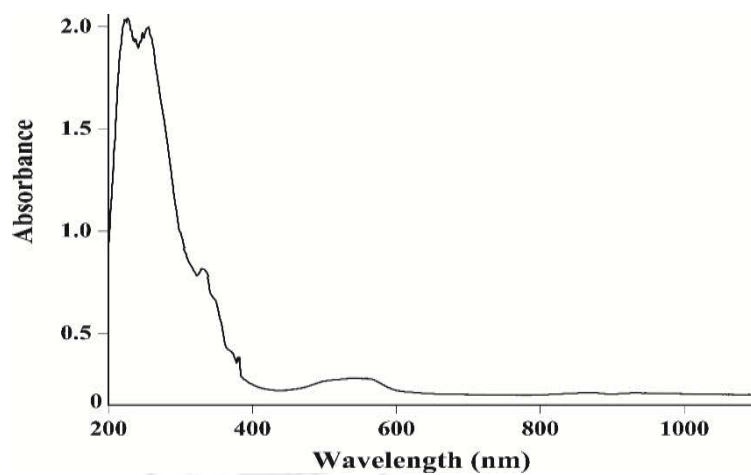


Figure A4.6. UV-visible spectrum of complex 5.2 in methanol.

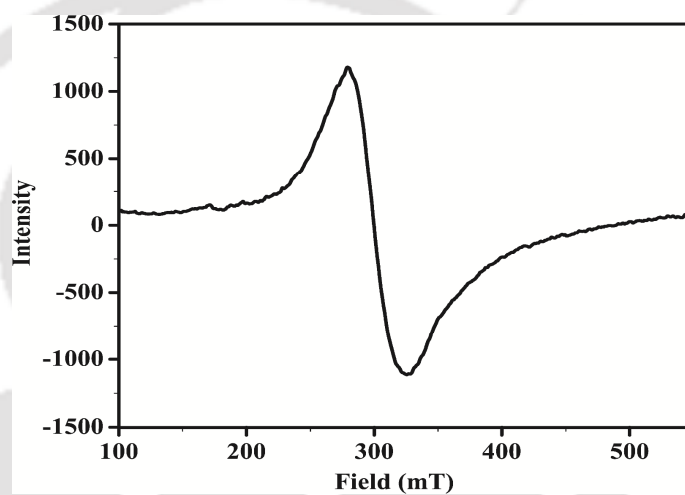


Figure A4.7. X-Band EPR spectrum of complex 5.2 in methanol at room temperature.

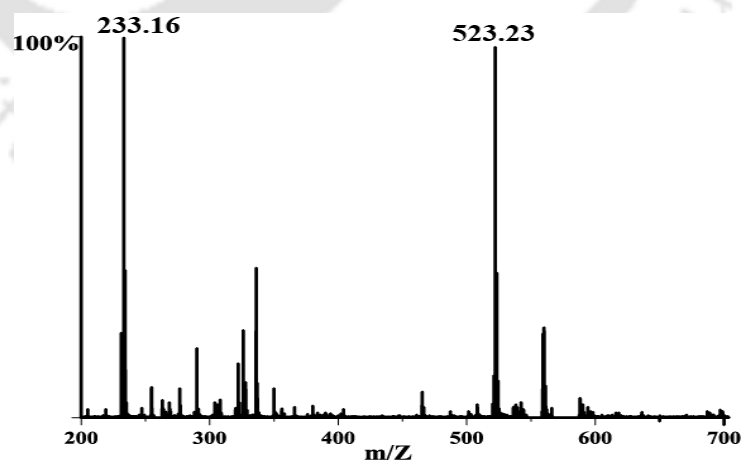


Figure A4.8. ESI Mass spectrum of complex 5.2 in methanol. The m/z, 523.23 peak corresponds to the $\{(L1)_2Co\}$ unit.

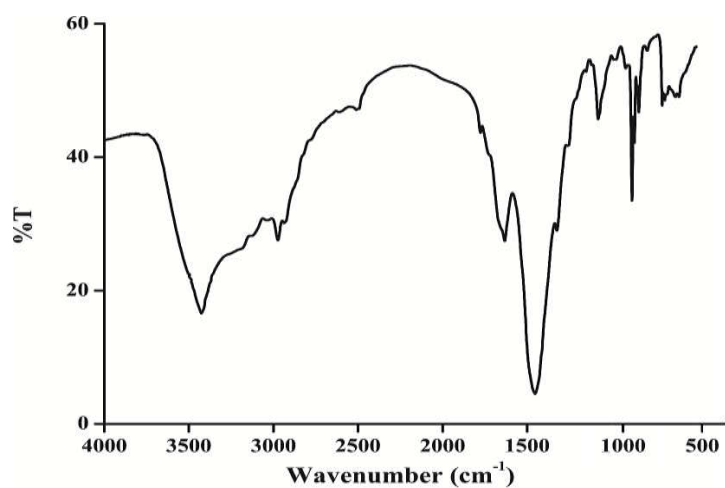


Figure A4.9. FT-IR spectrum of complex 5.3 in KBr pellet.

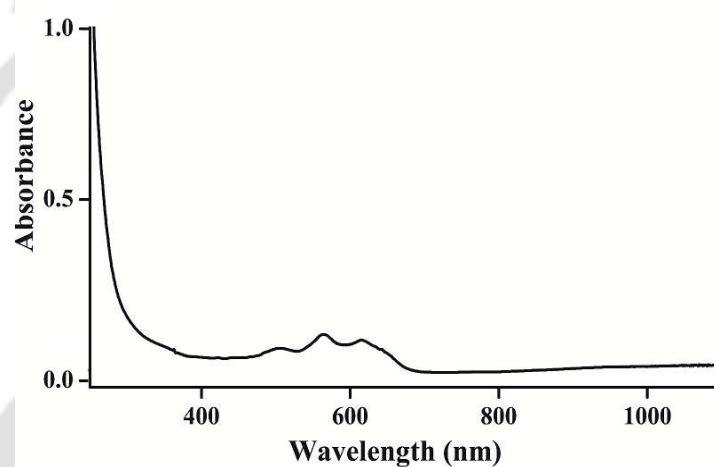


Figure A4.10. UV-visible spectrum of complex 5.3 in methanol.

Table A4.1. Crystallographic data for complex 5.2.

	5.2
Formulae	$C_{26}H_{40}ClN_9CoO_5$
Mol. wt.	653.05
Crystal system	Monoclinic
Space group	P 2/c
Temperature /K	293(2)
Wavelength / \AA	0.71073
$a / \text{\AA}$	9.4505(3)
$b / \text{\AA}$	9.5348(3)
$c / \text{\AA}$	18.4708(5)
$\alpha / ^\circ$	90.00
$\beta / ^\circ$	91.015(2)

$\gamma/^\circ$	90.00
$V/\text{\AA}^3$	1664.12(9)
Z	2
Density/ Mgm^{-3}	1.310
Abs. Coeff. / mm^{-1}	0.643
Abs. correction	None
F(000)	686
Total no. of reflections	2913
Reflections, $I > 2\sigma(I)$	2303
Max. $2\theta/^\circ$	24.99
Ranges (h, k, l)	-11 \leq h \leq 11 -11 \leq k \leq 11 -21 \leq l \leq 21
Complete to 2θ (%)	99.4
Refinement method	Full-matrix least-squares on F^2
Goof (F^2)	0.910
R indices [$I > 2\sigma(I)$]	0.0627
R indices (all data)	0.0763

Table A4.2. Selected bond lengths (\AA) for complex **5.2**.

Atoms	5.2
Co(1)-N(1)	2.087(3)
Co(1)-N(3)	2.099(3)
Co(1)-O(1)	2.287(4)
O(1)-N(5)	1.273(5)
O(2)-N(5)	1.15(1)

Table A4.3. Selected bond angles ($^\circ$) for complex **5.2**.

Atoms	5.2
N(3)-Co(1)-N(1)	98.2(1)
O(1)-Co(1)-N(1)	84.5(1)
O(1)-Co(1)-N(3)	103.6(2)
Co(1)-O(1)-N(5)	93.1(4)
O(2)-N(5)-O(1)	121.3(9)

List of Publications

- (1) “Reductive nitrosylation of nickel(II) complex by nitric oxide followed by nitrous oxide release”.
Ghosh, S.; Deka, H.; Dangat, Y. B.; **Saha, S.**; Gogoi, K.; Vanka, K.; Mondal, B. *Dalton Trans.* **2016**, *45*, 10200.
- (2) “Effect of ligand denticity on the nitric oxide reactivity of cobalt(II) complexes”.
Deka, H.; Ghosh, S.; **Saha, S.**; Gogoi, K.; Mondal, B. *Dalton Trans.* **2016**, *45*, 10979.
- (3) “Nitrogen dioxide reactivity of a nickel(II) complex of tetraazacyclotetradecane ligand”.
Ghosh, S.; Deka, H.; **Saha, S.**; Mondal, B. *Inorg. Chim. Acta* **2017**, *466*, 285.
- (4) “Nitric oxide reactivity of a Cu(II) complex of an imidazole based ligand: Aromatic C-nitrosation followed by the formation of N-nitrosohydroxylaminato complex”.
Deka, H.; Ghosh, S.; Gogoi, K.; **Saha, S.**; Mondal, B. *Inorg. Chem.* **2017**, *56*, 5034.
- (5) “Reaction of a nitrosyl complex of cobalt-porphyrin with hydrogen peroxide: Putative formation of peroxynitrite intermediate”.
Saha, S.; Gogoi, K.; Mondal, B.; Ghosh, S.; Deka, H.; Mondal, B. *Inorg. Chem.* **2017**, *56*, 7781.
- (6) “Reaction of a Co(III)-peroxo complex and NO: Formation of a putative peroxynitrite intermediate”.
Saha, S.; Ghosh, S.; Gogoi, K.; Deka, H.; Mondal, B.; Mondal, B. *Inorg. Chem.* **2017**, *56*, 10932.
- (7) “Dioxygenation reaction of a cobalt-nitrosyl: Putative formation of a cobalt-peroxynitrite via a $\{Co^{III}(NO)(O_2)\}$ intermediate”.

Gogoi, K.; **Saha, S.**; Ghosh, S.; Deka, H.; Mondal, B.; Mondal, B. *Inorg. Chem.* **2017**, *56*, 14438.

- (8) “Nitric oxide reactivity of Cu(II) complex of N- donor ligand: Formation of a stable nitrous oxide complex”.

Deka, H.; Dangat, Y. B.; **Saha, S.**; Gogoi, K.; Vanka, K.; Mondal, B. (*Under revision*).

- (9) “Reductive nitrosylation of cobalt(II) complex by nitric oxide followed by release of nitrous oxide”.

Saha, S.; Gogoi, K.; Mondal, B. (*Communicated*)

- (10) “Reactivity of a cobalt nitrosyl complex: Formation of a cobalt peroxyxynitrite intermediate and transfer the nitrosyl to a cobalt porphyrin complex”.

Saha, S.; Gogoi, K.; Mondal, B. (*Communicated*)

- (11) “Disproportionation of a $\{\text{FeNO}\}^7$ species into $\{\text{Fe}(\text{NO})_2\}^9$ and ferric complex”.

Gogoi, K.; Boro, M.; **Saha, S.**; Mondal, B. (*Communicated*).